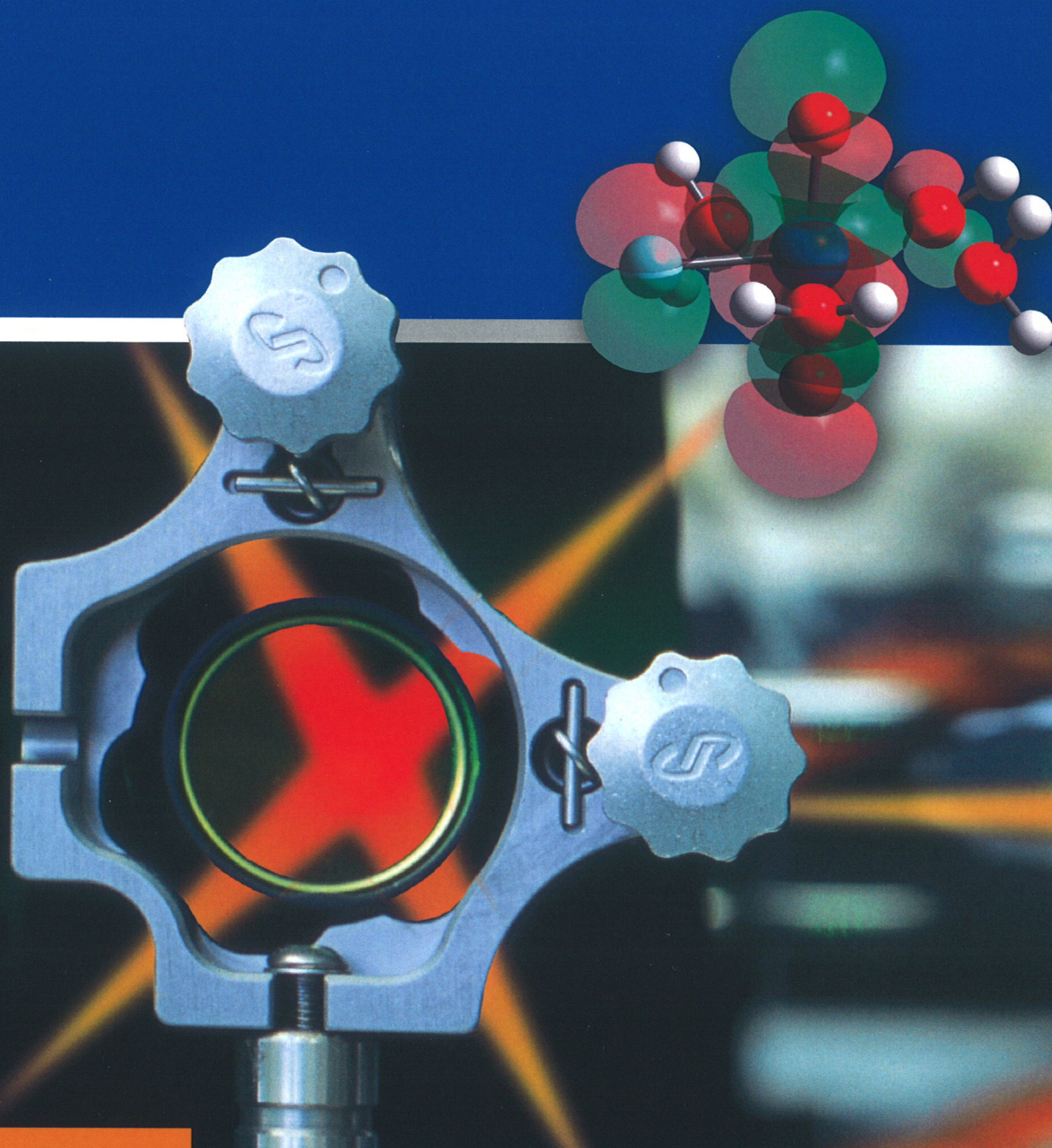


HZDR-027

Wissenschaftlich-Technische Berichte  
HZDR-027 2012 · ISSN 2191-8708



International Workshop on

## ADVANCED TECHNIQUES IN ACTINIDE SPECTROSCOPY (ATAS 2012)

ABSTRACT BOOK

**HZDR**



HELMHOLTZ  
ZENTRUM DRESDEN  
ROSSENDORF

Wissenschaftlich-Technische Berichte  
HZDR-027

# International Workshop on **Advanced Techniques for Actinide Spectroscopy (ATAS 2012)**

## **Abstract Book**

November 05-07, 2012  
HZDR – Helmholtz-Zentrum Dresden-Rossendorf  
Dresden, Germany

Organized by  
Helmholtz-Zentrum Dresden-Rossendorf e.V.  
Institute of Resource Ecology

Editors:  
H. Foerstendorf, K. Müller, R. Steudtner

**HZDR**

 **HELMHOLTZ**  
ZENTRUM DRESDEN  
ROSSENDORF

Print edition: ISSN 2191-8708

Electronic edition: ISSN 2191-8716

The electronic edition is published under Creative Commons License (CC BY-NC-ND):

Qucosa: <http://fzd.qucosa.de/startseite/>

Published by Helmholtz-Zentrum Dresden-Rossendorf e.V.

This abstract book is also available at <http://www.hzdr.de/FWO>

## Contact

Helmholtz-Zentrum Dresden-Rossendorf e.V.  
Institute of Resource Ecology

### *Postal Address*

P.O. Box 51 01 19  
D-01314 Dresden  
Germany

### *Address for visitors*

Bautzner Landstraße 400  
D-01328 Dresden  
Germany

Phone: ++49 (0) 351 260 3210

Fax: ++49 (0) 351 260 3553

e-mail: [contact.resourceecology@hzdr.de](mailto:contact.resourceecology@hzdr.de)

[ATAS@hzdr.de](mailto:ATAS@hzdr.de)

<http://www.hzdr.de/ATAS>

Wissenschaftlich-Technische Berichte  
HZDR-027

# International Workshop on **Advanced Techniques for Actinide Spectroscopy (ATAS 2012)**

## **Abstract Book**

November 05-07, 2012  
HZDR – Helmholtz-Zentrum Dresden-Rossendorf  
Dresden, Germany

Organized by  
Helmholtz-Zentrum Dresden-Rossendorf e.V.  
Institute of Resource Ecology

Editors:  
H. Foerstendorf, K. Müller, R. Steudtner

**HZDR**

 **HELMHOLTZ**  
ZENTRUM DRESDEN  
ROSSENDORF

Print edition: ISSN 2191-8708

Electronic edition: ISSN 2191-8716

The electronic edition is published under Creative Commons License (CC BY-NC-ND):

Qucosa: <http://fzd.qucosa.de/startseite/>

Published by Helmholtz-Zentrum Dresden-Rossendorf e.V.

This abstract book is also available at <http://www.hzdr.de/FWO>

## Contact

Helmholtz-Zentrum Dresden-Rossendorf e.V.  
Institute of Resource Ecology

### *Postal Address*

P.O. Box 51 01 19  
D-01314 Dresden  
Germany

### *Address for visitors*

Bautzner Landstraße 400  
D-01328 Dresden  
Germany

Phone: ++49 (0) 351 260 3210

Fax: ++49 (0) 351 260 3553

e-mail: [contact.resourceecology@hzdr.de](mailto:contact.resourceecology@hzdr.de)

[ATAS@hzdr.de](mailto:ATAS@hzdr.de)

<http://www.hzdr.de/ATAS>

## Contents

Preface.....	4
Scientific Committee .....	5
Local Committee.....	5
Sponsors.....	5
Information .....	7
Scientific Program .....	8
ORAL PRESENTATIONS.....	11
POSTER PRESENTATIONS.....	39
Index of Authors .....	64

## Preface

**M**ODERN SOCIETIES HAVE TO CONSIDER diverse tasks strongly related to geochemistry sciences. Examples intensively discussed in the public are restoration measures for contaminated industrial fallow grounds, the safe storage of chemical-toxic and radioactive waste, carbon dioxide sequestration to reduce green-house gas emissions, the construction and operation of deep geothermal power plants, the geochemical exploration of natural resources or water and waste water treatments, including desalination efforts. Direct and urgent aspects to be dealt with are analytical and geochemical consequences of the Fukushima Daiichi nuclear disaster. All these cases have one in common – they require reliable thermodynamic data in order to forecast the fate of chemicals in the respective environment.

Whereas a variety of standard methods, such as potentiometry, solubility studies, liquid-liquid extraction or electrochemical titrations, are in widespread use to generate thermodynamic data, it is far less straightforward to assign correct reaction pathways and structural patterns to the underlying chemical transformations. This especially holds for systems with strong tendencies to complexation and oligomerization. Here, it is essential to have proof of evidence for all involved species, which cannot be provided by the aforementioned methods, and is still lacking for various metal-containing systems.

Spectroscopic techniques in combination with approaches from quantum chemistry can be of great benefit for such tasks. However, their application ranges are often restricted with respect to the type of element (and redox state) that can be probed. Further handicaps are imposed by detection limits or other parameters such as pH or salinity. Moreover, the spectroscopic results are often difficult to interpret in an unambiguous way.

To overcome these complications at least partially, this workshop has been initiated. It shall significantly extend the application areas of spectroscopic tools important for lanthanide and actinide chemistry. Emphasis shall be placed on the development of spectroscopic methods towards more challenging environmental conditions – such as very basic pH values, elevated temperatures, pressures, or salinities – extending the range of covered elements and redox states. Furthermore, the exploration of options for lowering detection limits and increasing spatial resolution at sufficiently high signal-to-noise ratios will support future investigations on more complex systems. An approach combining the extension of spectroscopic tools with respect to elements and parameters, improvements of experimental setups, and applications of quantum chemical methods in predictive as well as interpretative ways certainly can be very beneficial.

The workshop hopefully will bundle and strengthen respective research activities and ideally act as a nucleus for an international network, closely collaborating with international partners. I am confident that the workshop will deliver many exciting ideas, promote scientific discussions, stimulate new developments and in such a way be successful.

This workshop would not take place without the kind support of the HZDR administration which is gratefully acknowledged. Finally, the organizers cordially thank all public and private sponsors for generous funding which makes this meeting come true for scientists working on the heavy metal research field.



Vinzenz Brendler  
Acting Director of the  
Institute of Resource Ecology

## Scientific Committee

### Christophe Den Auwer

Nice Sophia Antipolis University (France)

### Takaumi Kimura

Japan Atomic Energy Agency (Japan)

### Francis Livens

Manchester University (U.K.)

### Katharina Müller

Helmholtz-Zentrum Dresden-Rossendorf (Germany)

### Andreas C. Scheinost

Helmholtz-Zentrum Dresden-Rossendorf (Germany)

### Robin Steudtner

Helmholtz-Zentrum Dresden-Rossendorf (Germany)

### Thorsten Stumpf

Karlsruhe Institute of Technology (Germany)

### Jan Tits

Paul Scherrer Institute (Switzerland)

### Satoru Tsushima

Helmholtz-Zentrum Dresden-Rossendorf (Germany)

### Valérie Vallet

Lille University (France)

## Local Committee

### Katharina Müller

Astrid Barkleit

Vinzenz Brendler

Carola Franzen

Alix Günther

Satoru Tsushima

### Robin Steudtner

Frank Bok

Harald Foerstendorf

Gerhard Geipel

Henry Moll

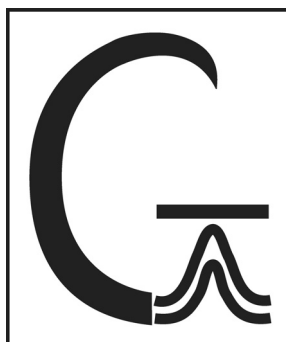
Manja Vogel

## Sponsors



Bundesministerium  
für Bildung  
und Forschung

**DFG**



**Gaussian Inc.**



**Newport®**

Experience | Solutions

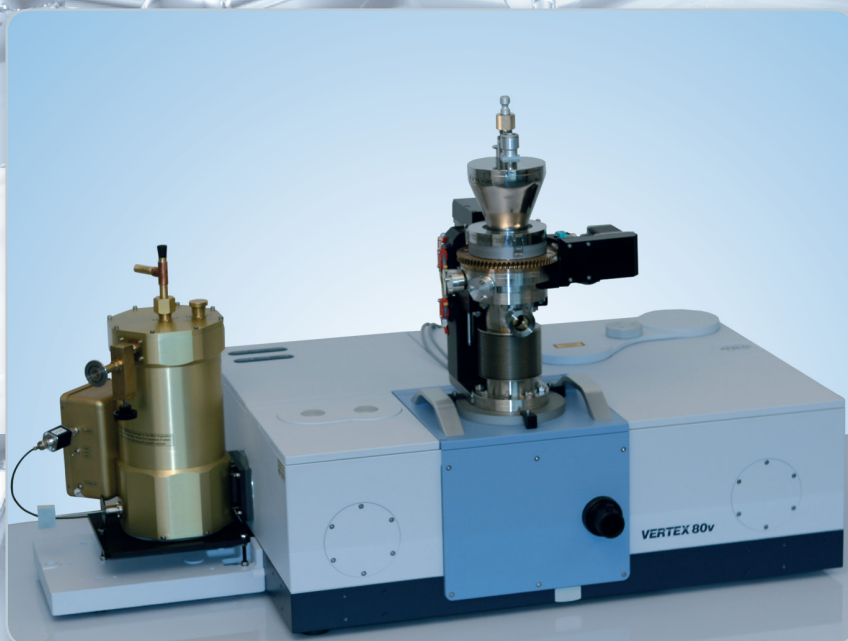


A Newport Corporation Brand



**HORIBA**  
Scientific





## VERTEX Series

### Research FT-IR Spectrometers

Bruker's VERTEX series FT-IR spectrometers are built on a fully upgradeable platform and share a variety of features for ease of use and ultimate performance. Vacuum models eliminate atmospheric moisture absorptions from the sample and the instrument for ultimate sensitivity and stability.

- VERTEX 70 and VERTEX 70v utilizes RockSolid™ permanently aligned interferometer.
- VERTEX 80 and VERTEX 80v utilizes UltraScan™ interferometer with precise linear air bearing scanner and TrueAlignment™ technology.
- **NEW:** Fully automated beamsplitter exchange for vacuum spectrometer VERTEX 80v

#### Bruker Optik GmbH

Rudolf-Plank-Str. 27  
76275 Ettlingen  
Tel. +49 7243 504 2000  
Fax. +49 7243 504 2050  
E-Mail: [info@brukeroptics.de](mailto:info@brukeroptics.de)  
[www.brukeroptics.de](http://www.brukeroptics.de)

Weitere Informationen finden Sie unter: [www.brukeroptics.de](http://www.brukeroptics.de) • [www.lumos-ir.de](http://www.lumos-ir.de)

## Information

### – Registration

Registration desk will be open as follows:

Monday, Nov. 5<sup>th</sup>: 9.30 a.m. - 3.00 p.m.

Tuesday, Nov. 6<sup>th</sup>: 9.30 a.m. - 12.00 p.m.

### – Instructions of Presentations

All speakers are asked to upload their presentations at the lecture hall before their session starts.

Poster dimensions should not exceed A0 size, that is ~124 x 87 cm (~48 x 35 inch) and should be in portrait format. The poster numbers are given in this abstract book and can also be found on the poster walls in front of the lecture hall. All posters can be presented throughout the workshop. Adhesives will be provided. All presenters are kindly asked to remove their posters before departure.

### – Lunch & Refreshments

Lunches will be served for the participants of the workshop during lunch breaks. Refreshments will be served during the breaks and poster session on Monday evening.

### – HZDR Tours

If you are interested in the research facilities at HZDR, you are invited to participate in one of the guided tours on Monday, 10 a.m.

Guided tours are offered for:

- Radiochemical Laboratories
- Free Electron Lasers at the ELBE Linac

The HZDR tours are for free for workshop participants. However, for organization reasons, we kindly ask you to register for these events.

More information on HZDR tours are available from the ATAS website.

(<http://www.hzdr.de/atas>).

### – Sightseeing Tour & Workshop Dinner

The sightseeing tour and workshop dinner will take place at Tuesday evening. The tour starts at 4.00 p.m. at HZDR. Historical buses will pick up all attendees at the gate of HZDR. The tour ends around 6.00 p.m. in town near the ibis hotels. Around 6.30 p.m. all participants are invited to gather at ibis hotel “Bastei” for a short walk (~ 20 min) to “*Kahnaletto*” restaurant at the ELBE riverside close to Augustusbrücke.

### – Shuttle Service

For your convenience, shuttle buses will be arranged between ibis Hotel „Bastei“ (Prager Straße 5) and HZDR.

Monday, November 5<sup>th</sup>:

- 9 a.m. and 12 p.m.: from ibis to HZDR
- 8.15 p.m.: from HZDR to ibis

Tuesday, November 6<sup>th</sup>:

- 8 a.m. from Ibis to HZDR

Wednesday, November 7<sup>th</sup>:

- 8 a.m. from Ibis to HZDR
- 1.30 p.m. from HZDR to main station (transport to Dresden airport will be organized if needed)

### – Public Transport

There is a bus line (no. 261, dest. “Sebnitz”) from Dresden main station to HZDR every hour. Departure time (a.m.): 7.15, 8.15, 9.15, 10.15,... Get off at bus stop “Forschungszentrum Rossendorf” (travel time: ~ 35-40 min).

From HZDR to Dresden city take bus no. 261, (dest. “Dresden Hbf”). Alternatively, take bus no. 229 (dest. “Bühlau”) with interchange to tram no. 11 (destination: “Zschertnitz”) for Dresden city. The buses leave HZDR in the afternoon as follows:

Bus 261	Bus 229
(Dest.: Dresden Hbf)	(Dest.: Bühlau)
3.13 p.m.	3.41 p.m.
4.13 p.m.	4.41 p.m.
5.13 p.m.	5.41 p.m.
6.13 p.m.	6.41 p.m.
7.19 p.m.	

One-way fare: 2,- €.

## Scientific Program

### Monday, November 5<sup>th</sup>

---

10:00 – 12:00 *HZDR tours*

---

12:00 – 13:00 *Lunch*

---

13:00 – 13:20 *Opening words*

---

#### ENVIRONMENTAL APPLICATIONS

Chairs: G. Geipel  
M. Zavarin

---

13:20 – 14:00	<i>I01:</i> <b>P. Yang</b> (PNNL, U.S.A.)	Computational studies on coordination, energetics, and spectra of actinyl ions in the natural environment
14:00 – 14:20	<i>O01:</i> <b>A. Kremleva</b> (Technical University Munich, Germany)	Density functional computational studies of uranyl(VI) complexation on solvated surfaces of clay minerals
14:20 – 14:40	<i>O02:</i> <b>M. Lübke</b> (Mainz University, Germany)	Spectroscopic study of the reaction of neptunium(V) with synthetic nanocrystalline mackinawite (FeS)
14:40 – 15:00	<i>Coffee break</i>	
15:00 – 15:20	<i>O03:</i> <b>J. Rothe</b> (KIT, Germany)	Soft X-ray spectromicroscopy of natural organics affecting actinide mobility - an overview
15:20 – 15:40	<i>O04:</i> <b>M. Merroun</b> (University of Granada, Spain)	Application of spectroscopic and microscopic techniques in bacterial/actinide interaction studies

---

#### NMR SPECTROSCOPY

Chair: V. Brendler

---

15:40 – 16:00	<i>O05:</i> <b>Z. Szabó</b> (KTH, Stockholm, Sweden)	<sup>17</sup> O NMR study of the oxygen exchange between uranyl(VI) oxygen and water oxygen in strongly alkaline solutions
16:00 – 16:20	<i>O06:</i> <b>H. Mason</b> (LLNL, U.S.A.)	Actinide NMR research at Lawrence Livermore National Laboratory
16:20 – 16:40	<i>O07:</i> <b>N. Huittinen</b> (University of Helsinki, Finland)	The specific sorption of Y(III) onto $\gamma$ -alumina: a solid-state <sup>1</sup> H MAS NMR study
16:40 – 17:00	<i>O08:</i> <b>J. Kretzschmar</b> (HZDR, Germany)	Eu <sup>3+</sup> in NMR spectroscopy - a helpful tool in tracking binding sites
17:00 – 17:20	<i>Break</i>	
17:20 – 20:00	<i>Poster session</i> with German pretzel and beer	

---

## Tuesday, November 6<sup>th</sup>

---

### VIBRATIONAL SPECTROSCOPY

Chair: T. Stumpf

09:00 – 09:40	<i>I02:</i> <b>P. Persson</b> (Umeå University, Sweden)	In-situ infrared spectroscopic studies of reactions at water-mineral interfaces
09:40 – 10:00	<i>O09:</i> <b>H. Foerstendorf</b> (HZDR, Germany)	In situ identification of the U(VI) surface speciation on iron oxide phases by ATR FT-IR spectroscopy
10:00 – 10:20	<i>O10:</i> <b>J. Heuser</b> (FZJ, Germany)	Short-range order investigations of LnPO <sub>4</sub> using Raman spectroscopy
10:20 – 10:40	<i>Coffee break</i>	

---

### X-RAY SPECTROSCOPY AND THEORY

Chair: T. Reich

10:40 – 11:00	<i>O11:</i> <b>M. Schmidt</b> (KIT, Germany)	X-ray reflectivity investigations on the interfacial reactivity of actinides
11:00 – 11:20	<i>O12:</i> <b>G. Creff</b> (IPNO, France)	Study of uranyl and thorium complexation with phosphorylated biomolecules
11:20 – 11:40	<i>O13:</i> <b>T. Vitova</b> (KIT, Germany)	Actinide speciation with high-energy resolution X-ray absorption spectroscopy and inelastic X-ray scattering
11:40 – 12:00	<i>O14:</i> <b>T. Dumas</b> (HZDR, Germany)	XAS study of actinide and lanthanide hexacyanoferrates

---

12:00 *Lunch*

---

### EMISSION SPECTROSCOPY AND THEORY

Chair: S. Tsushima

13:20 – 14:00	<i>I03:</i> <b>J. Li</b> (Tsinghua University, China)	Recent advances of computational spectroscopy in actinide chemistry
14:00 – 14:20	<i>O15:</i> <b>R. J. Baker</b> (Trinity College Dub- lin, Ireland)	Uranium(IV) luminescence: new tricks for an old dog
14:20 – 14:40	<i>O16:</i> <b>R. Polly</b> (KIT, Germany)	Quantum mechanical and spectroscopic investigation of the corundum water interface and sorption of lanthanides and actinides on this surface

---

14:40 – 15:00 *Coffee break*

---

### TECHNICAL APPLICATION: SEPARATION PROCESSES

Chair: I. Billard

15:00 – 15:20	<i>O17:</i> <b>D. Guillaumont</b> (CEA, France)	Experimental and theoretical structures of actinide ions with oxygen-donor ligands in organic solution
15:20 – 15:40	<i>O18:</i> <b>J. März</b> (Dresden University of Technology, Germany)	Fluorescent complexes of tripodal amides: TRIFS and multinuclear NMR spectroscopic studies

---

15:40 – 16:00 *Break*

---

16:00 – 19:00 *Sightseeing in Dresden by historical buses, rest and walk to restaurant*

---

19:00 *Workshop dinner at “Kahnaletto“*

---

## Wednesday, November 7<sup>th</sup>

---

### EMISSION SPECTROSCOPY

Chair: T. Kimura

- 09:00 – 09:40 *I04:* **T. Saito**  
(The University of Tokyo, Japan) Application of multi-mode factor analysis as a robust data reduction tool for time-resolved laser fluorescence spectroscopy
- 09:40 – 10:00 *O19:* **P. Reiller**  
(CEA, France) Commonalities and dissimilarities of Eu(III) interactions by simple organic acids and humic substances: complexation and sorption on Al<sub>2</sub>O<sub>3</sub>.
- 10:00 – 10:20 *O20:* **A. Heller**  
(HZDR, Germany) Spectroscopic and quantum chemical study of the curium(III) and europium(III) citrate speciation in biological systems
- 

10:20 – 10:40 *Coffee break*

---

- 10:40 – 11:00 *O21:* **B. S. Tomar**  
(Bhabha Atomic Research Centre, India) Uranium speciation at silica- water interface: a TRFS study
- 11:00 – 11:20 *O22:* **A. Martínez-Torrents**  
(Universitat Politècnica de Catalunya, Spain) Uranium speciation studies at alkaline pH and in presence of peroxide using TRLFS
- 

11:20 – 11:40 *Coffee break*

---

11:40 – 12:30 **PANEL DISCUSSION AND CLOSING WORDS**

Chairs: C. Den Auwer  
B. Schimmelpfennig  
S. Tsushima

---

12:30 – 13:30 *Lunch*

---

13:30 End of ATAS 2012

---

ABSTRACTS

---

## **ORAL PRESENTATIONS**



---

## Computational studies on coordination, energetics, and spectra of actinyl ions in the natural environment

P. Yang

W. R. Wiley Environmental Molecular Science Laboratory, Pacific Northwest National Laboratory, Richland, Washington, U.S.A.

Actinides are of environmental and health concern due to their introduction into groundwater and the natural environment via nuclear activities. In order to understand the chemical and radiological toxic effects of actinides elements on living creatures, we need to understand the mechanisms of actinide uptake and transport by biomolecules. A critical step is to understand the geometry and electronic structure associated to specific binding sites with selective recognition to actinides in homogeneous and heterogeneous environments, as well as the mechanisms of binding and unbinding processes at the molecular level. In this talk, we will study the interactions between actinyl cations and the elementary building blocks of protein, i.e. amino acids, in direct comparison to the experimental IR and EXAFS measurements. Relativistic density functional theory was applied in an effort to develop fundamental understanding of the interactions that drive the affinity of biological chelating ligands for actinyl ions. Furthermore, we study the dynamical behavior of actinide species interacting at a heterogeneous interface using *ab initio* molecular dynamics. Complimentary to modern experimental spectroscopic techniques, our calculations provide insights into the physico-chemical properties of actinide complexes in the natural environment, a step towards rational design of therapies for removing toxic actinyl cations and remediation technologies for environmental contaminants.



## In situ infrared spectroscopic studies of reactions at water-mineral interfaces

P. Persson

Department of Chemistry, Umeå University, Umeå, Sweden

Recent advances in infrared spectroscopic data collection and analysis have provided new insights into reactions at water-mineral interfaces, and compared to previous models that were based on macroscopic adsorption and dissolution data a more complex picture has emerged. In this paper, a simultaneous infrared and potentiometric technique for in situ studies of water-mineral interfaces will be described, and advanced methods for analyzing the spectroscopic data sets will also be presented. Examples of results will include adsorption and desorption reactions of oxoanions, particularly phosphate, sulfate and arsenate. A combination of in situ infrared and X-ray absorption spectroscopic data will show that arsenate bonds as monodentate ligand at water-mineral interfaces, and that the surface species are likely to gain additional stabilization from hydrogen bonding with neighboring surface sites [1]. It will further be shown that the adsorption mechanisms of phosphate and arsenate are very similar, and that desorption of these anions are strongly dependent on pH and thus on surface speciation and surface charge (Fig. 1).

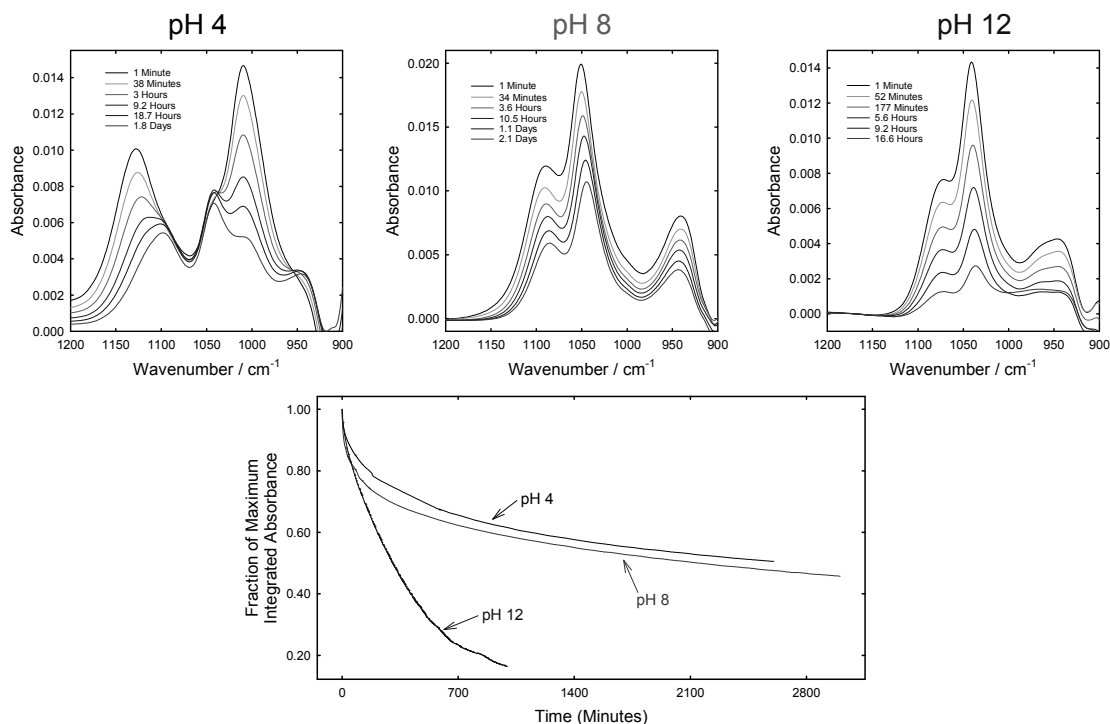


Fig. 1: Net forward rate of desorption of phosphate adsorbed onto  $\alpha$ -FeOOH as a function of pH. The pH dependent rates are determined from the in situ infrared spectra presented above.

The simultaneous infrared and potentiometric technique is also suitable for studying temperature dependence of reactions at water-mineral interfaces. Infrared results of sulfate adsorption in the temperature range 5-70 °C will be presented, which show that the sulfate bonding modes indeed are temperature dependent. Furthermore, these temperature excursion spectroscopic experiments help to distinguish between inner and outer sphere sulfate surface complexes. A final application of in situ infrared spectroscopy will be studies of hydrolysis reactions of organic phosphates at water-mineral interfaces; i.e. reactions often required to convert phosphorus in these molecules into a bioavailable form. Examples will be presented that show how infrared techniques may be used in real-time and at a molecular level to analyze abiotic and enzymatic hydrolysis reactions of organophosphates adsorbed at water-mineral interfaces.

[1] Loring, J. S. et al. (2009) Chem. Eur. J. 15, 5063.

---

## Recent advances of computational spectroscopy in actinide chemistry

J. Li

Department of Chemistry, Tsinghua University, Beijing, China

Actinide chemistry is an essential part of nuclear and radiochemistry. As the chemical behavior of actinides is rather complicated, various modern spectroscopy techniques provide critical information in characterization of actinides. Computational modeling is required in interpreting and predicting spectroscopic features of experimental spectra. Despite complicated electron correlation and relativistic effects, progress has been made in recent years in interpreting vibrational, electronic, and nuclear magnetic spectra of actinide systems. In this talk, an overview of recent advances in computational modeling of spectroscopic data relevant to actinide compounds will be presented. We will also discuss our recent computational results on the infrared, Raman, UV-Vis, fluorescence, NMR, and photoelectron spectra (PES) of actinide complexes using relativistic quantum chemistry methods [1-7]. A brief perspective will be given on future development in theoretical methodology and computational simulations of spectra involving actinides.

- 
- [1] Wei, F. et al. (2011) *Theor. Chem. Acc.* 129, 467–481.
  - [2] Wei, F. et al. (2011) *J. Chem. Theory Comp.* 7, 3223-3231.
  - [3] Su, J. et al. (2011) *J. Chem. Theory Comp.* 7, 3293-3303.
  - [4] Su, J. et al. (2011) *Inorg. Chem.* 50, 2082-2093.
  - [5] Su, J. et al. (2012) *Inorg. Chem.* 51, 3231-3238.
  - [6] Dau, P. D. et al. (2012) *Chem. Sci.* 3, 1137-1146.
  - [7] Dau, P. D. et al. (2012) *J. Chem. Phys.* 136, 194304.

## Application of multi-mode factor analysis as a robust data reduction tool for time-resolved laser fluorescence spectroscopy

T. Saito,<sup>1</sup> N. Aoyagi,<sup>2</sup> T. Kimura<sup>2</sup>

<sup>1</sup> Department of Nuclear Engineering and Management, School of Engineering, The University of Tokyo, Japan

<sup>2</sup> Nuclear Science and Engineering Directorate, Japan Atomic Energy Agency (JAEA), Japan

Radionuclides and other toxic ions readily react with various components of nature, resulting in a distribution of the chemical species, which is called speciation. Evaluating speciation is a key issue for the environmental behavior of such ions as it regulates their reactivity and migration in subsurface environments. Preferably, any speciation technique must possess the following three aspects: (i) separating chemical species of a target ion by their physicochemical properties such as size, charge and reactivity, (ii) quantifying (separated) species, and (iii) characterizing their chemical structures or reaction stoichiometry. Time-resolved laser fluorescence spectroscopy (TRLFS) is a particular speciation technique for fluorescent ions. TRLFS is well-balanced on the above aspects and provide in situ measurements with relatively low detection limits [1]. The structure of TRLFS data consists of two independent variables: wavelength and time. This multi-dimensionality provides a ground for good discrimination capability of TRLFS in speciation analyses, yet sometimes causes misinterpretation of data or insufficient use of the information contained in it. This is clearly shown in our early work, where the analysis of the TRLFS data of  $\text{Eu}^{3+}$ , a chemical homologue of trivalent actinide ions, with acetate ligand by simple exponential fitting gave erroneous results inconsistent with the known speciation [2]. In this talk, the application of a multi-mode factor analytical technique called PARAFAC (parallel factor analysis, Fig. 1) will be introduced to circumvent the above-mentioned difficulties.

PARAFAC is a multivariate technique used for multi-dimensional data with more than three (independent) variables, and thus it is used for a series of TRLFS data collected as a function of a physicochemical variable such as pH and ligand concentration. Adding another variable to data provides more constraints to the underlying chemical model and assures the robustness of the technique. One can also obtain the information on the relationship among samples; that is, the variation of the concentrations of common factors with a physicochemical variable investigated. Three instances of the application of PARAFAC for  $\text{Eu}^{3+}$  TRLFS data will be presented. The first one is the application for  $\text{Eu}^{3+}$  complexation by acetate, meant to demonstrate the applicability of TRLFS, using the system with known speciation [2]. In the remaining two examples  $\text{Eu}^{3+}$  interaction with natural heterogeneous sorbents, namely kaolinite and humic substances, are investigated [3, 4], both of which possess multiple binding sites and give more complicated speciation than the preceding example. The nature of factors obtained from PARAFAC is assessed by studying their fluorescence spectra, decay lifetimes and intensity profiles in terms of the properties of the sorbents and eventually used to deduce the corresponding speciation.

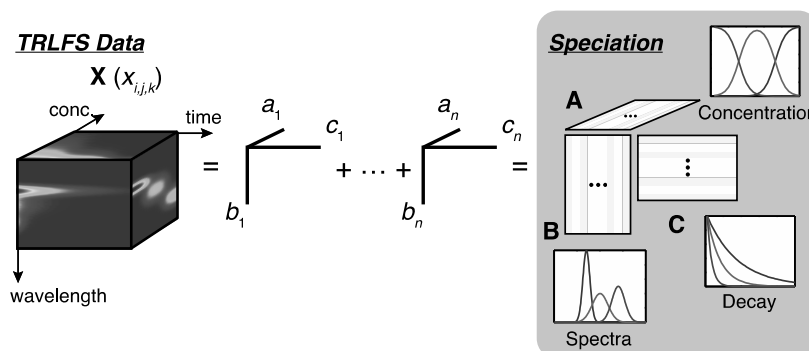


Fig. 1: Schematic representation of PARAFAC application for a TRLFS data array defined by three variables: wavelength, time and concentration of ligand, resulting in the spectra, decay curves and intensity profiles of factors.

[1] Collins, R. et al. (2011) *J. Environ. Quality* 40, 731-741.

[2] Saito, T. et al. (2010) *Environ. Sci. Technol.* 44, 5055-5060.

[3] Ishida, K. (2012) *J. Colloid Interface Sci.* 374, 258-266.

[4] Lukman, S. et al. (2012), *Geochim. Cosmochim. Acta* 88, 199-215.

## Density functional computational studies of uranyl(VI) complexation on solvated surfaces of clay minerals

A. Kremleva, S. Krüger, N. Rösch

Department Chemie & Catalysis Research Center, Technische Universität München, Garching, Germany

Adsorption of actinide ions on clay minerals surfaces is an important process for understanding the distribution and transport of actinide elements in geological repositories and under environmental conditions. Despite a considerable number of spectroscopic experiments, speciation and thermochemistry of actinide adsorption complexes at clay mineral surfaces are not well understood yet. Here computational studies offer helpful complementary information [1].

On the example of uranyl(VI) we studied adsorption complexes on various surfaces of the clay minerals kaolinite [1-3], pyrophyllite [4], and smectite-like model minerals. For the calculation of the electronic structure, we applied a density functional approach at the GGA level using the plane-wave based projector augmented wave method as implemented in the program VASP. Surfaces of clay minerals were modeled as periodic slabs. Surface solvation was approximated by about a monolayer of water molecules. Smectite-like clay minerals with substitutions in tetrahedral or octahedral layers were explored, compensating the permanent charge by  $\text{Na}^+$  counter ions.

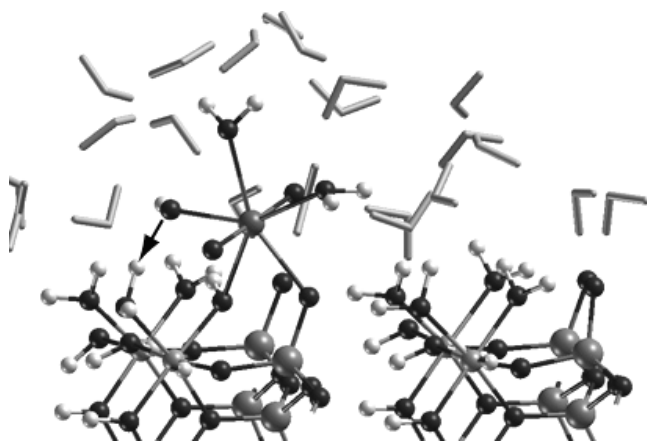


Fig. 1: Uranyl adsorbed on the (010) edge surface of kaolinite.

Pyrophyllite was chosen as a neutral reference mineral for the more complicated charged 2:1 clay minerals [4]. We mainly studied bidentate uranyl adsorption at deprotonated sites of (010), (100), and (110) edge surfaces, representing neutral or slightly higher pH, as inspired by experimental evidence. The various edge surfaces of 2:1 clay minerals exhibit different types of preferred adsorption sites. While uranyl adsorption on kaolinite edge surfaces commonly leads to deprotonation of aqua ligands, resulting in monohydroxide as adsorbate [3], this is rarely the case for 2:1 clay minerals [4]. The coordination numbers of calculated uranyl(VI) complexes at the

mineral surfaces vary between 4 and 5 [4], in contrast to EXAFS studies yielding commonly 5-6. Calculated adsorption energies suggest the (100) surface to be more reactive than the (010) and (110) surfaces. Substitution in the structure of 2:1 clay minerals hardly changed the results. Calculated geometry parameters are mainly determined by the surface groups uranyl is attached to and to a lesser degree by the mineral or the surface orientation. We also compare our calculated geometries to pertinent EXAFS results and suggest an extension of the current interpretation.

- [1] Kremleva, A. et al. (2010) *Radiochim. Acta* 98, 635.  
 [2] Martorell, B. et al. (2010) *J. Phys. Chem. C* 114, 13287.  
 [3] Kremleva, A. et al. (2011) *Geochim. Cosmochim. Acta* 75, 706.  
 [4] Kremleva, A. et al. (2012) *PCCP* 14, 5815.

## Spectroscopic study of the reaction of neptunium(V) with synthetic nanocrystalline mackinawite (FeS)

M. Lübke, S. Amayri, J. Drebert, T. Reich

Institute of Nuclear Chemistry, Johannes Gutenberg-Universität Mainz, Mainz, Germany

Due to its long half-life the radioactive isotope  $^{237}\text{Np}$  is considered to be one of the main contributors to the radiotoxicity of spent nuclear fuel after a storage time of more than 1000 years [1]. Over a wide range of pH and Eh the very mobile neptunyl cation,  $\text{NpO}_2^+$ , dominates the speciation in aqueous solutions. Under reducing conditions, as expected in a nuclear waste repository, Np(V) will be reduced to the less mobile and sparingly soluble  $\text{Np}(\text{OH})_4$  [2].

It is known that iron(II)-bearing minerals such as mackinawite (tetragonal FeS) play an important role in controlling the redox conditions in natural groundwaters. Thus, these minerals can affect the oxidation states of radionuclides, e.g. Np, and therefore also their mobility in the geosphere [3].

Batch experiments have been performed to study the uptake of Np(V) by synthetic nanocrystalline mackinawite as a function of the solid-to-liquid ratio, initial  $^{237}\text{Np}$  concentration, and pH value. Kinetic studies have been performed as well. All experiments showed an almost quantitative uptake of Np. For a better understanding of the reaction process at a molecular level, we combined these batch experiments with spectroscopic measurements. Therefore, mackinawite with different amounts of Np was investigated by X-ray photoelectron spectroscopy (XPS) and X-ray absorption fine structure (XAFS) spectroscopy. XAFS measurements were performed at the INE beamline at ANKA.

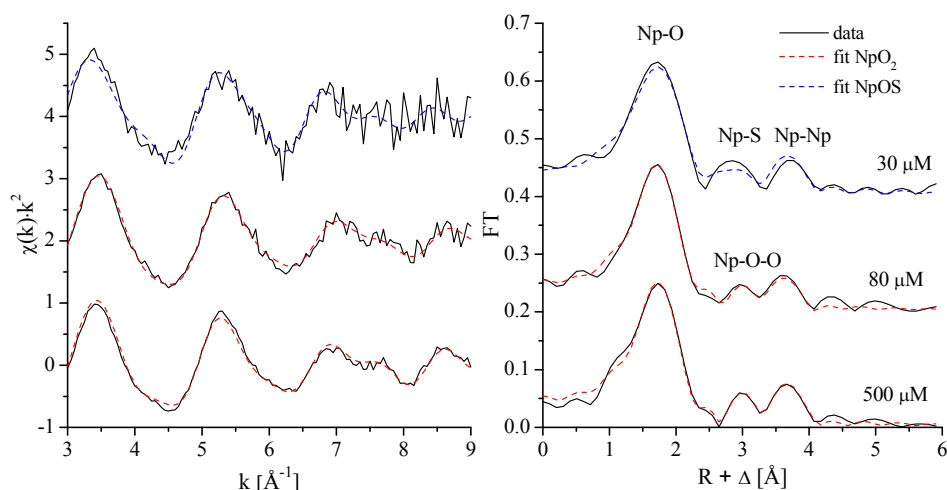


Fig. 1: Np  $L_{III}$ -edge EXAFS spectra (left) and the corresponding Fourier transforms (right) of Np reacted with FeS

XPS and Np  $L_{III}$ -edge XANES measurements (XANES: X-ray absorption near edge structure) showed that Np(V) is reduced to Np(IV) during the reaction with FeS under anaerobic conditions. This explains the nearly complete uptake of Np by mackinawite. The coordination environment of Np at the mineral surface was probed by Np  $L_{III}$ -edge EXAFS spectroscopy (EXAFS: extended X-ray absorption fine structure). The formation of  $\text{NpO}_2$ -like clusters was observed at higher Np concentrations, indicating precipitation of Np(IV) instead of surface complexation. At lower radionuclide concentration we found a sorbed surface species with a NpOS-like structure (Fig. 1).

As a conclusion, our spectroscopic studies showed that during the interaction with mackinawite the mobile pentavalent Np is reduced to Np(IV), which has a much lower mobility and a higher affinity for sorption on mineral surfaces. This greatly retards the migration of Np in the geosphere.

[1] Gompper, K. (2001) FZK, 154.

[2] Yoshida, Z. et al. (2006) in: The Chemistry of the Actinide and Transactinide Elements (Morss, L. R.; Edelstein, N. M.; Fuger, J., eds.), pp. 752, Springer, Dordrecht.

[3] Nakata, K. et al. (2002) Radiochim. Acta, 2002, 90, 665.

---

## Soft X-ray spectromicroscopy of natural organics affecting actinide mobility – An overview

J. Rothe, M. Plaschke, T. Schäfer, K. Dardenne, M. A. Denecke, H. Geckeis

Karlsruhe Institute of Technology (KIT), Institute for Nuclear Waste Disposal (INE), Karlsruhe, Germany

Securing nuclear repository safety requires profound understanding of molecular processes determining the mobility of released radionuclides (i.e., actinides). In this context, systematic spectromicroscopy studies have been performed over the last decade [1]. Scanning Transmission X-ray Microscopy (STXM) is an appropriate tool to visualize natural organics and their interactions with metal cations or mineral phases, providing excellent spatial resolution down to the nm-level in combination with high chemical sensitivity. This chemical speciation information can be obtained from K- or L-edge NEXAFS (Near Edge X-ray Absorption Fine Structure). STXM/NEXAFS investigations are performed at three different endstations: (1) X-1A-STXM, NSLS, USA, (2) PoLux-STXM, SLS, Switzerland, (3) ALS-MES-STXM, LBNL, USA. Moreover, STXM benefits from the ability to characterize environmental samples in thin films of aqueous suspensions or in thin sections. The studies cover various aspects of natural organics and their interactions with metal ions and mineral phases: (a) basic research on model compounds (e.g., polyacrylic acid (PAA)), (b) metal ion interaction with conditioned humic acid (HA) and (c) organic-mineral associations in natural systems (e.g., claystone). Appropriate model compounds are selected, helping to assign spectral features in the more complex natural matter. These assignments are corroborated by quantum-chemical calculations [2]. A distinct metal ion complexation effect is visible in both the C1s-NEXAFS of PAA and HA metal ion complexes depending on sample pH [3]. Metal cations are enriched in a HA minority fraction as determined in Eu(III)-HA aggregates [4]. Furthermore, HA are found associated and fractionated on certain mineral phases, e.g., Al-oxides. Characteristic organic-mineral associations are also observed in claystone samples originating from a possible repository site.

- 
- [1] Plaschke, M. et al. (2011) in: Actinide nanoparticle research, (Kalmykov, S. N. and Denecke, M. A., eds.), Springer-Verlag, Berlin, Heidelberg, pp. 161-184.  
[2] Bâldea, I. et al. (2007) *J. Electron Spec. Relat. Phenom.* 154, 109–118.  
[3] Armbruster, M. K. et al. (2009) *J. Electron Spec. Relat. Phenom.* 169, 51–56.  
[4] Naber, A. et al. (2006) *J. Electron Spec. Relat. Phenom.* 153, 71–74.

## Application of spectroscopic and microscopic techniques in bacterial/actinide interaction studies

M. L. Merroun,<sup>1</sup> F. Morcillo,<sup>1</sup> A. Barkleit,<sup>2</sup> J. M. Arias,<sup>1</sup> M. T. González-Muñoz<sup>1</sup>

<sup>1</sup> Department of Microbiology, University of Granada, Granada, Spain

<sup>2</sup> Helmholtz-Zentrum Dresden-Rossendorf, Institute of Resource Ecology, Dresden, Germany

The presence of the actinides uranium, plutonium, neptunium, americium and curium as well as of lanthanides in radioactive wastes is of major concern because of their potential for migration from the waste repositories and long-term contamination of the environment. It was demonstrated that abiotic processes strongly affect the migration of these elements in the environment. However, it is becoming increasingly evident that microbial processes are of importance as well. Microbial processes will act immobilizing or mobilizing radionuclides, depending on the type of process and the state of the microbes. This paper reviews the local coordination of uranium, as hexavalent actinide, and europium, as inactive analogue of trivalent actinides, by bacterial strains isolated from different environmental habitats including, Mediterranean seawater, and uranium mining wastes piles. For this propose, a combination of synchrotron-based X-ray absorption spectroscopy (XAS), time-resolved laser-induced fluorescence spectroscopy (TRLFS), transmission electron microscope (TEM) coupled with energy dispersive X-ray (EDX) analysis and electron diffraction were used. In the case of U, XAS and TRLFS, analysis indicated that the local coordination of this radionuclide in the U-complexes formed by the different bacterial strains is species specific. Monodentate binding of U to organic or inorganic phosphates, bidentate binding to carboxyl groups are the main types of molecular environment of U within the cells of the bacterial strains studied. TEM/EDX analysis confirms these results and showed strain-specific extracellular and/or intracellular uranium accumulation to varying degrees. In the case of europium, TRLFS analysis indicated the possible implication of biogenic carbonates precipitated by marine bacterium, *Idiomarina loihiensis* MAH1, in the speciation of this lanthanide at seawater conditions.

The results of this work will help in understanding the role of microbiological process in the chemical behavior of actinides in geological and environmental context for future nuclear waste disposals as well as in the optimization of bioremediation processes using these natural bacteria.

# $^{17}\text{O}$ NMR study of the oxygen exchange between uranyl(VI) oxygen and water oxygen in strongly alkaline solutions

Z. Szabó

School of Chemical Science and Engineering, Department of Chemistry, Royal Institute of Technology (KTH), Stockholm, Sweden

NMR spectroscopy is an excellent tool to provide information on both the structure of uranyl(VI) complexes and the rates and mechanisms of their ligand exchange reactions. We have previously used  $^{17}\text{O}$  enriched uranyl(VI), in combination with NMR spectroscopy to study equatorial ligand substitution reactions in various uranyl(VI) complexes, but we did not find evidence for “yl”-exchange with the solvent within a time scale of several days [1-3]. The test solutions used in these studies did not contain hydroxide complexes, indicating that “yl”-exchange requires the presence of terminal and / or bridging hydroxide groups in the equatorial plane of the uranyl(VI) ion. A few years ago, we studied the stoichiometric mechanism, rates and activation parameters for the exchange of the “yl”-oxygen atoms in the dioxo uranium(VI)-ion with solvent water oxygen using  $^{17}\text{O}$  NMR spectroscopy in the pH range of 1-2 and found that the predominant exchange pathway takes place via the OH-bridged binuclear complex  $(\text{UO}_2)_2(\text{OH})_2^{2+}$  [4]. Based on DFT calculations, a plausible pathway via an intramolecular proton transfer has been recently proposed for the “yl”-exchange [5].

The talk will give a brief summary of our recent study of the  $^{17}\text{O}$  isotope exchange in strongly alkaline solutions using tetramethyl-ammoniumhydroxide (TMA-OH) [6]. The exchange rates were studied over a range of uranium(VI) and TMA-OH concentrations by using  $^{17}\text{O}$  NMR inversion-transfer experiments. In this type of NMR experiments, inverting one of the signal using a  $180^\circ$  selective pulse (inversion-transfer) and then observing all of the peaks by a delayed ( $t$ )  $90^\circ$  hard pulse, the intensities of the signals depend on the longitudinal relaxation rate ( $1/T_1$ ) of the exchanging species, on the exchange rates between the sites, and on the variable delay ( $t$ ) value. The desired kinetic information can be calculated from the time dependence of the signal intensities by a non-linear fitting procedure.  $^{17}\text{O}$  NMR inversion-transfer does not seem to have been used previously because of limitations due to the fast longitudinal relaxation of the quadrupolar oxygen. The experimental rate equation indicates that the exchange takes place via a binuclear complex or a transition state with the stoichiometry  $[(\text{UO}_2(\text{OH})_4^{2-})(\text{UO}_2(\text{OH})_5^{3-})]$ . The inversion-transfer experiments were repeated at different temperatures (Fig. 1) and from the temperature dependence of the rate constants the activation parameters were calculated.

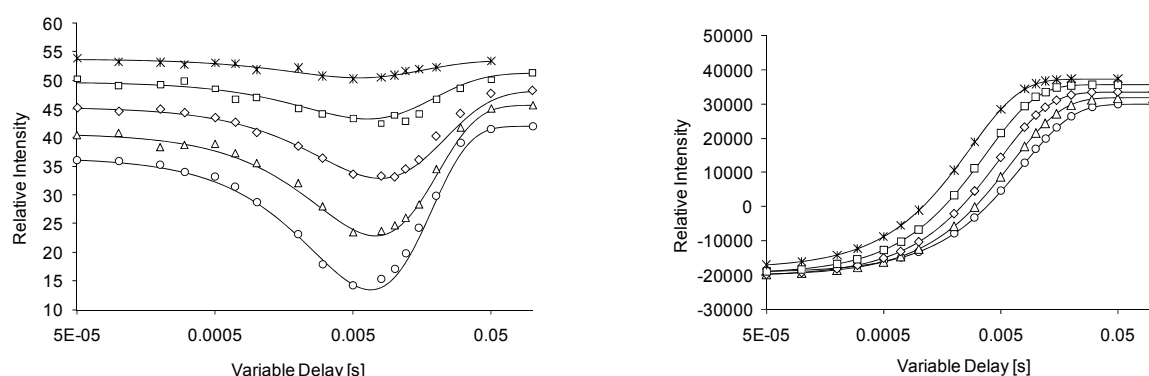


Fig. 1: Plots of peak intensities against the variable delays from  $^{17}\text{O}$ -NMR magnetization transfer experiments measured at various temperatures to determine the activation parameters for the oxygen exchange between the uranyl “yl”-oxygens and water. The curves show the intensity change of the inverted water signal (right) and the uranyl signal (left). The temperatures from top to bottom are 298, 308, 318, 328 and 338 K. The intensities are given in arbitrary units that reflect the relative ratio of the exchanging sites. The solid lines are generated by a non-linear fitting procedure of the experimental data. ( $[\text{UO}_2^{2+}]_{\text{total}} = 0.0315 \text{ M}$ ,  $[\text{TMA-OH}]_{\text{total}} = 2.91 \text{ M}$ ).

- [1] Szabó, Z.; Aas, W.; Grenthe, I. (1997) *Inorg. Chem.* 36, 5369.
- [2] Szabó, Z.; Grenthe, I. (2000) *I. Inorg. Chem.* 39, 5036.
- [3] Szabó, Z. (2000) *J. Chem. Soc., Dalton Trans.* 4242.
- [4] Szabó, Z., Grenthe I. (2007) *Inorg. Chem.* 46, 9372.
- [5] Tsushima, S. (2012) *Inorg. Chem.* 51, 1434.
- [6] Szabó, Z., Grenthe I. (2010) *Inorg. Chem.* 49, 4928.



## Actinide NMR research at Lawrence Livermore National Laboratory

H. Mason, S. Harley, P. Huang, S. Carroll, R. Maxwell, M. Zavarin, A. Kersting

Physical and Life Sciences Directorate, Lawrence Livermore National Laboratory, Livermore, CA, U.S.A.

As a part of the Transuranic Subsurface Transport Scientific Focus Area at Lawrence Livermore National Laboratory (LLNL), we are developing nuclear magnetic resonance (NMR) techniques focused on investigating geochemical and biogeochemical reactions with actinide species. The program builds upon the combined expertise of the group and has two major thrusts: 1) *The development of surface specific solid-state NMR techniques to investigate the sorption of actinide species to mineral surfaces;* 2) *The measurement of reaction rates of actinide solution species, and comparing these to rates calculated from ab-initio atomistic modeling.* The current status of this program has been benchmarking these techniques by investigating systems which allow safe technique development over a larger range of experimental conditions. This benchmarking has yielded results that will allow us to confidently extend these methods to systems containing low concentrations of actinide species. These goals are within reach at LLNL due to new capabilities in the NMR facility which allow us to investigate samples containing up to 10  $\mu\text{Ci}$  of ionizing radiation.

Many actinide species (e.g.  $\text{Pu}^{4+}$ ,  $\text{Pu}^{5+}$ , and  $\text{Np}^{5+}$ ) exhibit paramagnetic electronic ordering which can have a substantial effect on the NMR signal. Therefore, we have developed solid-state cross-polarization magic angle spinning (CP/MAS) NMR as a surface specific technique to probe the sorption of low loadings ( $1.6\text{-}54 \text{ nmol/m}^2$ ) of paramagnetic species ( $\text{Cu}^{2+}$  and  $\text{Ni}^{2+}$ ) to mineral surfaces. We used statistical methods to provide model-free analysis of the results from variable contact time  $^{29}\text{Si}\{^1\text{H}\}$  CP/MAS NMR spectra on amorphous silica which identified protonated and deprotonated silanol sites. These experiments established the deprotonated surface species as the preferential metal sorption site at pH 8, and show the ability to discern between precipitation of a separate phase and surface sorption. Additional experiments also proved the same results can be obtained under static (non-spinning) conditions, and can, therefore, be safely extended to systems containing low concentrations of paramagnetic actinide species such as  $\text{Pu}^{4+}$ . Experiments with trivalent lanthanide species ( $\text{Sm}^{3+}$  and  $\text{Eu}^{3+}$ ) are on-going to further constrain the effective concentration and pH range over which this method is valid.

We also are building on existing expertise in measuring ligand exchange and reaction rates of actinide species using solution state NMR spectroscopy. This work extends previous work in uranyl systems where both the apical oxygen and carbonate counter ion exchange mechanisms were investigated as a function of hydrostatic pressure and temperature. These types of measurements allow for the determination of the activation volume for the exchange process where the magnitude of this value elucidates the mechanism by which the transition state occurs. This is one of the few techniques that allows for direct observation of associative vs. dissociative exchange mechanisms. Further, the unique electronic environment of actinide systems allows for a wide range of NMR techniques to monitor exchange rates. In diamagnetic systems magnetization exchange through the use of tailored excitation allows for the direct detection of exchange rates. In paramagnetic systems it is more difficult to directly monitor exchange; however, the effect of exchange on line widths is well understood and will allow for quantifiable rate determination. Therefore we have accumulated the expertise required to investigate actinide exchange processes at LLNL, and we are moving forward with similar experiments designed to measure the exchange rates for actinide species such as  $\text{Np}^{5+}$ ,  $\text{Pu}^{4+}$ ,  $\text{Pu}^{5+}$ , and  $\text{Th}^{4+}$ . By analyzing such reaction rates we gain insight into the limiting reactions which may govern the reactions of these species with minerals surfaces, and complex organic species.

Prepared by LLNL under Contract DE-AC52-07NA27344. LLNL-ABS-543379.

# The specific sorption of Y(III) onto $\gamma$ -alumina: a solid-state $^1\text{H}$ MAS NMR study

N. Huittinen,<sup>1</sup> P. Sarv,<sup>2</sup> J. Lehto<sup>1</sup>

<sup>1</sup> Laboratory of Radiochemistry, Department of Chemistry, University of Helsinki, Finland

<sup>2</sup> Institute of Chemical Physics and Biophysics, Tallinn, Estonia

The specific sorption of the diamagnetic Y(III) ion, here taken as an analogue to the trivalent actinides, on the mineral phase  $\gamma$ -alumina ( $\gamma\text{-Al}_2\text{O}_3$ ) was investigated with solid state  $^1\text{H}$  MAS NMR spectroscopy. The aim of our study was to detect and identify those hydroxyl groups at the  $\gamma$ -alumina surface that participate in the complexation reaction of the trivalent metal. NMR samples were prepared under constant pH conditions,  $8.00 \pm 0.05$ , using a constant mineral concentration of 4 g/L and yttrium concentrations ranging from  $6.58 \cdot 10^{-7}$  M to  $3.95 \cdot 10^{-4}$  M.  $^1\text{H}$  NMR experiments were performed on a Bruker Avance III NMR spectrometer. The  $^1\text{H}$  resonance frequency was 800.13 MHz corresponding to a magnetic field of 18.8 T. The recorded proton spectra of all samples showed very remote differences

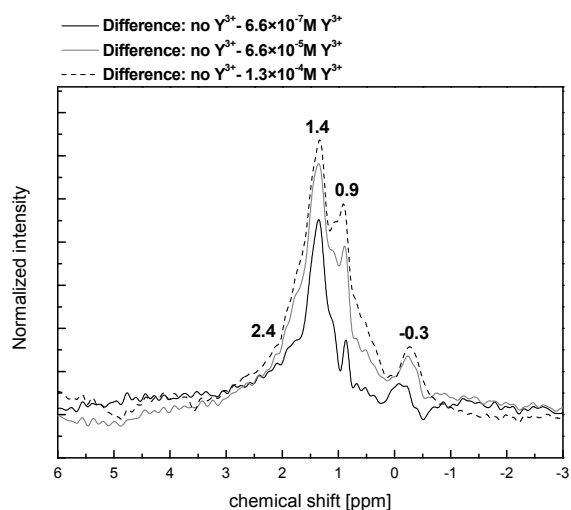


Fig. 1:  $^1\text{H}$  difference spectra produced by subtracting proton spectra of  $\gamma$ -alumina samples with  $\text{Y}^{3+}$  from the clean  $\gamma$ -alumina spectrum.

as a function of increasing metal-ion concentration. Therefore, in order to see the spectral changes induced by the sorption reaction itself difference spectra were produced by subtracting the proton spectra of the samples containing diamagnetic yttrium from that of the unreacted  $\gamma$ -alumina mineral, Fig. 1. In the difference spectra clear features at approximately 1.4, 0.9,  $-0.1$  and  $-0.3$  ppm can be distinguished. We based our interpretation of the proton signals on the so called Knözinger and Ratnasamy model of the gamma alumina surface [1]. According to this model, five distinct hydroxyls on the ideal surface planes of  $\gamma$ -alumina exist. These are presented in Fig. 2. The acidity of these protons increases from I to III. The most basic protons belonging to hydroxyls of type Ia or Ib show up in our difference spectra with chemical shifts below 0.0 ppm. These protons are being removed by complexation of the yttrium ion along with the bridging hydroxyls of type IIa and IIb that we assigned the peaks with chemical shifts around 1 ppm to. The most acidic hydroxyl group (type III) would appear in the proton spectra with chemical shifts above 2 ppm. Such proton signals cannot be witnessed in our difference spectra, indicating that this surface hydroxyl group does not participate in the complexation reaction.

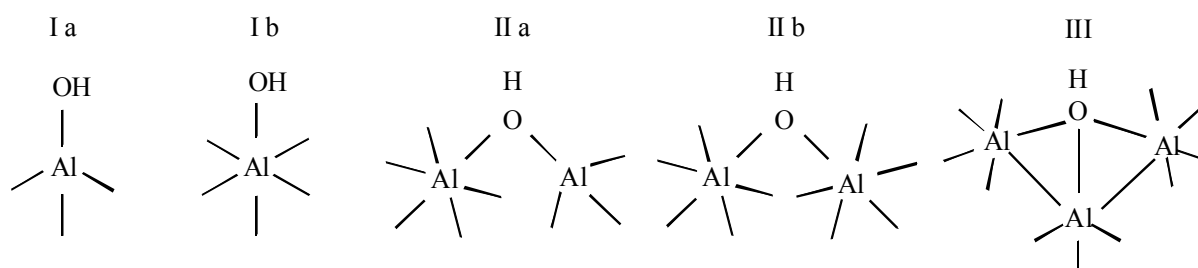


Fig. 2: Five different surface hydroxyl groups are defined for  $\gamma$ -alumina according to the Knözinger and Ratnasamy model [1].

[1] Knözinger, H. and Ratnasamy, P. (1978) Catal. Rev. 17, 31-70.

## Eu<sup>3+</sup> in NMR spectroscopy – A helpful tool in tracking binding sites

J. Kretzschmar, A. Barkleit, V. Brendler

Helmholtz-Zentrum Dresden–Rossendorf e.V., Institute of Resource Ecology, Dresden, Germany

Lanthanides have become a useful tool in NMR spectroscopy within the last 40 years. Due to their paramagnetic properties they can be utilized as probes to determine the binding sites of biologically or environmentally relevant organic molecules as they cause significant line broadenings and / or paramagnetic induced shifts [1-3].

Actual research deals with the interactions, thermodynamic and kinetic behaviour of actinides and biomolecules. Lanthanides can easily be used as inactive analogues for trivalent actinides in consequence of their similar chemistry.

Glutathione (GSH, Fig. 1) is a high concentrated intracellular reducing agent, playing a major role in detoxification processes. Important targets are electrophiles such as heavy metal ions. With its high natural abundance, different functional groups and reducing ability, this tripeptide provides outstanding characteristics for actinide complexation research. Furthermore, because of the small size, it is well suited as a model molecule in NMR spectroscopy.

As shown in Fig. 2, the <sup>1</sup>H-NMR signals are shifted and broadened by the paramagnetic induced shift of the Eu<sup>3+</sup> with their 4f<sup>6</sup> electron configuration. These interactions between nuclear spins and electron unpaired spins exhibit a strong distance dependency. The closer the binding site, the bigger the shift of the signals.

From these findings, it can be derived that the carboxylate group of the glutamate residue is the most potential binding site at pH 2.9. According to the aqueous speciation, the glycine carboxylic acid group is only partially deprotonated and therefore less involved in complexation. The thiol group does not interact with the metal ion.

Acknowledgement: We thank Dr. Erica Brendler, Technische Universität Bergakademie Freiberg, for

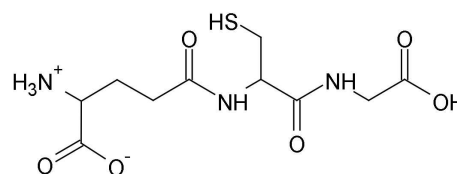


Fig. 1: Lewis structure of glutathione at pH 2.9.

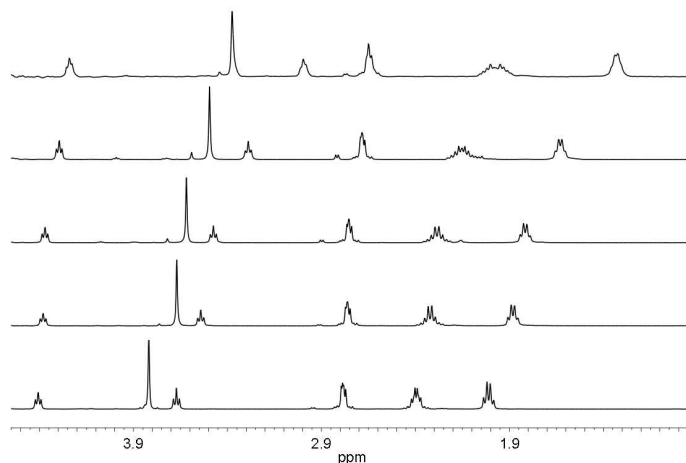


Fig. 2: <sup>1</sup>H-NMR spectra of 300 mM glutathione containing different Eu<sup>3+</sup> concentrations (from bottom to top: 0, 30, 50, 100 and 300 mM) at pH 2.9.

providing the possibility to acquire 2D-NMR spectra.

- [1] Hinckley, C. C. (1969) *J. Am. Chem. Soc.* 91, 5160-5162.  
 [2] Gansow, O. A. et al. (1971) *J. Am. Chem. Soc.* 93, 4295-4297.  
 [3] Bertini, I. et al. (2001) in: *Current methods in inorganic chemistry, Solution NMR of paramagnetic molecules*, Vol. 2, Elsevier, Amsterdam.

## In situ identification of the U(VI) surface speciation on iron oxide phases by ATR FT-IR spectroscopy

H. Foerstendorf, K. Heim, N. Jordan

Helmholtz-Zentrum Dresden-Rossendorf, Institute of Resource Ecology, Dresden, Germany

The identification of the molecular interactions occurring at solid-liquid interfaces is of great significance to the assessment of the migration behavior of heavy metal ions in the environment. In particular, the dissemination of radioactive metals, such as uranium (U), in soils and aquifers is determined by sorption and desorption processes at mineral surfaces.

Information of the molecular structures of the sorption complexes can be obtained by vibrational spectroscopy. The application of the Attenuated Total Reflection (ATR) technique in combination with a flow cell experiment potentially provides insights into the dynamic processes occurring during complex formation at the solid-liquid interface [1]. This technique allows an on line monitoring of the sorption processes with a time resolution in the sub minute range and under selective conditions approaching near environmental relevant conditions [2,3]. In particular, the variation of selective experimental parameter, e.g. pH,  $c(\text{UO}_2^{2+})$  or  $p\text{CO}_2$ , and the selection of modified solid phases are expected to generate selective spectral changes which potentially facilitate the identification of molecular features.

In this work, we provide vibrational spectroscopic data from binary and ternary U(VI) surface species on iron oxide mineral phases in the absence and presence of atmospherically derived  $\text{CO}_2$ , respectively. In a comparative study of two iron oxide phases, namely ferrihydrite and maghemite, the different character of sorption complexes can be spectroscopically identified. From the frequency of the  $\nu_3(\text{UO}_2)$  mode, the formation of different types of surface species, that is inner- and outer-sphere complexes, can be derived. This is corroborated by time-resolved spectra of the sorption step and of the subsequently induced desorption process. From the time courses of these reactions, a first assignment to the different types of surface species predominantly formed at the different mineral surfaces can be given.

Results from the ternary sorption systems (U(VI)/atm.  $\text{CO}_2$ /iron oxide phase) demonstrate significantly different affinities of the carbonate ions to the different mineral phases. While atm.  $\text{CO}_2$  forms binary and ternary sorption species on ferrihydrite in the absence and presence of U(VI), respectively, only ternary uranyl carbonate species were observed at the maghemite-water interface.

---

[1] Voegelin, A. et al. (2003) *Environ. Sci. Technol.* 37, 972-978.

[2] Müller, K. et al. (2012) *Geochim. Cosmochim. Acta* 76, 191-205.

[3] Foerstendorf, H. et al. (2012) *J. Colloid Interf. Sci.* 377, 299-306.

## Short-range order investigations of $LnPO_4$ using Raman spectroscopy

J. Heuser, H. Schlenz, D. Bosbach

Forschungszentrum Jülich GmbH, Institute of Energy and Climate Research – IEK-6: Nuclear Waste Management and Reactor Safety, Jülich, Germany

Lanthanide ( $Ln$ )-orthophosphate- and -phosphosilicate-ceramics represent promising materials for the immobilization of radionuclides like U, Pu and/or minor actinides resulting from the reprocessing of spent fuel. For the conditioning of radioactive waste, ceramics are a good alternative to the widely used borosilicate-glasses, especially for the conditioning of actinides. In terms of their crystal structures, e. g. monazite-type ceramics offer outstanding properties concerning chemical durability and radiation resistance [1, 2] which can also be confirmed by their natural analogues.

Therefore, we synthesized and characterized monazite-type solid solutions of sixteen different chemical compositions  $Sm_{1-x}Ce_xPO_4$  in the range  $0 \leq x \leq 1$ . Keeping in mind the efficiency of a future industrial synthesis we have chosen a Sm-component to make use of the relatively low melting point of  $SmPO_4$  ( $T_m = 1916$  °C) [3]. The products synthesized by hydrothermal synthesis (220 °C, ~25 bar) were thermally analyzed by coupled TG-DSC, chemically by EDX and structurally by XRD (Rietveld) and Raman spectroscopy after sintering at  $T = 1200$  °C. Raman data for the endmembers  $SmPO_4$  and  $CePO_4$  [4-6] are already available and are in good agreement to our own data. Ruschel et al. [6] published the value for  $\nu_1$  of the chemical composition  $Sm_{0.5}Ce_{0.5}PO_4$  that fits to our data in an excellent manner. New Raman data for the solid solution will be presented. Figure 1 shows the stretching vibrations  $\nu_1$  and  $\nu_3$  of the  $PO_4$ -tetrahedra exemplary for five compositions  $LnPO_4$  ( $Ln = Sm, Ce$ ).

Beside this, metastable monoclinic  $LnPO_4$  ( $Ln = Tb, Dy$ ) were prepared by precipitation. New Raman data could be generated. To the best of our knowledge no Raman data for these phases exist so far under standard conditions. Stavrou et al. [7] performed in situ Raman measurements of tetragonal  $TbPO_4$  and observed a transformation into the monoclinic phase at pressures of about 9.5 GPa.

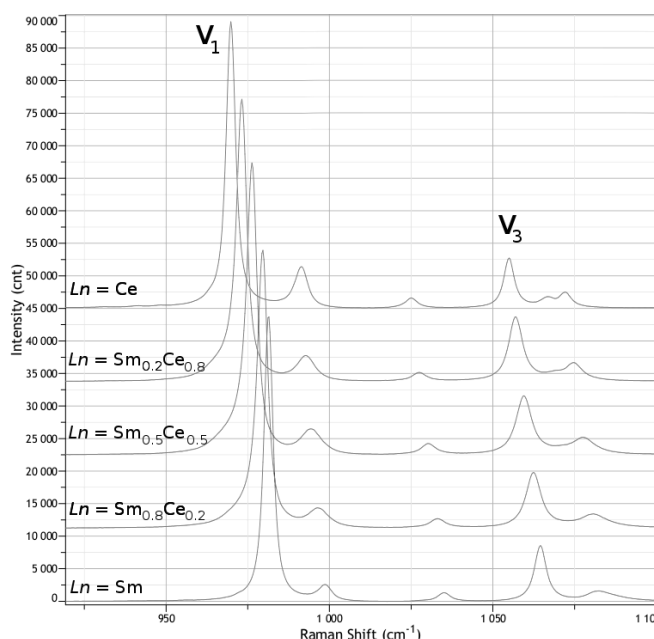


Fig. 1: Close up of five different Raman spectra of  $LnPO_4$  ( $Ln = Sm, Ce$ ) showing the stretching vibrations  $\nu_1$  and  $\nu_3$  of the  $PO_4$ -tetrahedra.

- [1] Lumpkin (2006) Elements 2, 365.
- [2] Meldrum et al. (1997) Physical Review B 56, 13805.
- [3] Hikichi and Nomura (1987) Journal of the American Ceramic Society 70, C-252.
- [4] Begun et al. (1981) Journal of Raman Spectroscopy 11, 273–278.
- [5] Silva et al. (2006) Optical Materials 29, 224-230.
- [6] Ruschel et al. (2012) Mineralogy and Petrology 105, 41-55.
- [7] Stavrou et al. (2008) Journal of Physics: Conference Series 121, 042016.

## X-ray reflectivity investigations on the interfacial reactivity of actinides

M. Schmidt,<sup>1</sup> S. S. Lee,<sup>2</sup> R. E. Wilson,<sup>2</sup> K. E. Knope,<sup>2</sup> L. Soderholm,<sup>2</sup> P. Fenter<sup>2</sup>

<sup>1</sup> Karlsruhe Institute of Technology (KIT), Institute for Nuclear Waste Disposal (INE), Karlsruhe, Germany

<sup>2</sup> Chemical Sciences and Engineering Division, Argonne National Laboratory, Argonne, IL, U.S.A.

The actinides' interaction with mineral phases is of foremost importance for the safety assessment of nuclear waste disposal sites as well as remediation efforts in legacy contamination sites [1, 2]. Actinide – mineral interactions will control the mobility and transport behavior of the actinides and thus their hazard potential in the biosphere. The complex nature of the aqueous – mineral interface system in conjunction with the multifaceted aqueous chemistry of plutonium requires techniques that are capable of selectively probing the complete near-interface regime while yielding molecular-level information of the structures and reactions in this system.

Application of X-ray reflectivity techniques offers exciting new possibilities for the study of interfacial systems. By combination of crystal truncation rod (CTR) analysis and resonant anomalous X-ray reflectivity (RAXR) full interfacial structures, from subsurface relaxation to the bulk liquid, can be elucidated with elemental selectivity [3]. Thus, the techniques allow the simultaneous *in situ* characterization of (structurally) incorporated, inner sphere, and outer sphere sorption species.

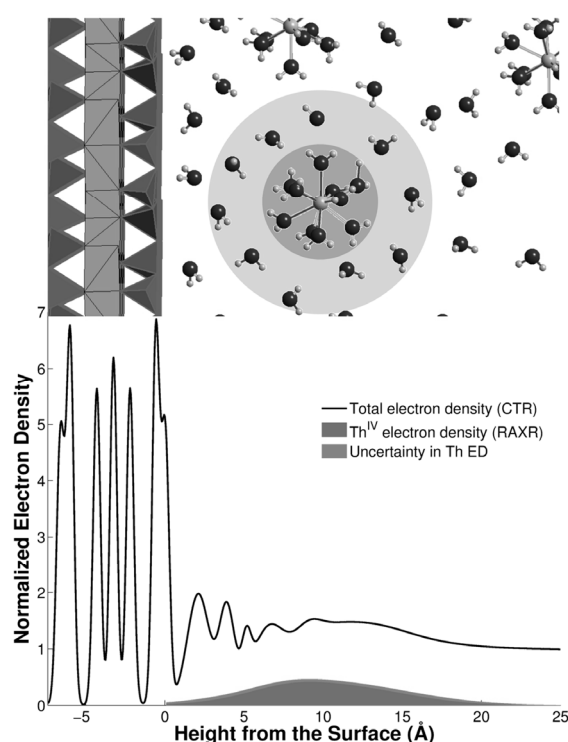


Fig. 1: Total electron density profile derived from CTR (black line) and Th electron density distribution derived from RAXR (grey area). The electron density is normalized to that of bulk water  $\rho(\text{bulk water}) = 0.33e^{-}/\text{\AA}^3$ , so that the normalized ED of water is 1.00. The average height of muscovite surface oxygens is set to be  $z = 0 \text{ \AA}$ . For illustration purposes a schematic representation of species contributing to the observed ED is shown in the upper part of the figure [4].

Recent results on the interaction of actinides (Th and Pu) with the (001) basal plane of muscovite from *in situ* surface X-ray diffraction experiments (CTR and RAXR) will be presented. The reactivity of the elements will be discussed in connection to their aqueous chemistry and with respect to implications for their transport behavior in geochemical system.

[1] De Paolo, D. J. *Basic Research Needs for Geosciences: Facilitating 21st Century Energy Systems*, 2007, U.S. Department of Energy, Office of Basic Energy Sciences: Bethesda, MD.

[2] Geckeis, H. and Rabung, T. (2008) *Journal of Contaminant Hydrology* 102, 187-195.

[3] Fenter, P. (2002) *Reviews in Mineralogy and Geochemistry* 49, 149-220.

[4] Schmidt, M. et al. (2012) *Geochimica et Cosmochimica Acta* 88, 66-76.

## Study of uranyl and thorium complexation with phosphorylated biomolecules.

G. Creff,<sup>1,2,3</sup> S. Safi,<sup>1</sup> A. Jeanson,<sup>1</sup> J. Roques,<sup>1</sup> P. Lorenzo Solari,<sup>4</sup> E. Simoni,<sup>1</sup>  
C. Vidaud,<sup>2</sup> C. Den Auwer<sup>3</sup>

<sup>1</sup> Institut de Physique Nucléaire d'Orsay (IPNO), UMR 8608, Orsay, France

<sup>2</sup> Laboratoire d'étude des protéines cibles, DSV/IBEB/SBTN, CEA Centre de Marcoule, France

<sup>3</sup> Institut de Chimie de Nice (ICN), UMR 7272, Université Nice Sophia Antipolis, Nice, France

<sup>4</sup> Synchrotron SOLEIL, St. Aubain, France

At the molecular scale, the study of actinides in interaction with biological molecules is essential in order to obtain a better description of the toxicological processes associated with these elements. Despite a significant number of studies on the interaction of these elements with living organisms, most of the available data are from a physiological point of view of the toxicology. In fact, there is very few data concerning the *bioactinidic* approach at the molecular level. Even so, the acquisition of structural information on complexes of radionuclides with molecules of biological interest (proteins) is essential to have a better understanding of the mechanisms of transfer (transport, storage and absorption) of these elements in the living cycles.

Among the different techniques used to probe the structure of the complexes between actinides and their biological environment (molecule, protein, matrix), X-ray absorption spectroscopy is a preferential tool. By probing the local environment of the cation which is targeted, this spectroscopy allows to overcome the size, chemical and physical forms of the considered system.

We have selected the interaction of uranyl and thorium with biological molecules of increasing complexity: an amino acid (p-Ser) and a phosphorylated peptide (His-p-Ser-Asp-Glu-p-Ser-Asp-Glu-Val) biomimetic of osteopontin (OPN) which is a hyper-phosphorylated protein particularly important in the process of osteogenesis and which is also studied in this work. The study of the interaction of Th(IV) with the same peptides allowed us to better understand the fate of actinides(IV) using a less radioactive surrogate with simpler redox chemistry than for the other An(IV) (such as Pu).

Molecular models of the different complexes: actinides-pSer, actinides-peptide and actinides-OPN are proposed (Fig. 1a) on the basis of EXAFS data (Fig. 1b) in combination with quantum chemical calculations.

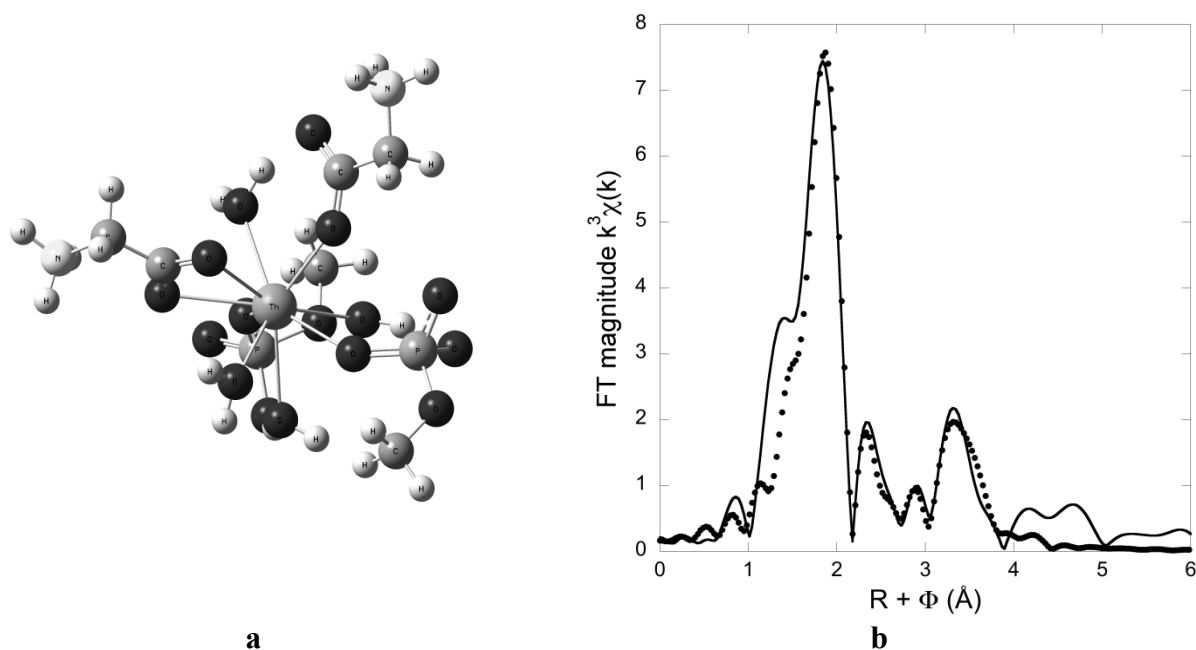


Fig. 3: Fragment of the Th-P-Ser hypothetical adduct (a); FT of the EXAFS spectrum of the Th-P-Ser complex (a). Straight line = experimental, dots = fit.

## Actinide speciation with high-energy resolution X-ray absorption spectroscopy and inelastic X-ray scattering

T. Vitova,<sup>1</sup> R. Caciuffo,<sup>2</sup> M. A. Denecke,<sup>1</sup> F. Huber,<sup>1</sup> T. Prüßmann,<sup>1</sup> J. Rothe,<sup>1</sup> T. Schäfer,<sup>1</sup> H. Geckeis<sup>1</sup>

<sup>1</sup> Karlsruhe Institute of Technology (KIT), Institute for Nuclear Waste Disposal (INE), Karlsruhe, Germany

<sup>2</sup> Institute for Transuranium Elements, Karlsruhe, Germany

High-energy resolution X-ray emission spectroscopy (HRXES) [1, 2] and non-resonant inelastic X-ray scattering (NIXS) [3] combined with quantum theoretical tools are gaining importance for understanding electronic and coordination structures of actinide (An) materials. HRXES is successfully used to remove lifetime broadening by registering the partial fluorescence yield emitted by the sample, thereby yielding highly resolved X-ray absorption near edge structure spectra (PFY-XANES), which often display resonant features not observed in conventional XAS [1, 2]. Resonant X-ray emission spectroscopy (RXES) and resonant inelastic X-ray scattering (RIXS) are applied to obtain bulk electronic configuration information in solids, liquids and gases. NIXS measures successfully, e.g., An  $O_{4,5}$  edge [3] and K edge XAS spectra of low  $Z$  elements in An materials. The high penetration depth of hard X-rays employed in NIXS ( $> 10$  keV) enables flexible containment concepts, facilitating investigations of radioactive materials in the liquid phase or under extreme conditions.

We demonstrate the structural characterization capabilities of these novel techniques by discussing results from both model [3, 4] and complex uranium materials [4]. For example, we observe U  $L_3$  PFY-XANES of U(VI) in a series of minerals to be more sensitive to changes in local coordination environment and crystal structure compared to U  $M_4$  PFY-XANES and U valence band RIXS (VB-RIXS). In contrast, U  $M_4$  PFY-XANES has higher sensitivity to changes in oxidation state compared to U  $L_3$  PFY-XANES. These results from reference systems are used to identify U(VI) as the dominant species in uranium sorbed onto magnetite ( $Fe_3O_4$ ) and maghemite ( $\gamma-Fe_2O_3$ ) nano-particles [4]. The NIXS technique and its advantages compared to standard XAS will be outlined by presenting examples of uranium [3] reference materials. Experimental results are supported by *ab initio* calculations (DFT, FDMNES, FEFF9).

We gratefully acknowledge Karlsruhe Institute of Technology and Helmholtz Association of German Research Centers (VH-NG-734) for the financial support. We thank ESRF and ANKA for the granted beamtime.

---

[1] Vitova, T. et al. (2010) Phys. Rev. B 82, 235118;

[2] Vitova T. et al. (2010) IOP Conf. Ser.: Materials Science and Engineering 9, 012053.

[3] Caciuffo, R. et al. (2010) Phys. Rev. B 81, 195104.

[4] Vitova, T. et al. (2011) ESRF user report.



## XAS study of actinide and lanthanide hexacyanoferrates

T. Dumas,<sup>1,2</sup> C. Den Auwer,<sup>3</sup> C. Fillaux,<sup>1</sup> D. Guillaumond,<sup>1</sup> D. Shuh,<sup>4</sup> T. Tyliczszak,<sup>4</sup>  
A. C. Scheinost,<sup>2</sup> S. Conradson<sup>5</sup>

<sup>1</sup> CEA, Nuclear Energy Division, RadioChemistry and Process Department, Bagnols sur Cèze, France

<sup>2</sup> Helmholtz-Zentrum Dresden-Rossendorf, Institute of Resource Ecology, Dresden, Germany

<sup>3</sup> University of Nice Sophia Antipolis, Nice Chemistry Institute, Nice, France

<sup>4</sup> Advanced Light Source Division, Lawrence Berkeley National Laboratory, Berkeley, CA, U.S.A.

<sup>5</sup> Los Alamos National Laboratory, Material Science and Technology Division, Los Alamos, NM, U.S.A.

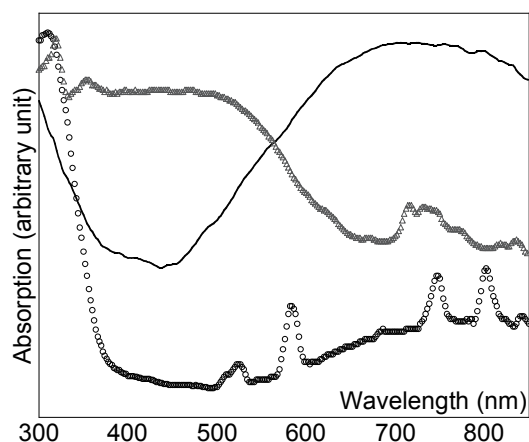


Fig. 1: Solid state UV-vis spectrum of prussian blue (black line), Nd (black circle) and Np (grey triangle) ferrocyanide adducts. The intermetallic charge transfer band appears only with prussian blue (730 nm) and Np ferrocyanide (470).

Hexacyanoferrate ligands form, with actinides, molecular solids derived from prussian blue. Transition metal prussian blue analogs family is known to foster long-range magnetic ordering at high temperature and specific optical characteristics (intense charge transfer band, Robin&Day class II) due to its specific metal-metal electronic exchange through the cyanide-bridge [1]. Structurally speaking, the 3d prussian blue derivatives form cubic phase structures when lanthanides and actinides form, hexagonal phases (nine coordinated) and orthorhombic phases (eight coordinated) [2]. From an electronic point of view, no intervalence charge transfer has been observed in the corresponding optical spectrum of the lanthanides compounds (Robin&Day class I), in agreement with ionic character of the lanthanide bonding. On the contrary, the actinides (oxidation state +III and +IV) analogs presents optical characteristics similar to the transition metals (intense charge transfer band, Robin&Day class II) as shown in Fig. 1. Considering this properties, the ferrocyanide ligand seems to be an ideal candidate to foster electronic delocalization resulting in potential covalent character in actinide bonding in comparison to lanthanides. The aim of this work was to develop an experimental and theoretical approach in order to characterize the intramolecular interactions between actinide and lanthanide elements (La, Nd, Eu, Th, U, Np, Pu) and the ferrocyanide ligand. Experiments are based on XAS spectroscopy performed at the iron L<sub>2,3</sub>-edges, the carbon and nitrogen K-edges (Fig. 2), together with the actinides N<sub>4,5</sub>- and lanthanides M<sub>4,5</sub>-edges which provide respective information on unoccupied iron 3d orbitals, nitrogen and carbon 2p orbitals and actinide 5f orbitals. XAS spectra are then confronted to DFT calculations in order to link experimental and theoretical results. As a last step the Mulliken charges obtained by DFT are used in the FDMNES program in order to simulate experimental edges. Using a phenomenological approach, a clear distinctive behaviour between actinides and lanthanides has been shown (Fig. 2) and between the actinides itself. Then the theoretical approach has shown more specifically the effect of covalency in the actinide-ferrocyanide bond. More specifically,  $\pi$  interactions with 5f orbitals were underlined by both theoretical and experimental methods and can be involve in the observed distinctive optical behaviour of the actinides compounds.

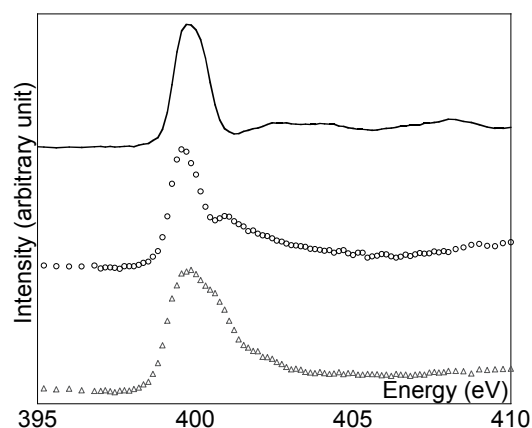


Fig. 2: Nitrogen K-edge of K (black line), Nd (black circle) and Np (grey triangle) ferrocyanides, representative of the cyano  $\pi^*$  orbitals, involved in chemical bonding.

[1] Robin, M. B. and Day, P. (1967) Adv. Inorg. Chem. Radiochem. 10, 247.

[2] Dupouy, G. et al. (2011) Eur. J. Inorg. Chem. 10, 1560-1569.

## Uranium(IV) luminescence: new tricks for an old dog

R. J. Baker,<sup>1</sup> E. Hashem,<sup>1</sup> J. A. Platts,<sup>2</sup> A. Kerridge<sup>3</sup>

<sup>1</sup> School of Chemistry, Trinity College, Dublin, Dublin 2, Ireland

<sup>2</sup> School of Chemistry, Cardiff University, Park Place, Cardiff, CF10 3TB, UK

<sup>3</sup> Department of Chemistry, University College London, London, UK

In order to fully assess any technologies for the treatment of nuclear waste, it is essential to understand the role of the 5f and 6d orbitals in bonding to chelating ligands. Therefore, the electronic structure of uranium in all oxidation states is important to understand, and predict, factors that may influence this bonding. We have taken a multi-technique synergistic approach to examine simple coordination compounds of uranium(IV) and will present our recent results here.

Whilst the photophysics of the uranyl ( $\text{UO}_2^{2+}$ ) moiety has been well studied, [1] the lower oxidation states have not been examined in much detail. There is only one report of fluorescence from a U(IV) compound in aqueous solution. [2] We will detail our studies on the photophysics of selected uranium(IV) compounds,  $[\text{Li}(\text{THF})_4][\text{UCl}_5(\text{THF})]$ ,  $[\text{Et}_4\text{N}]_2[\text{UCl}_6]$  and  $[\text{Et}_4\text{N}]_4[\text{U}(\text{NCS})_8]$ , [3] that display emissions that originate from excitation into the f-orbital manifold.

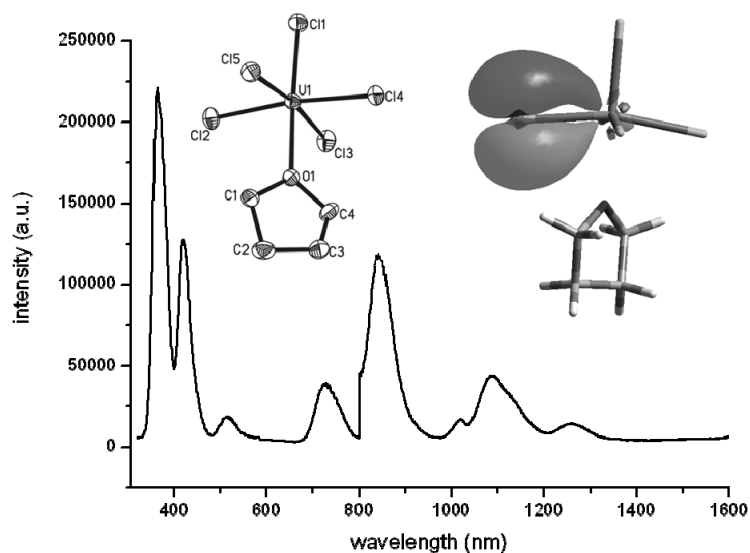


Fig. 1: Emission spectrum of  $[\text{Li}(\text{THF})_4][\text{UCl}_5(\text{THF})]$  in THF ( $\lambda_{\text{exc}} = 303 \text{ nm}$ ).  
Insert: X-ray structure and NBO representation of bonding in this compound.

A comprehensive computational study on some of these compounds will also be presented. We have assigned the absorption spectrum of  $[\text{Li}(\text{THF})_4][\text{UCl}_5(\text{THF})]$  and  $[\text{Et}_4\text{N}]_2[\text{UCl}_6]$  using spin-orbit coupled CASPT2 calculations. The bonding in this compound has also been examined and these calculations show substantial overlap between the Cl 3p orbitals and U 5f and 6d orbitals.

[1] Morss, L. R.; Edelstein, N. M. and Fuger, J. (eds.) (2010), *The Chemistry of the Actinide and Transactinide Elements*, Springer, Dordrecht, The Netherlands.

[2] Kirishima A., et al. (2003) *Chem. Commun.* 910-911.

[3] Countryman, R. and McDonald, W. S. (1971) *J. Norg. Nucl. Chem.* 33, 2213-2216.

## Quantum mechanical and spectroscopic investigation of the corundum water interface and sorption of lanthanides and actinides on this surface

R. Polly, B. Schimmelpfennig, M. Flörsheimer, T. Rabung, T. Kupcik, R. Klenze, H. Geckeis

Karlsruhe Institute of Technology (KIT), Institute for Nuclear Waste Disposal (INE), Karlsruhe, Germany

We present a joint theoretical and experimental investigation of the interaction of water and trivalent lanthanides/actinides with the corundum (001) and (110) surface. Theoretically, we employed ab initio methods, such as Møller Plesset perturbation theory of second order (MP2) or Coupled Cluster singles doubles with triple corrections (CCSD(T)), or Density Functional Theory (DFT) with different functional and basis sets. Experimentally, surface sensitive Sum Frequency spectroscopy (SF) was employed to probe the hydrated corundum surface and Time Resolved Laser Fluorescence Spectroscopy (TRLFS) was applied to investigate the actinide complexes formed on the two corundum surfaces.

As a preparation for both studies we determined in a thorough benchmark study, which showed that a combination of DFT functional and basis set are an appropriate choice to obtain accurate structures and frequencies. For this we compared DFT and ab initio results for small subsystems and assessed the accuracy of the DFT results. Based on this benchmark studies we carried out the rest of this study with the BP86 functional and the cc-pVDZ basis set.

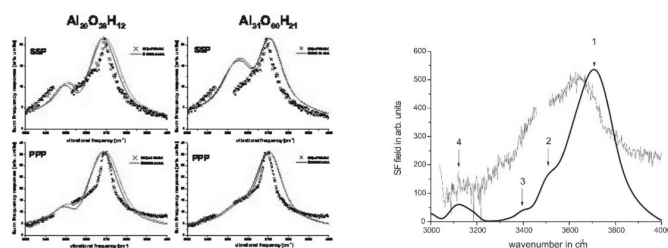


Fig. 1: Simulations of the SF spectra of the corundum (001) and (110) surface.

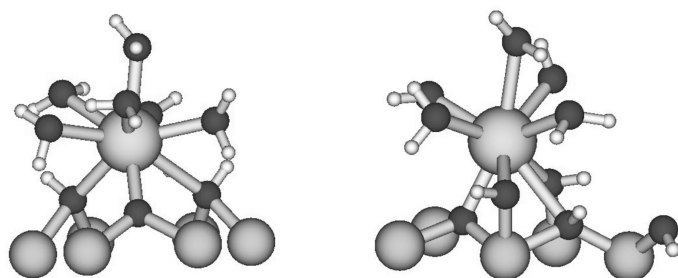


Fig. 2: Tri- and tetradentate inner-sphere complexes at the corundum (001) and (110) surfaces.

radendate inner-sphere complexes are formed at the corundum (110) surface. The results are consistent with TRFLS studies by T. Rabung *et al.* [5].

In summary, we could show the great advantage of a joint theoretical and experimental investigation. Due the consistency and agreement of the data, we understand the hydrated corundum surfaces and sorption of metal ions at these surfaces much better.

For both the corundum (001) [1] and (110) [2] surfaces we used cluster models which represent realistic models for the hydrated surfaces. We optimized the structures of these clusters with DFT using the BP86 functional and the cc-pVDZ basis set. In a second step the harmonic frequencies of the surface aluminol groups were determined. They are used to simulate the experimentally obtained SF spectra (Fig. 1). The excellent agreement between the theoretical and experimental results allowed an assignment of the observed species and a characterization of the surface aluminol groups on both surfaces.

Furthermore, we determined the structure of the inner-sphere complexes of trivalent lanthanides and actinides at the corundum (001) [3] and (110) [4] surfaces. While the metal cation is bonded to three surface groups (tridentate inner-sphere complex) at the corundum (001), tetradentate inner-sphere complexes are formed at the corundum (110) surface.

[1] Polly, R. *et al.* (2009) *J. Chem. Phys.* 130, 064702.

[2] Polly, R. *et al.*, in preparation.

[3] Polly, R. *et al.* (2011) *Rad. Chim. Acta* 98, 627.

[4] Polly, R. *et al.*, in preparation.

[5] Rabung, T. *et al.* (2004) *J. Phys. Chem* 108, 17160.

## Experimental and theoretical structures of actinide ions with oxygen-donor ligands in organic solution

D. Guillaumont,<sup>1</sup> C. Fillaux,<sup>1</sup> K. Ribokaité,<sup>1</sup> S. De Sio,<sup>1</sup> C. Den Auwer,<sup>2</sup> P. Guilbaud,<sup>1</sup> P. Moisy<sup>1</sup>

<sup>1</sup> CEA, Nuclear Energy Division, Radiochemistry & Processes Department, Bagnols sur Cèze, France

<sup>2</sup> Nice Sophia Antipolis University, Chemistry Institute of Nice, Nice, France

Actinide ions in solution present a wide variety of coordination environments which are very often unknown even though a detailed knowledge of their molecular structures and dynamics in a given media is essential to predict their behavior and to control a ligand affinity toward the metal ions. Understanding the structure of actinide ions in organic solution is of particular interest in the development of effective solvent extraction separations for waste remediation in advanced nuclear fuel cycles.

In the present study, we have combined theoretical calculations and experimental measurements in order to determine the preferred structures of actinide ion complexes in the presence of neutral oxygen-donor ligands and nitrate ions in organic solution. The investigated systems are representative of those encountered in actinide liquid-liquid extraction processes. In such systems, precise structural information is often lacking because of the difficulty to resolve the structures purely from experimental data.

Theoretical chemistry calculations were used to construct and optimize molecular structures corresponding to metal-ion complexes that may form in the organic solution. EXAFS and IR-Raman were simulated for the optimized structures. By comparing the simulated spectra with experimental EXAFS and IR-Raman spectra, we are able to deduce the coordination environments of a series of actinide(IV) and (VI) ions in the systems of interest.

## Fluorescent complexes of tripodal amides: TRLFS and multinuclear NMR spectroscopic studies

J. März, M. Abraham, A. Heine, Ke. Gloe, K. Gloe

Dresden University of Technology, Department of Chemistry and Food Chemistry, Dresden, Germany

Designing ligands for lanthanide and actinide ion complexation is of much interest according to their importance in the nuclear fuel cycle as well as for applications as luminescent probes in medicine or as catalysts [1,2]. Ligands like malonamides are used for separation of lanthanides and actinides in extraction processes [2].

Here, we report the synthesis of novel carboxamides which can act as N,O donor ligands for *d*- and *f*-block elements. The ligand **L1** itself shows a triple helical hydrogen bond arrangement in the solid state (Fig. 1).

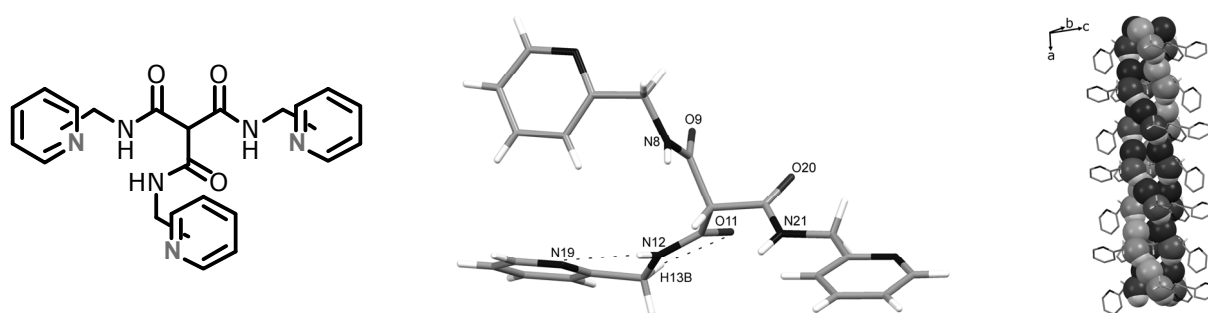


Fig. 1: Picolyl substituted Methanetricoxamides **L1-3** (left), X-ray structure of *N,N',N''*-Tris(2-picolyl)methanetricoxamide (**L1**) (middle) and triple helical hydrogen bond arrangement in solid **L1** (right).

The tendency to self-organization provides an indication of biological activity concerning metal ion complexation as well.

The coordination behavior of these tricarbonylamides to lanthanides and actinides is analyzed by  $^1\text{H}$  NMR, UV-vis and fluorescence spectroscopy. The fluorescence intensities of rare earth metal complexes of **L1** obtained by TRLFS spectra are showing a strong dependency on the metal ion. Though the wavelength of emission is only reliant on the solvent (Fig. 2).

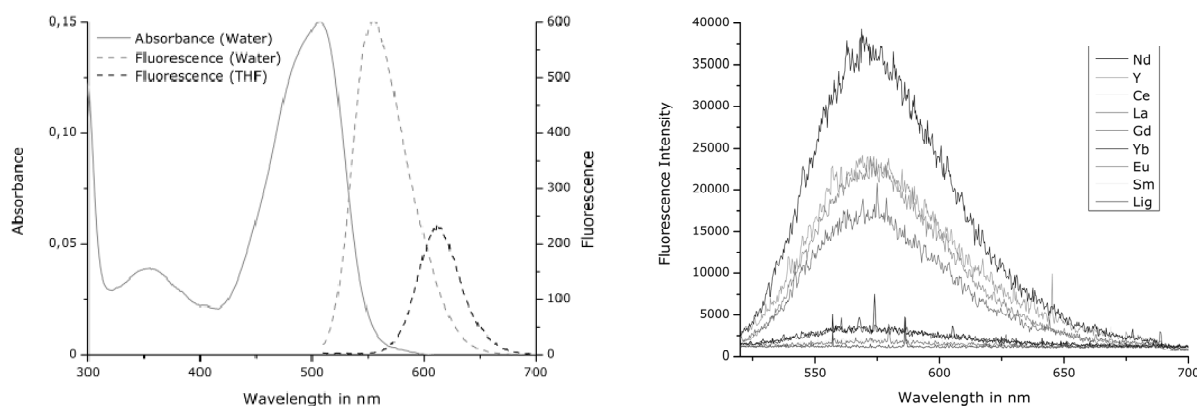


Fig. 2: Absorbance and fluorescence spectra of the La(III) complex of **L1** (left) and TRLFS spectra of various rare earth metal complexes of **L1** (right).

[1] Yang, Y. et al. (2010) *Inorg. Chim. Acta* 363, 3448-3452.

[2] Drew, M. G. B. et al. (2007) *J. Chem. Cryst.* 30, 455-458.

## Commonalities and dissimilarities of Eu(III) interactions by simple organic acids and humic substances: complexation and sorption on Al<sub>2</sub>O<sub>3</sub>

P. E. Reiller,<sup>1,2</sup> N. Janot,<sup>3</sup> P. Moreau,<sup>1</sup> S. Colette-Maatouk,<sup>1</sup> C. Auriault,<sup>1</sup> P. Gareil,<sup>4</sup> M. Benedetti<sup>3</sup>

<sup>1</sup> CEA/DEN/DANS/SEARS/LANIE, Gif-sur-Yvette, France

<sup>2</sup> Université d'Evry Val d'Essonne, LAMBE, Evry, France

<sup>3</sup> Institut de Physique du Globe de Paris, Université Denis Diderot, Paris, France

<sup>4</sup> Chimie Paritech, PECSA, Paris, France

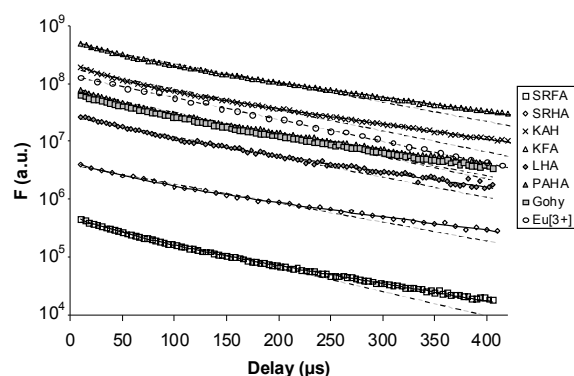


Fig. 1: Comparison mono-exponential decay of Eu<sup>3+</sup> (empty circles) and bi-exponential of Eu(III)-complexes [2].

[4]. Recently, some hydroxobenzoic acids have been shown decreasing the Eu(III) decay time [5, 6]. It seems then justified to compare the luminescence properties of both Eu(III)-HS and -hydroxobenzoic acid complexes under varying conditions, i.e., during complexation and sorption experiments.

Figure 1 and 2 are showing typical bi-exponential decay of Eu(III)-HS, and decreasing decay during complexometric titration of Eu(III)-parahydroxybenzoic (PHBA) acid and -protocatechuic (PROTOA) complexes, respectively. After determination of the Eu(III)-hydroxobenzoic acids complexation constants [6], both the spectra and  $\tau$  can be compared with the Eu(III)-HS complex(es). If the complex formation of Eu(III)-PHBA only merely decreases  $\tau$ , Eu(III)-PROTOA is showing a large  $\tau$  decrease (Fig. 2), which is in agreement with  $\tau_1$  of Eu(III)-HS complexes [2, 3]. Luminescence spectra are also showing similarities with Eu(III)-HS complexes.

Conversely, luminescence behavior of sorbed Eu(III)-hydroxobenzoic and -HS complexes [7] before Eu(III) the sorption edge on Al<sub>2</sub>O<sub>3</sub> are markedly different. Evidence of a weak ternary surface complex is obtained both for Eu(III)-PHBA and -PROTOA complexes with a moderate increase of  $\tau$ . For HS, the strong sorption enhancement of Eu(III)-HS complex is accompanied by an increase in the slowest  $\tau_2$ ; both spectrum and  $\tau_1$  being unchanged. Implication of commonalities and dissimilarities will be discussed.

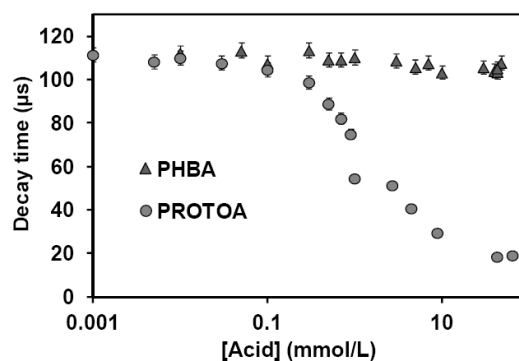


Fig. 2: Evolution of Eu(III) decay time during complexometric titration by PHBA and PROTOA [6].

[1] Buckau, G. et al. (1992) *Radiochim. Acta* 57, 105-111.

[2] Brevet, J. et al. (2009) *Spectrochim. Acta A* 74, 446-453.

[3] Reiller, P. E. and Brevet, J. (2010) *Spectrochim. Acta A* 75, 629-636.

[4] Horrocks, W. et al. (1979) *J. Am. Chem. Soc.* 101, 334-340.

[5] Kuke, S. et al. (2010) *Spectrochim. Acta A* 75, 1333-1340.

[6] Moreau, P. et al. (submitted) *Inorg. Chem.*

[7] Janot, N. et al. (2001) *Environ. Sci. Technol.* 45, 3224.

## Spectroscopic and quantum chemical study of the curium(III) and europium(III) citrate speciation in biological systems

A. Heller,<sup>1</sup> A. Barkleit,<sup>1,2</sup> H. Foerstendorf,<sup>1</sup> S. Tsushima,<sup>1</sup> K. Heim,<sup>1</sup> G. Bernhard<sup>2</sup>

<sup>1</sup> Helmholtz-Zentrum Dresden-Rossendorf, Institute of Resource Ecology, Dresden, Germany

<sup>2</sup> Dresden University of Technology, Professorship Radiochemistry, Dresden, Germany

Heavy metals, particularly radionuclides, represent a serious health risk to humans in case of incorporation. For the understanding of their (radio-) toxicity, distribution, deposition and elimination, it is crucial to investigate their aqueous speciation and molecular transport mechanisms in biosystems. Unfortunately, only little is known about the behavior of artificial, radioactive trivalent actinides (An(III)) and naturally occurring, nonradioactive lanthanides (Ln(III)) in the human organism. Nevertheless, quite recently, we showed that citrate complexes are the dominant binding form of An(III) and Ln(III) in human urine at pH < 6 [1]. Hence, an accurate prediction of the speciation of these elements in the presence of citrate is crucial for the understanding of the impact on the metabolism of the human organism and the corresponding health risks.

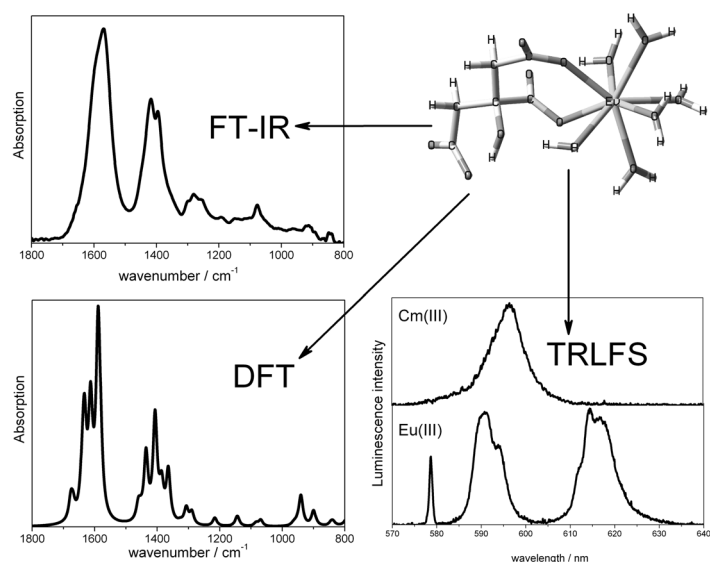


Fig. 1: Measured and calculated IR and TRLFS spectra of  $\text{MCitH}^0$  complexes.

With ATR FT-IR and DFT, structural details of the  $\text{EuHCit}$  and  $\text{EuCit}^-$  complexes were obtained. The combination of both methods gave clear evidence for the deprotonation of the hydroxyl group of the citrate ion in the  $\text{EuCit}^-$  complex, what also revealed that the complexation of the  $\text{Eu}^{3+}$  ion takes place not only through the carboxylate groups, like in  $\text{EuCit}^0$ , but additionally via the hydroxylate group. In both  $\text{EuCit}^0$  and  $\text{EuCit}^-$  the carboxylate binding mode is predominantly mono-dentate.

At a very low metal-citrate ratio, which is typical for human body fluids, the Cm(III) and Eu(III) speciation was found to be strongly pH-dependent. The Cm(III) and Eu(III) citrate complexes dominant in human urine at pH < 6 were identified to be  $\text{Cm}(\text{HCitH})\text{HCit}^{2-}$  and a mixture of  $\text{Eu}(\text{HCitH})\text{HCit}^{2-}$  and  $\text{EuHCit}^0$ . The results specify our previous *in vitro* study using natural human urine samples [1] and point out the importance of low molecular weight ligands for An(III) and Ln(III) complexation in body fluids and other biological systems.

Therefore, we studied the complexation of Cm(III) and Eu(III), as representatives of An(III) and Ln(III), respectively, in aqueous citrate solution over a wide pH range using a combined approach of Time-Resolved Laser-induced Fluorescence Spectroscopy (TRLFS), Attenuated Total Reflection Fourier-Transform Infrared (ATR FT-IR) spectroscopy and Density Functional Theory (DFT) calculations (Fig. 1).

With TRLFS, four citrate complexes were identified for both Cm(III) and Eu(III), which are  $\text{MHCit}^0$ ,  $\text{M}(\text{HCitH})\text{HCit}^{2-}$ ,  $\text{M}(\text{HCit})_2^{3-}$ , and  $\text{M}(\text{Cit})_2^{5-}$ . Furthermore, the stability constants were determined (Tab. 1). Additionally, there were also indications for the formation of  $\text{MCit}^-$  complexes.

Tab. 1: Complex formation constants of identified Cm(III) and Eu(III) citrate species ( $I = 0.1 \text{ M}$ , room temperature).

Complex	Cm	Eu
$\text{MHCit}^0$	$7.4 \pm 0.2$	$7.5 \pm 0.2$
$\text{M}(\text{HCitH})\text{HCit}^{2-}$	$11.0 \pm 0.3$	$10.8 \pm 0.5$
$\text{M}(\text{HCit})_2^{3-}$	$11.3 \pm 0.7$	$11.4 \pm 0.4$
$\text{MCit}_2^{5-}$	–	$21.0 \pm 0.2$

[1] Heller, A. et al. (2011) Chem. Res. Tox. 24, 93-103.

## Uranium speciation at silica-water interface: a TRFS study

A. S. Kar,<sup>1</sup> S. V. Godbole,<sup>2</sup> B. S. Tomar<sup>1</sup>

<sup>1</sup> Radioanalytical Chemistry Division, Bhabha Atomic Research Centre, Mumbai, India

<sup>2</sup> Radiochemistry Division, Bhabha Atomic Research Centre, Mumbai, India

U(VI) migration and transport in aquatic environment is vital issue as huge quantities of U(VI) are left in the mill tailing ponds near the U(VI) mining sites. U(VI) can also be considered as an analogue of hexavalent actinides viz., Np(VI) and Pu(VI) which have high specific activity. Silica is one of the common constituents of the minerals and clays present in earth's crust and hence U(VI) interaction with silica will help in understanding its migration in geosphere.

Figure 1 shows the photoluminescence spectra of U(VI) sorbed onto silica surface at room temperature and varying pH values in the range of 4-8, having several characteristic peaks in 500-600 nm region. The intense luminescence is seen as outcome of charge transfer transition from  $5f_{\delta}$  and  $5f_{\phi}$  orbitals of  $U^{6+}$  ion to  $\sigma_u$  orbitals of  $O^{2-}$  ion which in turn couples with vibrational modes of uranyl ion to give rise to different peaks in uranyl spectra [1].

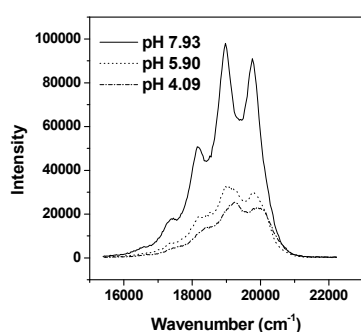


Fig. 1: Emission spectra of uranium sorbed on silica.

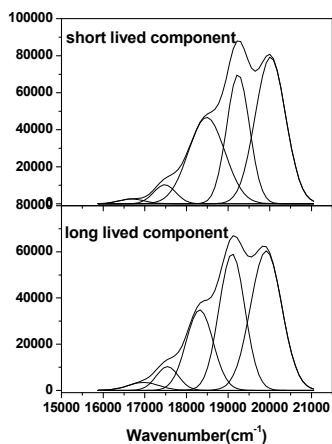


Fig. 2: Deconvoluted fluorescence emission spectra of short and long lived component of pH 4.62.

The sorbed uranyl species have their peak maxima red shifted with respect to the uranyl aquo ion which is attributed to the complexation of the uranyl ion and the surface sites of silica ( $\equiv Si-OH$ ). The lifetime of U(VI) species is dependent on many factors such as sample preparation, presence of quenchers, temperature in addition to the coordination environment, therefore its lifetime decay profile is only used to gather information about the number of species present [2]. The magnitude of two lifetimes increased with pH. However, the emission characteristics of the two species remained same in the entire pH range suggesting the existence of two sorbed uranyl species on silica surface. The representative spectra of two components are shown in Figure 2. A pure electronic luminescence transition at  $20,015\text{ cm}^{-1}$  for short lived species and at  $19,912\text{ cm}^{-1}$  for long lived species is followed by a coupling of the  $O=U=O$  vibrations resulting in the other peaks in the spectrum. Larger red shift observed for long-lived species suggests a stronger equatorial bonding for the same in comparison to short lived species. Table 1 gives the characteristic peak positions of two components along with that of the aquo ion for comparison. Thus, the TRFS studies validate the proposition of two surface complexes of uranium sorbed on silica by surface complexation modeling [3].

Tab. 1: Peak maxima of two components for  $UO_2^{2+}$  sorbed on silica.

Sample	$\nu\text{ (cm}^{-1}\text{)}$
Short lived species	20015, 19238, 18484, 17477, 16684
Long lived species	19912, 19092, 18316, 17542, 16973
$UO_2^{2+}$ ion (pH) [2]	21276, 20492, 19646, 18761, 17889, 17094

[1] Matsika, C. et al. (2001) J. Phys. Chem. A, 105, 3825-3828.

[2] Al-Abadleh, H. A. and Grassian, V. H. (2010) Molecules 15, 8431-8468.

[3] Kar, A. S. et al. (2012) Colloids Surf., A 395, 240-247.



## Uranium speciation studies at alkaline pH and in presence of peroxide using TRLFS

A. Martínez-Torrents,<sup>1,2</sup> S. Meca,<sup>2</sup> N. Baumann,<sup>3</sup> V. Martí,<sup>1,2</sup> J. Giménez,<sup>1</sup> J. de Pablo,<sup>1,2</sup> I. Casas<sup>1</sup>

<sup>1</sup> Chemical Engineering Dept. Universitat Politècnica de Catalunya (UPC), Barcelona, Spain

<sup>2</sup> Environmental Technology Area, CTM-Centre Tecnològic, Manresa, Spain

<sup>3</sup> Helmholtz-Zentrum Dresden-Rossendorf, Institute of Resource Ecology, Dresden, Germany

In the waters in contact with the spent nuclear fuel (SNF) pH values higher than 11 may be reached in the presence of concrete [1], which is proposed to be used in structural parts of the high level nuclear waste repositories [2]. In addition, hydrogen peroxide might be formed through the radiolysis of water. Time-resolved laser-induced fluorescence spectroscopy (TRLFS) studies were made at three different pH values and at room temperature in absence of CO<sub>2</sub>. At pH 11, two different lifetimes appeared, and were attributed to species UO<sub>2</sub>(OH)<sub>3</sub><sup>-</sup> and (UO<sub>2</sub>)<sub>3</sub>(OH)<sub>7</sub><sup>-</sup> [3]. At pH 13, fluorescence was not measured, indicating that the predominating species, UO<sub>2</sub>(OH)<sub>4</sub><sup>2-</sup>, is not fluorescent. At pH 12, the lifetime obtained is attributed to the predominant species UO<sub>2</sub>(OH)<sub>3</sub><sup>-</sup>.

Because the absence of fluorescence of the UO<sub>2</sub>(OH)<sub>4</sub><sup>2-</sup> species at room temperature, measurements at 10K were made, obtaining two different lifetimes in the pH range between 12 and 13.5, indicating the presence of two different species. The difference between the lifetimes allowed calculating the contribution of each species to the total fluorescence spectra (Fig. 1). The peaks for each species were similar to the data found in the bibliography [4].

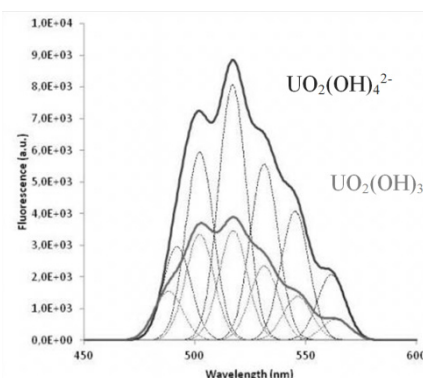


Fig. 1: Fitting of the fluorescence spectra of species UO<sub>2</sub>(OH)<sub>3</sub><sup>-</sup> and UO<sub>2</sub>(OH)<sub>4</sub><sup>2-</sup> at pH 13 [U(VI)]: 5 · 10<sup>-6</sup> M and 10 K.

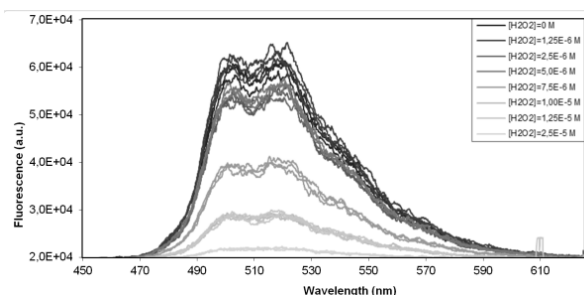


Fig. 2: Fluorescence spectra of the samples with different hydrogen peroxide concentrations. [U(VI)] of 10<sup>-5</sup> mol·dm<sup>-3</sup>, pH 12, ionic strength 0.1 M, and [H<sub>2</sub>O<sub>2</sub>] between 0 and 2 · 10<sup>-5</sup> mol·dm<sup>-3</sup> (Fluorescence intensity diminishes as hydrogen peroxide concentration augments).

From the experiments carried out in the presence of hydrogen peroxide, it was observed that hydrogen peroxide produces a quenching effect of the uranium species (Fig. 2). At pH 12 the quenching is static, which points to the formation of a non-fluorescent complex between U(VI) and hydrogen peroxide [5,6]. Using the Stern-Volmer equation for static quenching the equilibrium formation constant of the first species UO<sub>2</sub>O<sub>2</sub>(OH)<sub>2</sub><sup>2-</sup>, was calculated to be: K<sub>1</sub> = 28.7 ± 0.4, which is similar to the one determined using UV-vis spectrometry, 28.1 ± 0.2 [5].

[1] Stegemann, J.A. and Buenfeld, N.R. (2002) Journal of Hazardous Materials B90, 169-188.

[2] Pointeau, I. et al. (2004) Radiochim. Acta 92, 645-650.

[3] Eliet, V. et al. (1995) J. Chem. Soc. Faraday Trans. 91, 2275-2285.

[4] Kitamura, A. et al. (1998) Radiochim. Acta 82, 147-152.

[5] Meca, S. et al. (2011) Dalton Trans. 40, 7976-7982.

[6] Zanonato, L. et al. (2012) Dalton Trans. 41, 3380-3386.

ABSTRACTS

---

# **POSTER PRESENTATIONS**



## Time-resolved laser-induced fluorescence spectroscopy (TRLFS) of aqueous Am(III) complexes at ambient and elevated temperature

A. Barkleit,<sup>1,2</sup> M. Acker,<sup>3</sup> G. Geipel,<sup>1</sup> G. Bernhard<sup>1,2</sup>

<sup>1</sup> Helmholtz-Zentrum Dresden-Rossendorf, Institute of Resource Ecology, Dresden, Germany

<sup>2</sup> Radiochemistry, Dresden University of Technology, Dresden, Germany

<sup>3</sup> Central Radionuclide Laboratory, Dresden University of Technology, Dresden, Germany

Time-resolved laser-induced fluorescence spectroscopy (TRLFS) has been extensively used as a sensitive and selective technique to analyze actinide complexation with inorganic and organic ligands in trace metal concentrations. However, the application of TRLFS onto Am(III) complexation systems was up to now limited because of the much lower luminescence intensity and much shorter lifetime of Am(III) in comparison to U(VI) or Cm(III).

We investigated the complexation behavior of Am(III) complexes with lactate (Lac) and substituted benzoic acids like pyromellitic acid (1,2,4,5-benzenetetracarboxylic acid, BTC) at ambient and elevated temperatures with TRLFS.

Using the emission of the  $^5D_1 \rightarrow ^7F_1$  transition at around 691 nm, spectral data like luminescence lifetimes, luminescence maxima and complex stability constants were calculated. Temperature dependent stability constants were determined to estimate thermodynamic data (reaction enthalpy, reaction entropy).

The Am(III) aquo ion shows at pH 4-6 a luminescence lifetime of 23 ns, corresponding to approximately 9 coordinating water molecules. Complexation with BTC shows no change of the excitation and emission maximum but an increase of the luminescence intensity and lifetime. The luminescence lifetime was prolonged to 27 ns, corresponding to 8 remaining water molecules in the first coordination shell. This indicates an exchange of 1 water molecule with 1 coordination site of the ligand, resulting in an Am-BTC 1:1 complex [1]. In contrast, complexation with lactate causes a red shift of the excitation wavelength of Am(III) (Fig. 1), resulting in a red shift of the luminescence emission maximum of about 5 nm. The luminescence lifetime is prolonged up to 37 ns which corresponds to 5-6 remaining water molecules. This indicates an exchange of about 3-4 water molecules with coordination sites of ligand molecules which implies the formation of 1:1, 1:2 and 1:3 complexes. The stability constants increase slightly with rising temperature which is consistent with an endothermic complexation reaction.

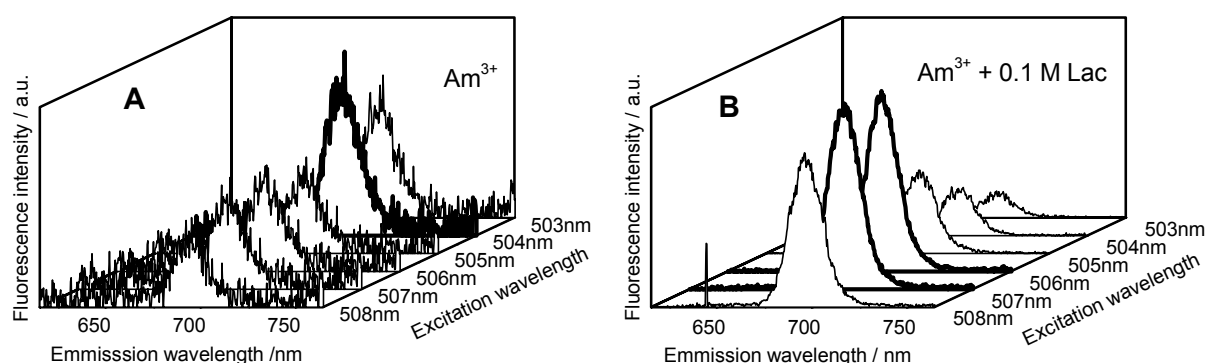


Fig. 1: Emission spectra of (A) 5  $\mu\text{M}$   $\text{Am}^{3+}$  and (B) 5  $\mu\text{M}$   $\text{Am}^{3+}$  + 0.1 M lactate in dependence of the excitation wavelength ( $I = 0.1 \text{ M NaClO}_4$ , pH = 6.0).

[1] Barkleit, A. et al. (2011) Spectrochim. Acta A: Mol. Biomol. Spectrosc. 78, 549-552.

## Investigation of uranium(VI) speciation in cementitious environments by direct laser excitation

J. Tits,<sup>1</sup> T. Stumpf,<sup>2</sup> C. Walther,<sup>3</sup> E. Wieland<sup>1</sup>

<sup>1</sup> Paul Scherrer Institute, Laboratory for Waste Management, Villigen, Switzerland

<sup>2</sup> Karlsruhe Institute of Technology (KIT), Institute for Nuclear Waste Disposal (INE), Karlsruhe, Germany

<sup>3</sup> Institut für Radioökologie und Strahlenschutz, Leibniz Universität Hannover, Hannover, Germany

Sufficient knowledge of the local coordination environment of U(VI) sorbed by calcium silicate hydrates (C–S–H), the main component of hardened cement paste, is necessary to obtain a better understanding of the mechanisms controlling the immobilisation of this actinide in cementitious materials. In this study, the coordination environment of U(VI) sorbed on C–S–H phases under hyperalkaline conditions was examined with the help of luminescence spectroscopy using direct laser excitation at cryogenic temperature (~15 K). The luminescence spectra recorded after broadband excitation ( $\lambda_{\text{ex}} < 480$  nm), of trace amounts of U(VI) sorbed onto cementitious materials, are characterized by the presence of three to five broad, structureless bands [1]. These wide band structures result from the superposition of many narrower bands associated with slightly different non-interacting U(VI) luminescence centres in the nearly amorphous cementitious material. Each of these U(VI) luminescence centres experiences a somewhat different coordination environment, as the exact position of neighboring atoms is less well defined in amorphous than in crystalline materials. Selectively exciting these U(VI) centres with direct excitation using a tunable laser as a narrow-band light source, results in a significant decrease of the band width and an improved resolution of the spectra (see e.g. [2]).

Luminescence spectroscopy measurements were performed on two reference systems; i). U(VI) solutions in 0.5 M TMA-OH at pH ~13.5. ii) U(VI) sorbed on rutile at pH 13.3. The first reference system was chosen to determine the luminescence behaviour of  $\text{UO}_2(\text{OH})_4^{2-}$ , the hydroxy species dominating the aqueous uranyl speciation at pH = 13.3. The U(VI) sorption onto rutile was studied as rutile is a well defined crystalline material, stable under high pH conditions and U(VI) is known to sorb on this material via a surface complexation mechanism. The spectra of the U(VI) surface complexes on rutile were further compared with spectra from U(VI) sorbed onto C–S–H phases.

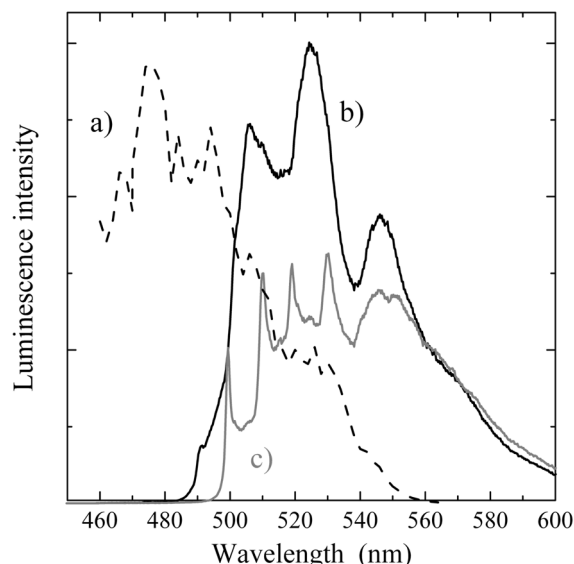


Fig. 1: Excitation and luminescence spectra of  $10^{-6}$  M U(VI) sorbed on a C–S–H phase at pH = 13.3. a) Excitation spectrum. b) Luminescence spectrum after broadband excitation at  $\lambda_{\text{ex}} = 470$  nm. c) Luminescence spectrum after direct excitation at  $\lambda_{\text{ex}} = 500$  nm.

High resolution spectra of U(VI) solutions in 0.5 M TMA-OH indicate the presence of 3 U(VI) species: The dominant  $\text{UO}_2(\text{OH})_4^{2-}$  species together with  $\text{UO}_2(\text{OH})_3^-$  and a  $\text{UO}_2(\text{CO}_3)_3^{4-}$ , the latter originating from carbonate impurities.

For the solids loaded with U(VI), broadband laser excitation results in typical poorly resolved U(VI) emission spectra with three to five broad bands (e.g. spectrum b in Fig. 1) corresponding to the coupling of the O=U=O symmetric stretch vibration with the pure electronic charge transfer transition. Under direct excitation at longer wavelengths, the spectra of U(VI) sorbed on C–S–H phases exhibit detailed fine structure (e.g. spectrum c in Fig. 1) whereas the spectra of U(VI) sorbed on rutile remain poorly resolved due to energy transfer to neighboring uranyl luminescence centres on the rutile surface having a slightly lower excitation energy. Evaluation of the highly resolved luminescence spectra of U(VI) sorbed on C–S–H phases recorded at different excitation wavelengths, allowed the identification and characterization of different U(VI) sorbed species in different geometries.

[1] Tits, J. et al. (2011). *J. Coll. Interf. Sci.* 359, 248-256.

[2] Flint, C. and Tanner, P. A. (1983). *Chem. Phys. Lett.* 102, 249-253.

## Development and application of a polarizable force-field for actinides in aqueous solution including cooperative charge-transfer terms

B. Schimmelpfennig,<sup>1</sup> M. Trumm,<sup>1</sup> M. Masella,<sup>2</sup> F. Réal,<sup>3</sup> Y.O. Guerrero Martinez,<sup>3</sup> V. Vallet<sup>3</sup>

<sup>1</sup> Karlsruhe Institute of Technology (KIT), Institute for Nuclear Waste Disposal (INE), Karlsruhe, Germany

<sup>2</sup> Laboratoire de Chimie du Vivant, Service d'ingénierie moléculaire des protéines, Institut de biologie et de technologies de Saclay, CEA Saclay, Gif sur Yvette Cedex, France

<sup>3</sup> Université Lille 1 (Sciences et Technologies), Laboratoire PhLAM, CNRS UMR 8523, Villeneuve d'Ascq Cedex, France

Detailed understanding of actinide complexation in aqueous solution at ambient and elevated temperatures is essential for predictive risk assessment of transport phenomena after water intrusion at a nuclear waste repository. The theory can help in understanding and predicting experimental results as well as providing a more narrow error-margin as often shown by experiments. In an international cooperation, we have developed a highly-accurate polarizable force-field including cooperative charge-transfer terms [1], which are usually not included in existing MD codes. The force-field parameters are herein adjusted to state-of-the art ab initio calculations on the MP2 or CCSD(T) level. We will present the implemented terms to describe the interatomic interactions and the training set used for fitting the force-field parameters for the case of an actinide ion interacting with water. Our goal is to develop predictive force-field parameters which are independent of experimental input. MD-simulations were carried out in the time-scale of 10 ns and the trajectories were analyzed for structural, thermodynamic and reaction properties like, e.g., the mean residence time of water in the first coordination shell. There are several possibilities to describe non-additive charge-transfer, for example by taking into account only the water density around the ion or by an explicit three-body term, which is even able to describe the angular behavior of the interactions. We compare both approaches and discuss also the influence of limitations in the water-water potential, which are caused by all water models for molecules in the first coordination sphere of the solvated ion [3]. The first actinides studied with our approach are Th(IV) and Cm(III) for which experimental data indicates coordination numbers in the range of 8-10 and esp. for Cm(III) a strong temperature dependence leading to a change from mainly nine-coordination at room temperature to mainly eight-coordination at higher temperatures. We could reproduce this temperature dependence as well as the structural parameters obtained by EXAFS and HEXS, the same holds for mean-residence times and diffusion parameters. To reproduce the experimental setups, we also studied the halide ions from fluoride to bromide in solution [2] and their effect on the actinide's aquo ion. Recent HEXS data indicates high bromide concentrations to increase the mean water coordination of Th(IV) and our ansatz is capable of reproducing such a behavior.

[1] Real, F. et al. (2010) *J. Phys. Chem. B* 114, 15913-15924.

[2] Trumm, M. et al. (2012) *J. Chem. Phys.* 136, 044509.

[3] Real, F. et al. *J. Comp. Chem.* (submitted).

## Structural analysis of the aqueous $(\text{UO}_2)_2\text{CO}_3(\text{OH})_3^-$ -complex – A combined approach using ATR FT-IR spectroscopy and DFT-calculations

K. Gückel, S. Tsushima, H. Foerstendorf, A. Rossberg

Helmholtz-Zentrum Dresden-Rossendorf, Institute of Resource Ecology, Dresden, Germany

The migration behavior of heavy metal contaminants like actinyl ions ( $\text{UO}_2^{2+}$ ) in ground water aquifers is mainly controlled by sorption processes at water-mineral interfaces. Sorption and therewith the retardation of uranium in the environment depends predominately on its aqueous speciation.

From our recent spectroscopic study, the formation of a dimeric uranyl carbonate hydroxo complex on the surface of gibbsite was derived [1]. The found interatomic distances and coordination numbers for the surface complex are in line with the results of Szabo et al. [2] for the mixture of aqueous  $(\text{UO}_2)_2\text{CO}_3(\text{OH})_3^-$ -complexes. However, an unequivocal verification of the molecular structure is still lacking. According to previous investigations [2, 3] and predicted aqueous speciation of uranium(VI), a uranyl carbonate hydroxo complex is predominant over a broad pH range. Under near neutral pH conditions, similar to those of natural waters, the  $(\text{UO}_2)_2\text{CO}_3(\text{OH})_3^-$ -complex is the dominating species over a wide concentration range (Fig. 1). Maya et al. [3] determined the stability constant ( $-\log \beta = 18.63 \pm 0.08$ ) and measured the Raman spectrum [4] of the complex. The stoichiometry of this complex and the coordination geometry of the uranyl ion was discussed by means of four possible structures [2] of which the preferred structure is shown in Fig. 2.

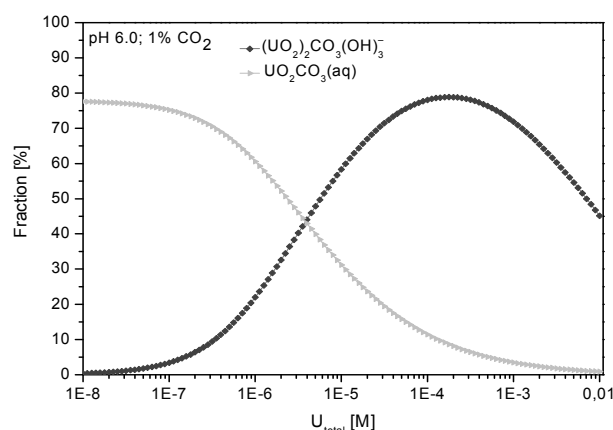


Fig. 1: Speciation of U(VI) under inert gas with 1%  $\text{CO}_2$  conditions at pH 6.

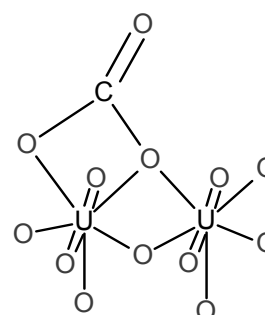


Fig. 2: Possible structure of the  $(\text{UO}_2)_2\text{CO}_3(\text{OH})_3^-$ -complex.

Up to date, no vibrational spectra of the aqueous complex are available in the literature potentially providing further structural information particularly about the configuration of the carbonate ion. We prepared the dimeric complex under well defined atmospheric conditions and recorded IR spectra. In combination with DFT calculations, the assignment of the spectroscopic data to the respective isomer is accomplished.

[1] Gückel, K. et al. (2012) *Chemical Geology*, under revision.

[2] Szabo, Z. et al. (2000) *Journal of the Chemical Society-Dalton Transactions*, 3158-3161.

[3] Maya, L. (1982) *Inorganic Chemistry* 21, 2895-2898.

[4] Maya, L. and G.M. Begun (1981) *Journal of Inorganic & Nuclear Chemistry* 43, 2827-2832.

## NMR-investigations on paramagnetic effects in $^{241}\text{PrBTP}$ complexes of trivalent lanthanides and americium

P. Kaden,<sup>1</sup> C. Adam,<sup>1,2</sup> A. Geist,<sup>1</sup> P. J. Panak,<sup>1,2</sup> M.A. Denecke<sup>1</sup>

<sup>1</sup> Karlsruhe Institute of Technology (KIT), Institute for Nuclear Waste Disposal (INE), Karlsruhe, Germany

<sup>2</sup> University of Heidelberg, Department of Physical Chemistry, Heidelberg, Germany

Partitioning and transmutation (P&T) is a strategy for reducing the long term radiotoxicity of spent nuclear fuel. P&T involves separating actinides and converting them into shorter-lived or stable fission products. In this context the separation of trivalent actinides from the chemically similar lanthanides is a key step. This separation can be performed by liquid-liquid extraction using selective N-donor extracting ligands. BTP-type (alkylated bis-triazinyle pyridine) ligands have high separation factors ( $> 100$ ) for Am(III) over Eu(III). However, little is known about the molecular origin of their selectivity. Previous studies have shown that BTP complexes of An(III) and Ln(III) are isostructural, allowing a comparative study of the different binding modes of actinides and lanthanides. Variation of the metal ion type will lead to changes in electron density distribution on the ligand. NMR spectroscopy is an excellent tool to study these effects on the electron density around the observed nuclei as chemical shift.

To obtain an understanding of the differences between Ln and An-complexes on a molecular level, NMR focusing on the paramagnetism of the compounds is a sensitive and versatile spectroscopic method. Lanthanide and actinide ions show paramagnetic properties to a variable extent. Am(III) is known to have only a weak anisotropy of the magnetic susceptibility tensor, leading to a nearly diamagnetic behavior in solution. NMR investigations at KIT-INE on  $\text{Am}(\text{PrBTP})_3^{3+}$  complexes show that there is a small paramagnetic relaxation enhancement and a temperature dependent paramagnetic shift in  $^1\text{H}$  and  $^{13}\text{C}$  spectra. Furthermore, strong chemical shifts ( $> 300$  ppm) of the coordinating nitrogen atoms in the pyridine and triazine moiety, which are not observed for the non-coordinating nitrogens, indicate that the binding mode in the americium complexes differs from isostructural lanthanide complexes. We present strong evidence that this difference lies in covalence being the predominant interaction of Am(III) in complexes with BTP-type N-donor ligands.

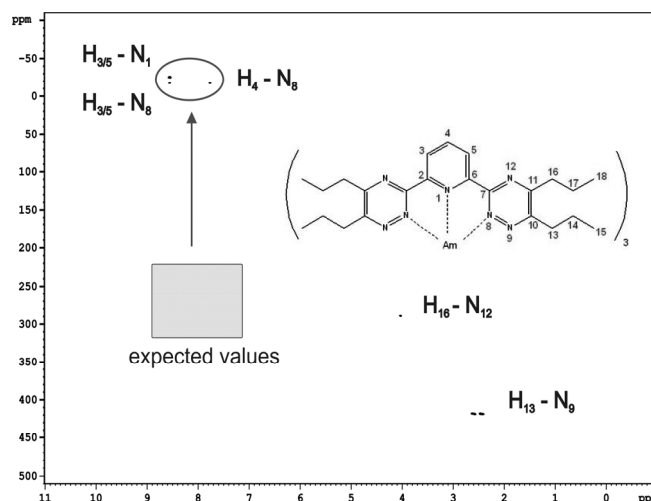


Fig. 1: 2D  $^1\text{H}$ ,  $^{15}\text{N}$ -HMQC NMR spectrum of  $\text{Am}(\text{PrBTP})_3(\text{NO}_3)_3$  in MeOD/ $\text{D}_2\text{O}$  solution. The  $^{15}\text{N}$  signals of the Am-binding nitrogen atoms show strong chemical shifts. To obtain this correlation partial  $^{15}\text{N}$  labelling of the vicinal triazine nitrogens is necessary.

[1] This work is supported by the German Federal Ministry of Education and Research (BMBF) under contract numbers 02NUK012A, 02NUK012D and 02NUK020A and 02NUK020D.

[2] Desreux, Reilley (1976) *J. Am. Chem. Soc.* 98, 2105-2109.

[3] Piguet, Geraldes (2003) in: *Handbook on the Physics and Chemistry of Rare Earths*, Vol. 33, Elsevier, pp. 353-463.



## Selective Extraction of $^{85}\text{Sr}^{2+}$ with modified Calix[4]arenes in a liquid-liquid system

M. Poetsch,<sup>1</sup> A. Mansel,<sup>1</sup> R. Schnorr,<sup>2</sup> S. Haupt,<sup>2</sup> B. Kersting<sup>2</sup>

<sup>1</sup> Helmholtz-Zentrum Dresden-Rossendorf, Institute of Resource Ecology, Department of Reactive Transport, Research Site Leipzig, Leipzig, Germany

<sup>2</sup> Institute of Inorganic Chemistry, Faculty of Chemistry and Mineralogy, University of Leipzig, Leipzig, Germany

$^{90}\text{Sr}$  is a long-lived radionuclide ( $T_{1/2} = 28.6$  a), which is produced as a by-product in nuclear power plants in the decay chain of uranium. In case of release in the biosphere, it can be concentrated in aquatic systems or in soil. It follows the food chain from environment to fauna and human. Due to its chemical similarity to calcium, it can be incorporated in bones. Stable isotopes of strontium might not be harmful, but radioactive analogues can lead to bone disorders and diseases, including leukaemia [1].

Calix[4]arenes represent an important class of supramolecules having various applications, e.g. in the recovery of nuclear fission products of uranium, like cesium or strontium [2]. We synthesized and structurally analyzed calix[4]arene-based extractants as shown in Fig. 1 in order to investigate their binding ability towards strontium in liquid-liquid extraction systems.

An aqueous phase was traced using the short-lived radionuclide  $^{85}\text{Sr}$  ( $T_{1/2} = 64.9$  d), which was produced and purified at the in-house 18 MeV-cyclotron [3]. To quantify the extraction behaviour of the calix[4]arenes, the remaining amounts of  $^{85}\text{Sr}$  in the aqueous phases after the extraction, were recorded using gamma spectrometry. We systematically investigated the influence of various experimental parameters. Figure 1 shows extraction behaviour of various calix[4]arene derivatives depending on the pH of the aqueous strontium phase. Under alkaline conditions of the aqueous strontium phase, extraction yields of  $> (90 \pm 4)\%$  were obtained for calix[4]arenes derivatives having carbonyl binding sites. Furthermore, the competition of inorganic and organic impurities to the extraction performance was studied. The impurities are in naturally occurring concentrations of ions like sodium, calcium, acetate or tartaric acid as groundwater ingredients. By simulating a synthetic groundwater, extraction of strontium was performed in yields up to  $(86 \pm 6)\%$ .

In further experiments, the calix[4]arene-strontium complex is going to be analyzed spectroscopically with the aim to investigate the complex formation behaviour.

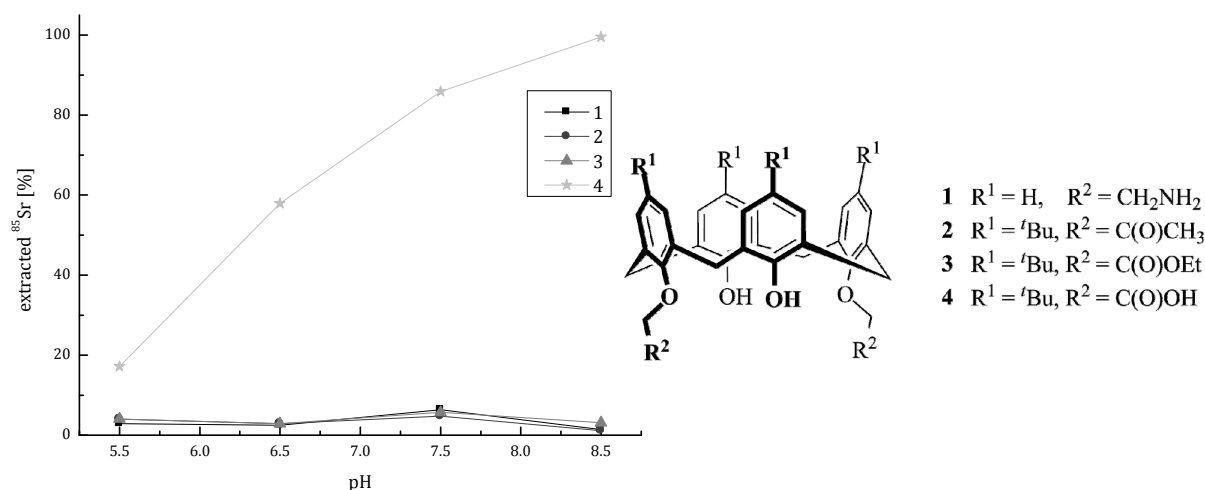


Fig. 1: Extraction capacity of various calixarene derivatives depending on pH value of the aqueous strontium phase.

The authors gratefully thank the German Federal Ministry of Education and Research (BMBF) for financial support of this study (project no. 02NUK014).

[1] Wallova, G. et al. (2012) Journal of Environmental Radioactivity 107, 44-50.

[2] Otho, K. (2010) Solvent Extraction Research and Development 17, 1-18.

[3] Mansel, A., et al. (2012) submitted.

## 2,6-Bis(5-(2,2-dimethylpropyl)-1H-pyrazol-3-yl)pyridine as a ligand for efficient actinide(III)/lanthanide(III) separation

A. Bremer,<sup>1,2</sup> Ch. M. Ruff,<sup>1,2</sup> D. Girnt,<sup>3</sup> U. Müllich,<sup>1</sup> J. Rothe,<sup>1</sup> P. W. Roesky,<sup>3</sup>  
P. J. Panak,<sup>1,2</sup> A. Karpov,<sup>4</sup> T. J. J. Müller,<sup>4</sup> M. A. Denecke,<sup>1</sup> A. Geist<sup>1</sup>

<sup>1</sup> Karlsruhe Institute of Technology (KIT), Institute for Nuclear Waste Disposal (INE), Karlsruhe, Germany

<sup>2</sup> University of Heidelberg, Department of Physical Chemistry, Heidelberg, Germany

<sup>3</sup> Karlsruhe Institute of Technology, Institut für Anorganische Chemie, Karlsruhe, Germany

<sup>4</sup> Institut für Organische Chemie und Makromolekulare Chemie, Heinrich-Heine-Universität Düsseldorf, Düsseldorf, Germany

The N-donor complexing ligand 2,6-bis(5-(2,2-dimethylpropyl)-1H-pyrazol-3-yl)pyridine (C5-BPP) was synthesized and screened as an extracting agent selective for trivalent actinide cations over lanthanides [1]. C5-BPP extracts Am(III) from up to 1 mol/L HNO<sub>3</sub> with a separation factor over Eu(III) of approximately 100. Due to its good performance as an extracting agent, the complexation of trivalent actinides and lanthanides with C5-BPP was studied.

The solid-state compounds [Ln(C5-BPP)(NO<sub>3</sub>)<sub>3</sub>(DMF)] (Ln = Sm(III), Eu(III), Fig. 1) were synthesized, fully characterized, and compared to the solution structure of the Am(III) 1:1 complex [Am(C5-BPP)(NO<sub>3</sub>)<sub>3</sub>] (Fig. 2). The high stability constant of  $\log \beta_3 = 14.8 \pm 0.4$  determined for the Cm(III) 1:3 complex is in line with C5-BPP's high distribution ratios for Am(III) observed in extraction experiments.

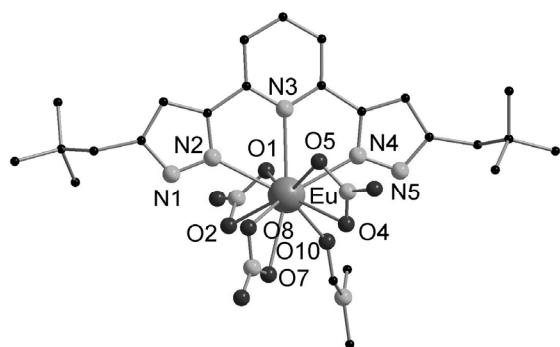


Fig. 1: Solid-state structure of [Eu(C5-BPP)(NO<sub>3</sub>)<sub>3</sub>(DMF)] showing the atom labeling scheme, omitting hydrogen atoms.

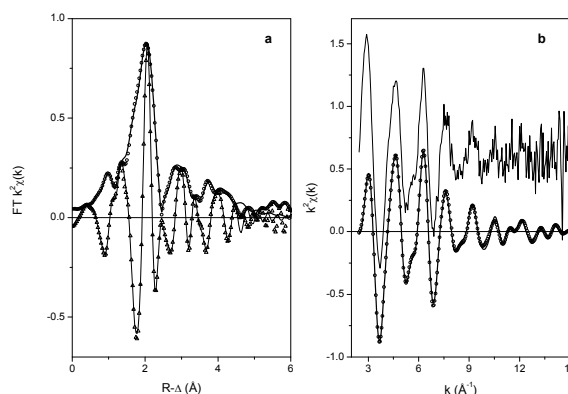


Fig. 2: Am L<sub>3</sub>-EXAFS for Am(III)-C5BPP (a) experimental Fourier transform (FT) magnitude (circles) and real part (triangles), with solid lines giving theoretical curves from the fit results (b) experimental k<sup>2</sup>-weight data (thin solid line, vertically shifted for clarity), back-transformed data (circles), and theoretical fit curves (solid line).

[1] Bremer, A. et al. (2012) Inorg. Chem. 51, 5199-5207.

## Combination of spectroscopic methods for the identification of U(VI) species formed by selected bacteria, algae and fungi

A. Günther, M. Vogel, A. Rossberg, J. Raff, G. Bernhard

Helmholtz-Zentrum Dresden-Rossendorf, Institute of Resource Ecology, Dresden, Germany

Microorganisms like bacteria, algae and fungi have a significant influence on the immobilization, mobilization and transport of radionuclides like uranium and other heavy metals in the biological and geological environment via the soil and water path. To understand the mechanisms of uptake, transport, deposition, degradation and the behavior of actinides in different biological and geological systems structural knowledge about the formed actinides species are of great importance and are essential for a reliable assessment of these processes.

*Arthrobacter* (bacteria), *Chlorella vulgaris* (green algae) and *Schizophyllum commune* (fungi) bind significant amounts of uranium(VI) in the pH range from 4 to 7 and contact time of two days. Results from transmission electron and scanning electron microscopy investigations demonstrate predominant interactions of uranium with parts of cell walls of the selected biomass. However, from experiments

with transparent fungal cells, additional uranium containing accumulates are identified inside originally living cells.

For the determination of the functionalities, which are important for the binding and mobilization or immobilization of uranium, the interaction of uranium(VI) with metabolic active bacterial, algal and fungal cells was investigated by means of time-resolved laser-induced fluorescence spectroscopy (TRLFS) and X-ray absorption fine structure spectroscopy (EXAFS). The measured luminescence spectra of uranyl containing cell species of all investigated organisms show bathochromic shifts of the uranyl emission bands in comparison to the corresponding emission signals of the uranyl species in the initial solution independent of the uranium concentration and the pH value of the solution. The comparison of the

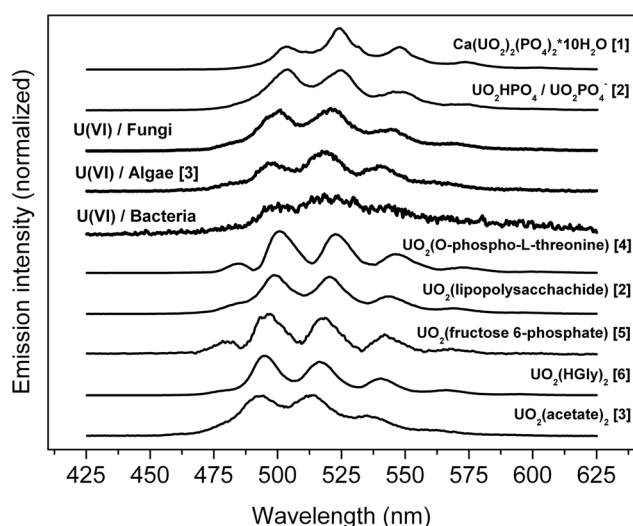


Fig. 1: Luminescence spectra of uranium containing bacteria-, algae- and fungi samples in comparison to the spectra of selected uranyl model compounds.

spectra obtained from biomass with those of uranyl model compounds demonstrates that the carboxylic and organic/inorganic phosphate groups are responsible for uranium binding on the biomass. The contributions of these functional groups to uranium complexation is dependent on the cell status and on uranium concentration in the initial sorption solution (Fig. 1). The dominant interaction of uranium(VI) with organic/inorganic phosphate groups could be verified by corresponding EXAFS investigations.

- [1] Geipel, G. et al. (2000) *Radiochim. Acta* 88, 757-762.  
 [2] Barkleit, A. et al. (2008) *Dalton Trans.*, 2879-2886.  
 [3] Vogel, M. et al. (2010) *Science of the Total Environment* 409, 384-395.  
 [4] Günther, G. et al. (2006) *Radiochim. Acta* 94, 845-851.  
 [5] Koban, A. et al. (2004) *Radiochim. Acta* 92, 903-908.  
 [6] Günther, G. et al. (2007) *Polyhedron* 26, 59-65.

## TRLFS of Cm and Eu doped $\text{La}_2\text{Zr}_2\text{O}_7$ with the defect fluorite and the pyrochlore crystal structure

S. Finkeldei,<sup>1</sup> K. Holliday,<sup>2,3</sup> S. Neumeier,<sup>1</sup> C. Walther,<sup>3,4</sup> D. Bosbach,<sup>1</sup> T. Stumpf<sup>3</sup>

<sup>1</sup> Forschungszentrum Jülich, Institute of Energy and Climate Research - IEK-6: Nuclear Waste Management and Reactor Safety, Jülich, Germany

<sup>2</sup> Lawrence Livermore National Laboratory, Livermore, CA, U.S.A.

<sup>3</sup> Karlsruhe Institute of Technology (KIT), Institute for Nuclear Waste Disposal (INE), Karlsruhe, Germany

<sup>4</sup> Leibniz Universität Hannover, Institute of Radioecology and Radiation Protection, Hannover, Germany

Minor actinides (MA = Am, Cm, Np) are the main contributors to the long-term radiotoxicity of spent fuel. Due to their inherent stability, crystalline waste forms seem to be superior to borosilicate glasses for the immobilization of these MA. The embedding of the radionuclides on well-defined atomic positions within the crystal structure procures a high stability. Specifically zirconate based pyrochlores ( $\text{A}_2\text{B}_2\text{O}_7$ ) have favorable properties with respect to their radiation resistance and their high durability in aqueous environments [1]. Radiation damages in the zirconate based pyrochlores are expected to occur as an order to disorder transition [2]. Therefore, a transformation of the pyrochlore to the defect fluorite structure would be caused. The defect fluorite structure exhibits disordered vacancies within the crystal structure, whereas the vacancies of the pyrochlore crystal structure are ordered.

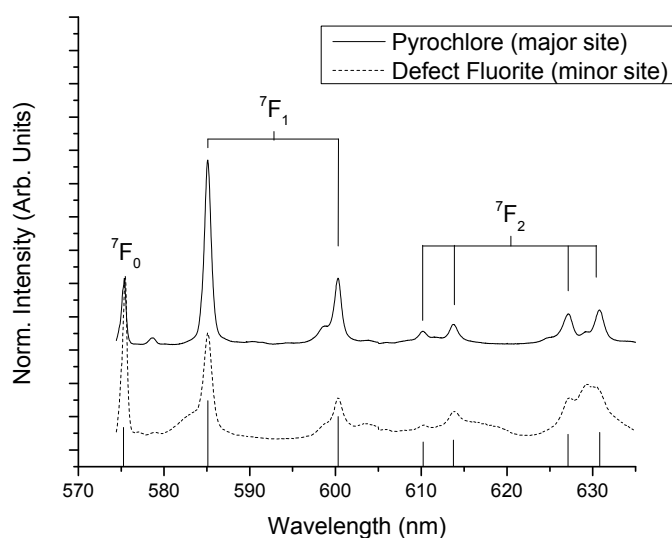


Fig. 1: Emission spectra after direct excitation to the  $^5\text{D}_0$  band for the major species in the pyrochlore and the defect fluorite crystal structure of Eu doped  $\text{La}_2\text{Zr}_2\text{O}_7$  [3].

and the minor species in the pyrochlore structure are caused by the disordered vacancies in the nearby environment in the defect fluorite crystal structure. For the Cm doped pyrochlore sample a minor Cm species was found with the same environment as the major species in the defect fluorite structure and vice versa. This phenomenon could be used in future studies to quantify the radiation damage in a zirconate based pyrochlore.

Here, the local environment of  $\text{Cm}^{3+}$  and  $\text{Eu}^{3+}$  in  $\text{La}_2\text{Zr}_2\text{O}_7$  was investigated with time resolved laser fluorescence spectroscopy (TRLFS). The fluorescence spectra by UV excitation, direct excitation and lifetime measurements were performed for lanthanum zirconates with the defect fluorite and the pyrochlore crystal structure. It was found that in both  $\text{Eu}^{3+}$  doped materials there are two Eu species. Figure 1 compares two spectra of the direct excitation of  $\text{Eu}^{3+}$  to the  $^5\text{D}_0$  band. Apparently the minor species in the defect fluorite structure has adopted the pyrochlore site symmetry even though no long range ordering into the pyrochlore crystal structure could be observed.

The maximum splitting observed of the  $^5\text{D}_0 \rightarrow ^7\text{F}_{1,2}$  transition for the major Eu species in the defect fluorite structure

[1] Ewing, R. C. (2011) C.R. Geosci. 343, 219-229.

[2] Sickafus, K. E. et al. (2007) Nature Mater. 6, 217-223.

[3] Holliday, K. S. et al. submitted to J. Nucl. Mater.

## Multifunctional complexation agents for *d*- and *f*-elements

S. Ullmann, R. Schnorr, S. Haupt

Universität Leipzig, Fakultät für Chemie und Mineralogie, Institut für Anorganische Chemie, Leipzig, Germany

Calix[4]arenes are very potent host molecules and their conformational properties have been widely exploited to induce selectivity in the recognition of ions and neutral molecules [1]. Their controlled synthetic functionalization and versatile complexation properties along with unique three-dimensional structures arouse considerable attention in the field of supramolecular chemistry. They are commonly employed as molecular building blocks for the design of various receptor sites for the specific recognition of several guests [2]. They can be selectively functionalized both at the phenolic hydroxyl groups (*lower rim*) and at the *para* positions of the phenol rings (*upper rim*).

In our case, we do not use the calix[4]arene itself as ligand or receptor but as scaffold that bears two coordination sites with various chemical affinities. Particularly, these attributes shall be employed, for example in the selective extraction, coordination and migration of radionuclides like  $^{85}\text{Sr}$ ,  $^{131}\text{I}$ ,  $^{137}\text{Cs}$ , as well as *d*-elements, e.g.  $^{60}\text{Co}$  and  $^{64}\text{Cu}$  and also actinides like uranium. Hence, we developed new synthetic approaches to such bifunctional calix[4]arenes based on the de-alkylated 25,26,27,28-tetrahydroxycalix[4]arene. In our group we pursue two strategies: on the one hand, we develop synthetic approaches to bifunctional *lower* and *upper* rim modified calix[4]arenes in the *cone* conformation with exhausting substitution at the *exo* and *endo* face. On the other hand, we acquire the syntheses of bifunctional *lower rim* modified calix[4]arenes in the *partial cone* or *1,3-alternate* conformation with partial or total substitution at the *endo* face (Fig. 1).

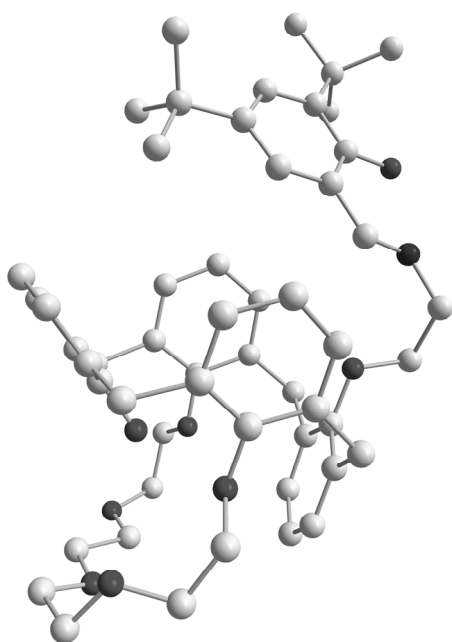


Fig. 1: Molecular structure of *partial cone* 25-(di-*tert*-butylsalicylidene)-diaminoethoxy-27-hydroxy-26,28-crown-5-calix[4]arene bearing a crown ether moiety as well as a salicylidene moiety.

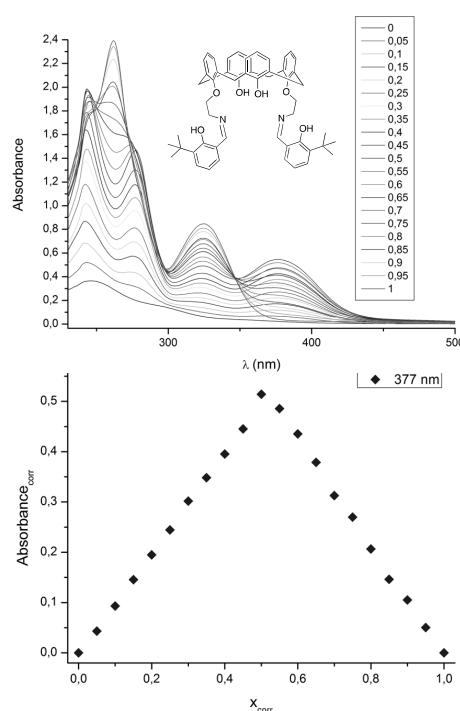


Fig. 2: Complex formation of 25,27-Bis-(*tert*-butylsalicylidene)-26,28-dihydroxycalix[4]arene-Cu(II) in  $\text{CHCl}_3/\text{MeOH}$  (1 : 1, v/v) solution at ambient temperature. Job plot obtained from UV/vis spectral intensity at 377 nm.

Therefore, we present an up-to-date outline of the synthetic strategies towards such novel multifunctional calix[4]arenes. Furthermore, we present syntheses, complexation studies (Fig. 2) and structural characterizations of selected compounds. This research project is funded by the Federal Ministry for Education and Research under grant number 02NUK014C.

[1] Gutsche, C. D. (2008) Calixarenes. An Introduction, 2<sup>nd</sup> Edition, RSC Publishing, Cambridge.

[2] Baldini, L. et al. (2007) Chemical Society Reviews 36, 254-266.

## Coordination compounds of trivalent rare earth metals with hydrazone-supported tripodal $\kappa^6N$ donor ligands

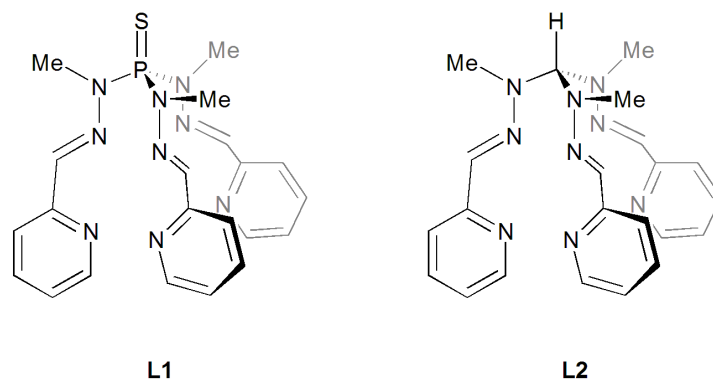
S. Hohnstein,<sup>1</sup> M. Löble,<sup>1,2</sup> I. Trapp,<sup>1</sup> J. Meyer,<sup>1</sup> D. Matioszek,<sup>1</sup> I. Fernández,<sup>3</sup> P. Oña-Burgos,<sup>1</sup> T. Vitova,<sup>2</sup> J. Rothe,<sup>2</sup> K. Dardenne,<sup>2</sup> P. Lindqvist-Reis,<sup>2</sup> M. A. Denecke,<sup>2</sup> F. Breher<sup>1</sup>

<sup>1</sup> Karlsruhe Institute of Technology (KIT), Institute of Inorganic Chemistry, Karlsruhe, Germany

<sup>2</sup> Karlsruhe Institute of Technology (KIT), Institute for Nuclear Waste Disposal (INE), Karlsruhe, Germany

<sup>3</sup> Universidad de Almería, Laboratory of Organic Chemistry, Almería, Spain

Rare earth metal coordination compounds of *N*-donor ligands are of special interest because of their variety of applications, e.g. in catalysis [1] and medicine [2]. They play an important role in the reprocessing of spent nuclear fuels [3] by extracting the minor actinides (e.g., curium, americium) from high-level radioactive waste. This operation is followed by transmutation of the actinides into short-lived isotopes. To improve the performance of existing extraction ligands and to develop more suitable ones understanding their selectivity for actinides over the chemically similar lanthanide cations is essential. Crucial factors are the characterization of the metal-ligand bond in the complex, the influence of counter-anions and the behavior of all existing species in solution. In order to investigate these influencing factors, our group became interested in tripodal ligands with podand topology, which provide intrinsically well-defined coordination geometries [4]. This poster presentation will focus on the coordination chemistry of the recently synthesized multisite ligands (S)P[N(Me)N=C(H)Py]<sub>3</sub> (**L1**) and HC[N(Me)N=C(H)Py]<sub>3</sub> (**L2**) [5, 6].



Several complexes with various trivalent rare earth metal cations will be presented. The coordination compounds of the general formulas [M(**L1**)](OTf)<sub>3</sub> and [M(**L2**)](OTf)<sub>3</sub> have been characterized by several methods including X-ray diffraction on single crystals, NMR spectroscopy, TRLFS, or XAS, either in the solid-state or in solution [7].

[1] Edlmann, F. T. (2009) Chem. Soc. Rev. 38, 2253-2268.

[2] Thompson, K. H. and Orvig, C. (2006) Chem. Soc. Rev. 35, 500-511.

[3] Kolarik, Z. (2008) Chem. Rev. 108, 4208-4252.

[4] Breher, F. et al. (2008) Dalton Trans., 5836-5865.

[5] Hormes, J. et al. (2010) IOP Conf. Series: Materials Science and Engineering 9, 012053.

[6] Breher, F. et al. (2011) Inorg. Chim. Acta 374, 373-384.

[7] Roesky, P. W. et al. (2012) Chem. Eur. J. 18, 5325-5334.

## Investigations into the formation of neptunium(IV)-silica colloids

R. Husar, S. Weiss, H. Zänker, G. Bernhard

Helmholtz-Zentrum Dresden-Rossendorf, Institute of Resource Ecology, Dresden, Germany

Knowledge on the mobility of actinides is crucial in predicting potential release of radionuclides from nuclear waste repositories. Under the reducing conditions expected for such repositories, the tetravalent form of the actinides, An(IV), is predominant. Due to the low solubility at neutral pH, An(IV) are considered to be immobile. Nevertheless, high environmental mobility has been found e.g. for Pu(IV) [1, 2]. This is obviously related to the formation of An(IV) eigencolloids or to the sorption onto other colloids. In the laboratory An(IV)O<sub>2</sub>·xH<sub>2</sub>O colloids have been produced [3, 4]. For U(IV) and Th(IV), there is evidence for the formation of silica-containing colloids [5, 6].

We developed a method to generate solutions of Np(IV) and tried to figure out if Np(IV), too, can form silica-containing colloids. Under anaerobic conditions Np(IV) carbonate solutions in presence and absence of silicate were investigated by UV-Vis spectroscopy, ultrafiltration, LSC and Dynamic light scattering (DLS).

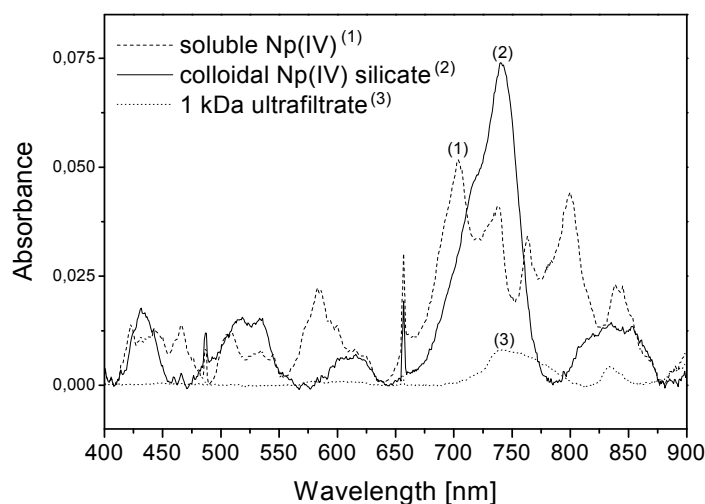


Fig. 1: UV-Vis spectra of the soluble Np(IV) carbonate (1) ( $1.82 \cdot 10^{-3}$  M Np(IV), 1 M NaHCO<sub>3</sub>), the colloidal Np(IV) (2) ( $1.72 \cdot 10^{-3}$  M Np(IV),  $3.2 \cdot 10^{-3}$  M Si, 0.1 M NaHCO<sub>3</sub>), and the ultrafiltrate of colloidal Np(IV) silicate (3).

Figure 1 shows UV-Vis absorption spectra of solutions containing Np(IV) species determined after 24 h equilibration time. Curve (1) represents the spectrum of a typical Np(IV) solution in 1 M carbonate. In the case of solution 2 (curve 2), the carbonate concentration was only 0.1 M. At that concentration carbonate is not able to stabilize Np(IV) in solution as carbonate complexes and Np(IV) precipitates with total decrease of UV-vis spectrum [7]. However, also silicate was admixed to solution 2 which prevented the Np(IV) from precipitation.

A characteristic spectrum (curve 2) of colloidal Np(IV) silicate is

generated which differs from that of truly dissolved Np(IV) carbonate complexes. The light absorption is significantly higher and the peaks are shifted as shown by the absorption band at 741 nm. The colloid-disperse Np(IV) silicate solution exhibits an increased scattering light intensity. DLS gave diameters < 20 nm. Ultrafiltration removes these particles and decreases the UV-vis absorbance (curve 3) resulting in the disappearance of the absorption band at 741 nm; it also reduces the concentration of Np from  $1.8 \cdot 10^{-3}$  to  $0.3 \cdot 10^{-3}$  M. All these observations are caused by colloidal behaviour.

In presence of silicate we observed a stabilized dispersion of precipitated Np(IV) colloids. The existence of such colloids has never been reported so far. Consequently, Np(IV) can form silicate-containing colloids and may become waterborne even if the limit of solubility is exceeded.

- [1] Buddemeier, R. et al. (1988) *Appl. Geochem.* 3, 535.
- [2] Utsunomiya, S. et al. (2009) *Environmental Science & Technology* 43, 1293.
- [3] Altmaier, M. et al. (2004) *Radiochim. Acta* 92, 537.
- [4] Neck, V. et al. (2001) *Radiochim. Acta* 89, 439.
- [5] Dreissig, I. et al. (2011) *Geochimica et Cosmochimica Acta* 75, 352.
- [6] Hennig, C. et al., *Geochimica et Cosmochimica Acta* (submitted).
- [7] Rai, D. et al. (1999) *Radiochim. Acta* 84, 159.

## UV-vis studies of 2-hydroxy-3-methoxyphenyl and 2-hydroxy-3-ethoxyphenyl diimines with *f*-elements

N. Kelly, A. Heine, F. Taube, Ke. Gloe, K. Gloe

Dresden University of Technology, Department of Chemistry and Food Chemistry, Dresden, Germany

The coordination chemistry of multifunctional *Schiff* bases with lanthanide and actinide ions has been the focus of a considerable number of investigations [1]. In their complexes, lanthanides and actinides show specific affinities to oxygen and nitrogen donor atoms.

In this work, we report the synthesis and UV-vis studies of complexes of novel 2-hydroxy-3-methoxyphenyl and 2-hydroxy-3-ethoxyphenyl diimines ( $\text{H}_2\text{L}^1$  and  $\text{H}_2\text{L}^2$ ) having different linking elements. According to similar ligands in the literature these *Schiff* bases lead to complexes with *d*- or *f*-block elements using the  $\text{N}_2\text{O}_2$  and  $\text{O}_4$  donor sets [2]. As a consequence, heterobinuclear complexes can be formed, which contain *d*-elements and Ln(III) or U(VI) together.

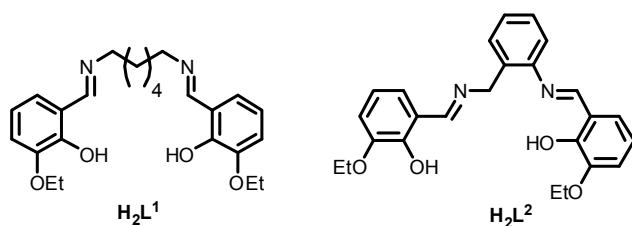


Fig. 1: Structures of ligands  $\text{H}_2\text{L}^1$  and  $\text{H}_2\text{L}^2$ .

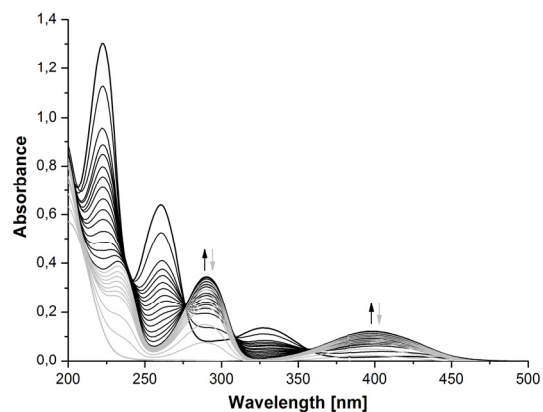


Fig. 2: Absorbance spectra of  $\text{H}_2\text{L}^1$  and  $\text{Eu}(\text{NO}_3)_3$  in acetonitrile ( $c = 2.5 \cdot 10^{-5}$  mol/L).

[1] Vigato, P.A. and Tamburini, S. (2004) *Coord. Chem. Rev.* 248, 1717-2128.

[2] Costes, J.-P. et al. (2003) *Inorg. Chem.* 43, 7792-7799.



## Mo<sub>n</sub>O<sub>m</sub> species distributions in acidic solution measured by electrospray ionization mass-spectrometry

M. Cheng, M. Steppert, C. Walther

Institut für Radioökologie und Strahlenschutz, Leibniz Universität Hannover, Hannover, Germany

Within the scope of the development of advanced fuels for generation IV reactors, molybdenum oxide is investigated as inert matrix to embed the fissile material. The application of these matrices should enhance the retention of radionuclides, especially of Pu(IV) and Am(III)/Cm(III), during operation, reprocessing and disposal of the spent nuclear fuel. Before the leaching of actinides from these matrices can be investigated, the species formed upon dissolution of the molybdenum oxide have to be known. To that end, electrospray ionization mass spectrometry [1, 2], which can probe the stoichiometry and relative abundances of solution species, was applied [3].

MoNa<sub>2</sub>O<sub>4</sub>·2H<sub>2</sub>O (natural isotopic distribution) was dissolved in nitric acid ([HNO<sub>3</sub>] = 0.5 M through [HNO<sub>3</sub>] = 3 M) to give [Mo] = 5 mM through 30 mM. In a second set of measurements, Mo metal powder was dissolved in conc. (67%) nitric acid and after 1 day the sample was diluted with distilled water to give a stock solution of ([HNO<sub>3</sub>] = 3 M, [Mo] = 60 mM). This stock solution was aged for 13 days. Prior to each measurement the actual samples were prepared by dilution with 3 M nitric acid to give the appropriate concentration. 1-10 μL sample was introduced into a spray capillary (New Objective) and sprayed into vacuum using mild declustering conditions [1, 2], preserving a solvent shell.

An example of an ESI TOF mass-over-charge spectrum in logarithmic representation is shown in Fig. 1. Each envelope corresponds to one polymer size Mo<sub>x</sub>O<sub>y</sub> with various numbers of water molecules in the droplet causing clusters of peaks. In all samples, Mo polymerizes strongly, the monomer does not play an important role. In contrast to measurements on Zr, Th and Pu polymers [3, 4], the Mo(VI) polymers carry a charge due to an additional H<sup>+</sup> (Na<sup>+</sup>) ion. The size distribution extends well beyond the decamer in all cases, with the dimer being the most abundant species. In many solutions the hexamer is almost absent and the pentamers and heptamers are somewhat suppressed, possibly due to a geometrical destabilization of the hexamer.

From the present measurements, we conclude that nano ESI is well suited for quantifying the species distribution of Mo in highly acidic media. Spectra were unambiguously evaluable and measurements were well reproducible. Depending on concentration more or less pronounced ageing of solutions was observed over a time span up to 45 d, leading in all cases to formation of larger polymers. The dependence on acidity was not very pronounced between [HNO<sub>3</sub>] = 0.5 M and 3 M. In the future, the leaching behavior of radionuclides embedded in molybdenum oxide matrices will be investigated by spectroscopic and mass spectrometric means.

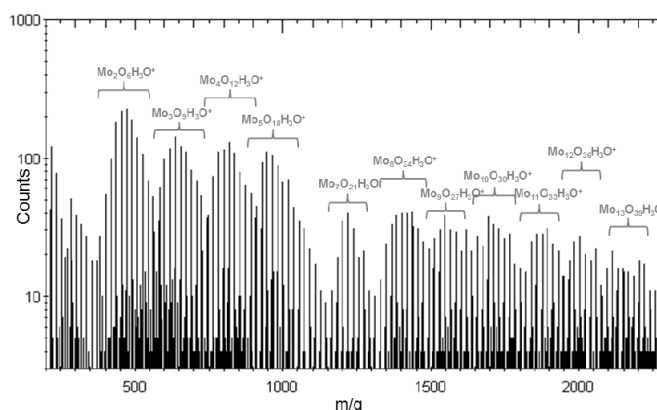


Fig. 1: Time-of-flight mass spectrum of a sample with [Mo] = 40 mM, [HNO<sub>3</sub>] = 3 M.

[1] Wilm, M. and Mann, M. (1996) *Anal. Chem.* 68, 1-8.

[2] Cole, R. B. (1997) *Electrospray ionization mass spectrometry*, John Wiley and Sons, New York.

[3] Walther, C. (2007) *Anal. Bioanal. Chem.* 388, 409-431.

[4] Walther, C. (2012) *Dalton Trans.*, DOI: 10.1039/C2DT30243H.

## Complexation behaviour of U(VI) and Eu(III) with Schiff Bases investigated by laser-induced spectroscopy

K. Lindner, A. Günther, G. Bernhard

Helmholtz-Zentrum Dresden-Rossendorf, Institute of Resource Ecology, Dresden, Germany

Actinides can be released into the environment particularly from mining areas by weathering and erosion processes, anthropogenic activities as well after incidents at nuclear power plants representing potential health issues for human beings. Lanthanides rarely occur in nature, but they constitute major players in the production chain in glass and ceramics industries, in metallurgy and in the cracking of petroleum. Therefore, new supramolecular complexing agents with N, O, S donor function are developed to selectively separate elements of the d- and f-block and to enrich rare earth elements. Schiff Bases are essential basic components of these new organic ligands.

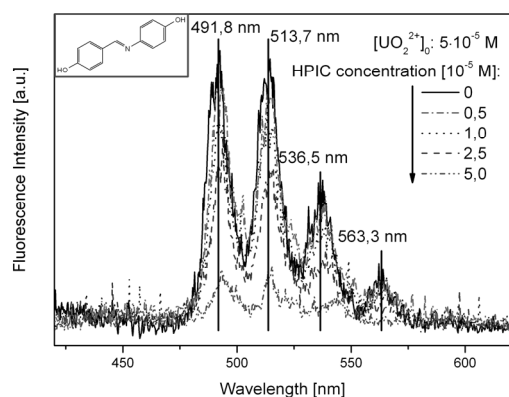


Fig. 1: Uranium(VI) luminescence spectra of different complex solutions at 240 mV and 153 K.

sity in presence of the Schiff Base (cf. Fig. 1). Because of the peak maxima were not shifted, it is obvious that the complexes do not show specific fluorescence properties.

At room temperature, the fluorescence of Eu(III) was not affected by methanol. But it turned out that the Eu(III) in methanol solution forms an asymmetric complex in comparison to the Eu(III)-water complex [1]. The Eu(III) fluorescence decreased in presence of the Schiff Bases. The observed splitting of the peaks suggests the presence of two different Eu(III) species in the samples.

Femtosecond (fs) TRLFS investigations provide the possibility to determine very short-lived organic complex species. The fs-TRLFS as a sensitive speciation technique was used to determine the fluorescence properties of the free ligand and the complexes in the U(VI)-NBA, U(VI)-HBAP and U(VI)-HPIC systems. The emission signals show bathochromic shifts in comparison to the emission maxima of the uncomplexed ligand (Fig. 2). The intensity of the ligand fluorescence increased with the increasing U(VI) concentration. Corresponding to the first analyses of the time resolved measurements, the luminescence lifetimes of the free ligand and the U(VI) complex species are in the range from 2-4 ns. By the change of the emission properties of organic ligands or metals, the complexation with U(VI) and Eu(III) can be observed and corresponding complex formation constants can be calculated.

In this study, the complexation of uranium(VI) and europium(III) with the Schiff bases N-benzylidene-aniline (NBA), 2-(2-hydroxybenzylidene-amino)phenol (HBAP) and alpha-(4-hydroxyphenyl-imino)-p-cresol (HPIC) was investigated in methanolic solution using time-resolved laser-induced fluorescence spectroscopy (TRLFS) at room and cryogenic temperature and in the case of the U(VI)-Schiff bases systems by applying of TRLFS with ultrashort laser pulses (fs-TRLFS).

The measurements of the uranyl luminescence in alcoholic solution at room temperature showed strong quenching effects by the solvent which could be minimized by measurements at cryogenic temperature (153 K). At low temperature, the same spectra were observed with a significantly decreased inten-

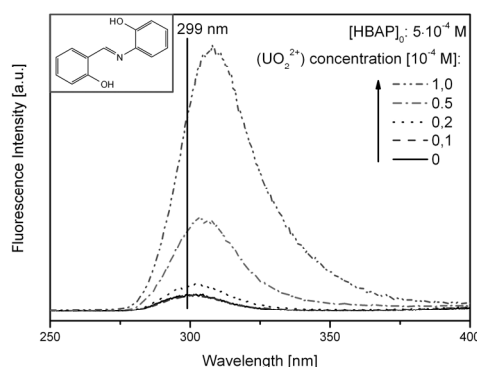


Fig. 2: fs-TRLFS spectra of U(VI)-HBAP system at 120 mV and room temperature.

[1] Choppin, G. R. and Peterman, D. R. (1998) Coord. Chem. Rev. 147, 283-299.

## Spectroscopic study on structure of 2,2'-(Methylimino)bis(N,N-Dioctylacetamide) complex with $\text{Re(VII)O}_4^-$ and $\text{Tc(VII)O}_4^-$

M. Saeki,<sup>1</sup> Y. Sasaki,<sup>2</sup> A. Nakai,<sup>3</sup> A. Ohashi,<sup>3</sup> D. Banerjee,<sup>4</sup> A. C. Scheinost,<sup>4</sup> H. Foerstendorf<sup>4</sup>

<sup>1</sup> Quantum Beam Science Directorate, Japan Atomic Energy Agency, Japan

<sup>2</sup> Nuclear Science and Engineering Directorate, Japan Atomic Energy Agency, Japan

<sup>3</sup> College of Science, Ibaraki University, Japan

<sup>4</sup> Helmholtz-Zentrum Dresden-Rossendorf, Institute of Resource Ecology, Dresden, Germany

2,2'-(Methylimino)bis(N,N-Dioctylacetamide) (MIDOA) was found to be a compatible receptor for  $\text{M(VII)O}_4^-$  ( $\text{M} = \text{Re}$  and  $\text{Tc}$ ) in the liquid-liquid extraction [1], although the molecular interaction of MIDOA with  $\text{M(VII)O}_4^-$  was unclear. We prepared the MIDOA complexes with  $\text{M(VII)O}_4^-$  by the liquid-liquid solvent extraction and obtained information about their structures and chemical states from  $^1\text{H-NMR}$ , EXAFS and FT-IR spectroscopy [2].

The  $^1\text{H-NMR}$  spectra of the complex of MIDOA with  $\text{Re(VII)O}_4^-$  prepared in the organic solution suggest the transfer of a proton from aqueous to organic solution and the formation of the  $\text{H}^+\text{MIDOA}$  ion. The EXAFS spectra of the complexes of  $\text{H}^+\text{MIDOA}$  with  $\text{Re(VII)O}_4^-$  and  $\text{Tc(VII)O}_4^-$  show only the  $\text{M-O}$  coordination of the aquo complexes, suggesting that the chemical state of  $\text{M(VII)O}_4^-$  was unchanged during the extraction process. The results from  $^1\text{H-NMR}$  and EXAFS provide therefore evidence of  $\text{M(VII)O}_4^- \cdots \text{H}^+\text{MIDOA}$  complex formation in the organic solution.

Detailed structure of the  $\text{M(VII)O}_4^- \cdots \text{H}^+\text{MIDOA}$  complex was investigated by IR spectroscopy and DFT calculation. As shown in Fig. 1, the IR spectrum of  $\text{Re(VII)O}_4^- \cdots \text{H}^+\text{MIDOA}$  shows appearance of a sharp band at  $910\text{ cm}^{-1}$  and a broad one centering at  $3400\text{ cm}^{-1}$ . The sharp band is assigned to the  $\nu_3$  antisymmetric stretching mode of  $\text{Re(VII)O}_4^-$ . The broad band assigned to the hydrogen-bonded stretching mode of  $\text{N-H}^+$  in  $\text{H}^+\text{MIDOA}$ , because in the IR spectrum of  $\text{Re(VII)O}_4^- \cdots \text{D}^+\text{MIDOA}$  the band is shifted to  $\sim 2600\text{ cm}^{-1}$  upon deuteration. The B3LYP/cc-pVDZ calculation suggests the structure in Fig. 2 is most stable in isomers of  $\text{Re(VII)O}_4^- \cdots \text{H}^+\text{MIDOA}$ . The  $\text{Re(VII)O}_4^-$  ion interacts with  $\text{H}^+\text{MIDOA}$  through multiple  $\text{C-H}_n \cdots \text{O}$  hydrogen bonds. In addition, the  $\text{H}^+\text{MIDOA}$  ion is stabilized by formation intramolecular hydrogen bond. The calculated IR spectrum reproduced the observed one very well. In the  $\text{Tc(VII)O}_4^- \cdots \text{H}^+\text{MIDOA}$  complex, the IR spectrum and calculated structure was similar with those of  $\text{Re(VII)O}_4^- \cdots \text{H}^+\text{MIDOA}$ . Thus, we concluded that the  $\text{M(VII)O}_4^- \cdots \text{H}^+\text{MIDOA}$  complex has the structure shown in Fig. 2.

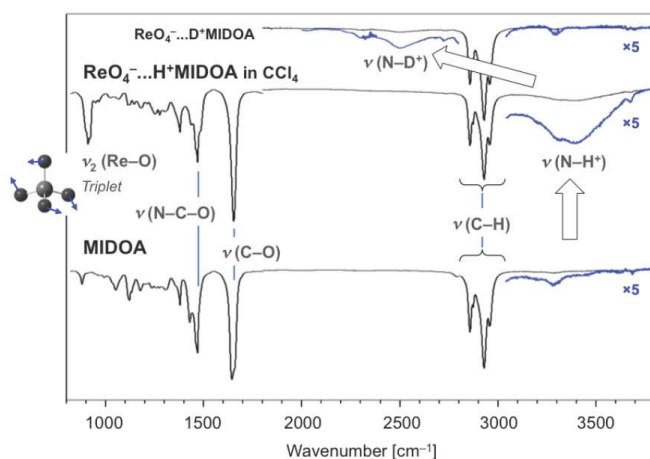


Fig. 1: IR spectra of  $\text{Re(VII)O}_4^- \cdots \text{H}^+\text{MIDOA}$ ,  $\text{Re(VII)O}_4^- \cdots \text{D}^+\text{MIDOA}$  and MIDOA.

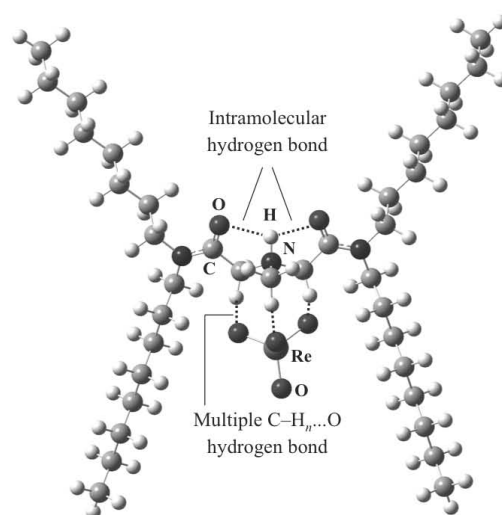


Fig. 2: Structure of the  $\text{Re(VII)O}_4^- \cdots \text{H}^+\text{MIDOA}$  complex determined from the IR spectrum and DFT calculation.

[1] Sasaki, Y. et al. (2007) Chem. Lett. 36, 1394-1395.

[2] Saeki, M. et al. (2012) Inorg. Chem. 51, 5814-5821.

---

## Curium(III) as intrinsic luminescence probe for direct speciation studies in biogeochemical systems

H. Moll, L. Lütke, J. Raff, V. Brendler, G. Bernhard

Helmholtz-Zentrum Dresden-Rossendorf, Institute of Resource Ecology, Dresden, Germany

Knowledge concerning the speciation of actinides is essential to understand their fate and behavior in the environment. Moreover, the speciation of actinides influences their behavior in biological systems (e.g., microbes) in terms of chemical toxicity and radiotoxicity. For many years we are successfully operating a unique pulsed flash lamp pumped Nd:YAG-OPO laser system (Powerlite Precision II 9020 laser equipped with a Green PANTHER EX OPO from Continuum, Santa Clara, CA, U.S.A.) designed especially to detect the luminescence of trivalent actinides and lanthanides (e.g., Cm, Eu). The luminescence spectra were detected using an optical multi-channel analyzer-system, consisting of an Oriel MS 257 monochromator and spectrograph with a 300 or 1200 line mm<sup>-1</sup> grating and an Andor iStar ICCD camera (Lot-Oriel Group, Darmstadt, Germany). The high performance of this system for direct speciation studies of Curium(III) in biogeochemical systems will be presented on the basis of selected examples. These examples cover geochemical systems: the aqueous Cm(III) phosphate system [1] and biological systems: (a) Cm(III) speciation studies with cells of a groundwater strain of *Pseudomonas fluorescens* [2] and (b) Cm(III) complexation with bacterial surface-layer proteins [3].

Acknowledgement: This work was partly funded by BMWi under contract number 02E10618. The authors are indebted to the U.S. Department of Energy, Office of Basic Energy Sciences, for the use of <sup>248</sup>Cm via the transplutonium element production facilities at Oak Ridge National Laboratory; <sup>248</sup>Cm was made available as part of collaboration between HZDR and the Lawrence Berkeley National Laboratory (LBNL).

---

[1] Moll, H. et al. (2011) *Radiochim. Acta* 99, 775-782.

[2] Moll, H. et al. (2012) *Geomicrobiol. J.*, in press.

[3] Moll, H. et al. (2011) Poster at the 13th International Conference on the Chemistry and Migration Behavior of Actinides and Fission Products (MIGRATION 2011), Sept. 18-23, 2011, Beijing, PR China.

## A theoretical and experimental study of actinide complexes of nitrate, amide and phosphine oxide

K. Ribokaité,<sup>1</sup> P. Guilbaud,<sup>1</sup> N. Boubals,<sup>1</sup> R. D. Guillaumont,<sup>1</sup> R. Vuilleumier<sup>2</sup>

<sup>1</sup> CEA Marcoule DRCP/SCPS/LILA, Bagnols sur Cèze, France

<sup>2</sup> ENS, Departement of Chemistry, Paris, France

A comprehensive theoretical and experimental study has been carried out to investigate the coordination environment of uranyl and actinide(IV) in water and methanol in the presence of nitrate ions and amide or phosphine oxides ligands. Short alkyl chain amide and phosphine oxide ligands were chosen as models of lipophilic extractant ligands [1, 2]. The ligands studied are shown in Fig. 1.

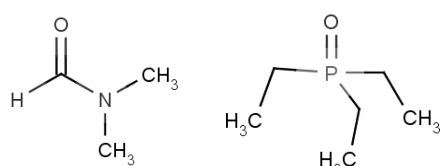


Fig. 1: Ligands: DMF and TEPO.

and nitrate ions in the first coordination sphere are analyzed.

Experimentally the molecular properties of the complexes in the liquid phase were probed by, UV-Visible, EXAFS, Infra-red and Raman spectroscopy at a low pH range. The complexation of the water-soluble ligands to uranyl was monitored through optical absorbance spectroscopy, and stability constants were obtained. In the 600-1800  $\text{cm}^{-1}$  region, the experimental IR/Raman bands were identified and assigned to specific molecular vibrations of investigated complexes in water and methanol using the theoretical calculations obtained by DFT (B3LYP) (Tab.1).

The main objective of the study is to explore how small modifications of the ligands may alter the molecular structures of the complexes in solution by using a combination of theoretical and experimental methods.

The theoretical part has been carried out using density functional theory and molecular dynamics approaches. The solvent was approximated by a dielectric continuum model or through explicit water/methanol molecules. Structural and dynamical properties of the ligands

Tab. 1: Calculated frequencies of the symmetric ( $\nu_s$ ) and antisymmetric ( $\nu_{as}$ ) stretching vibrations of uranyl in the complexes ( $\text{cm}^{-1}$ ) and distance of U- $\text{O}_{yl}$  (Å) in water.

Complexes	$\nu_s$	$\nu_{as}$	R(U- $\text{O}_{yl}$ )
$\text{UO}_2(\text{H}_2\text{O})_5$	923	987	1.757
$\text{UO}_2(\text{H}_2\text{O})_4(\text{NO}_3^-)$ mono	902	969	1.763
$\text{UO}_2(\text{H}_2\text{O})_3\text{DMF}(\text{NO}_3^-)$ mono	889	955	1.768
$\text{UO}_2(\text{H}_2\text{O})_3\text{TEPO}(\text{NO}_3^-)$ mono	872	946	1.771

[1] Musikas, C. (1988) Separation Science and Technology 23, 1211-1226.

[2] Laskorin, B. N. et al. (1974) Journal of Radioanalytical Chemistry 21, 65-79.

## A study of the sorption of U(VI) onto SiO<sub>2</sub> in the presence of phosphate by ATR FT-IR spectroscopy

M. J. Comarmond,<sup>1</sup> H. Foerstendorf,<sup>2</sup> K. Gückel,<sup>2</sup> K. Müller,<sup>2</sup> V. Brendler,<sup>2</sup>  
T. E. Payne<sup>1</sup>

<sup>1</sup> Australian Nuclear Science and Technology Organisation, Locked Bag, Kirrawee, Australia

<sup>2</sup> Helmholtz-Zentrum Dresden-Rossendorf, Institute of Resource Ecology, Dresden, Germany

Adsorption onto mineral surfaces is a key process for controlling the migration of actinides in the environment, and is influenced by a number of factors including pH, ionic strength, partial pressure of CO<sub>2</sub>, mass loading, actinide concentration, and the presence of ligands [1]. Attenuated total reflection Fourier-transform infrared (ATR FT-IR) spectroscopy is a powerful technique for *in situ* investigation of the solid-liquid interface at the molecular level, providing information on sorption mechanisms and the identification of surface complexes [2], as has been successfully demonstrated in studies of actinide sorption onto model minerals [3, 4].

In the present work, ATR FT-IR spectroscopy was used for an *in situ* investigation of uranyl sorption on SiO<sub>2</sub> at pH 4.0 in the presence of phosphate. The phosphate ligand is known to influence uranium sorption on model minerals, with batch sorption studies showing an increase in the uptake of uranium at low pH values [1, 5]. The formation of ternary surface complexes and/or precipitation has been suggested as possible mechanisms for this increase in sorption [1, 5].

ATR FT-IR studies were conducted for the U(VI)/SiO<sub>2</sub>/phosphate ternary system containing 20 µM U(VI), 20 µM NaH<sub>2</sub>PO<sub>4</sub> and 0.1 M NaCl at pH 4 and compared to a similar reference system without silica present. Chemical speciation modeling indicates that the solution speciation of uranyl is predominantly UO<sub>2</sub><sup>2+</sup>, with minor amounts of UO<sub>2</sub>HPO<sub>4</sub> (aq), UO<sub>2</sub>Cl<sup>+</sup>, UO<sub>2</sub>OH<sup>+</sup> and UO<sub>2</sub>H<sub>2</sub>PO<sub>4</sub><sup>+</sup>, and the solution is slightly oversaturated with (UO<sub>2</sub>)<sub>3</sub>(PO<sub>4</sub>)<sub>2</sub>·4H<sub>2</sub>O. The vibrational spectroscopy for the ternary system shows that the spectra at the early stage of sorption differ from that after prolonged sorption. The results indicate the possible formation of two species/complexes and two types of binding sites provided by the SiO<sub>2</sub> surface. We postulate that the early stage of uptake is dominated by the sorption of free uranyl species as an outer sphere complex with bands at ca 920 cm<sup>-1</sup>, 1452 cm<sup>-1</sup> and 1530 cm<sup>-1</sup> [6] in addition to a transient species reflected by the new band at ca. 1030 cm<sup>-1</sup>. The sorption then becomes dominated by the precipitation of uranyl phosphate with bands at 1125 cm<sup>-1</sup>, 993 cm<sup>-1</sup> and 919 cm<sup>-1</sup>.

[1] Payne, T. E. et al. (1998) in: Adsorption of Metals by Geomedia (Jenne, E. A., ed.), p. 75-97, Academic Press, San Diego.

[2] Lefèvre, G. (2004). Adv. Colloid Interface Sci. 107, 109-123.

[3] Müller K. et al. (2009). Env. Sci. Technol. 43, 7665-7670.

[4] Gückel, K. et al. (2012). Chem. Geol. 326-327, 27-35.

[5] Zhang, H. and Tao, Z. (2001). J. Rad. Nucl. Chem. 254, 103-107.

[6] Müller, K. et al. (2008) Inorg. Chem. 47, 10127-10134.

## Surface interaction studies of Ln(III)/ An(III) with site-selective time resolved laser fluorescence spectroscopy

S. Hofmann, T. Stumpf, M. Schmidt

Karlsruhe Institute of Technology (KIT), Institute for Nuclear Waste Disposal (INE), Karlsruhe, Germany

The time resolved laser fluorescence spectroscopy (TRLFS) is a suitable method for the determination of the chemical environment of many lanthanides and the actinide ions Pa(IV), U(IV), U(VI), Am(III) und Cm(III) at trace concentrations in both solid and liquid phase. After excitation by pulsed laser light, fluorescence is detected in a nano to milisecond time scale and the obtained luminescence lifetimes are correlated with the quantity of water molecules in the first coordination shell of the ion [1]. The site-selective TRLFS of Eu(III) and Cm(III) doped mineral phases yields additional information about the ion-surface interaction.

**SITE-SELECTIVE TRLFS.** We used europium as a homologue for the trivalent actinides due to its spectroscopic properties and chemically similar behaviour. Earlier TRLFS studies [2] have shown that Eu forms solid solutions with calcite under certain conditions ( $T = 25\text{ }^{\circ}\text{C}$ ,  $IS = 0.01\text{ M}$ ,  $\text{ClO}_4^-$  trace concentration). Direct excitation of the  ${}^7\text{F}_0 \rightarrow {}^5\text{D}_0$  transition in the range of 575-585 nm results in spectra that show different Eu species in the sample. Three different sites were determined (solid line, Fig. 1) with this method: These have been identified as one surface sorbed (site A) and two incorporated species (sites B and C, Tab. 1). After excitation of the single species, the splitting patterns of the  ${}^7\text{F}_1$  and  ${}^7\text{F}_2$  emission bands give information about the respective ligand field geometry.

**RECENT RESULTS.** By using  $2\text{ }\mu\text{M}$  europium nitrate ( $T = 25\text{ }^{\circ}\text{C}$ ,  $IS = 0.02\text{ M}$ ) instead of perchlorate, a bathochromic shift of the excitation maximum of about  $0.5\text{ nm}$  was observed (dotted line, Fig. 1). The long emission lifetime of this species ( $\bar{\tau} = 602 \pm 59\text{ }\mu\text{s}$ , Tab. 2) indicates that there is only one water molecule left in the first coordination sphere of the lanthanide ion (Horrock's equation [2]). An increase of pH to 9 and 10 results in expanded excitation spectra with only one peak (dashed line, Fig. 1). Lifetime measurements show that at pH 9 two Eu species are present and at pH 10 only one of them remains. Considering the ubiquity of nitrate, hydroxide and other anions in the geosphere, this will highly affect modelling calculations for long term safety assessment of nuclear waste deposits.

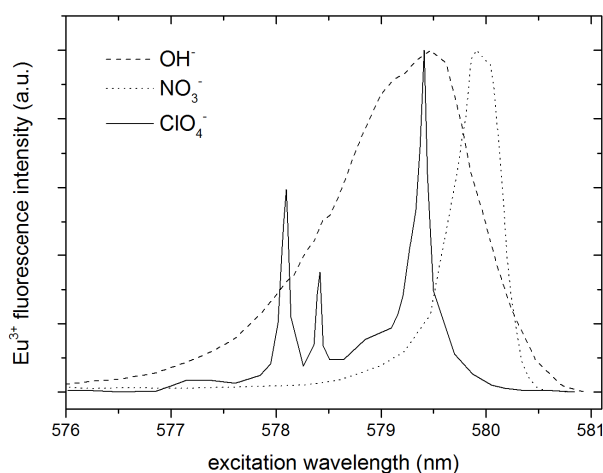


Fig. 1: TRLFS excitation spectra of Eu(III) doped calcite samples in presence of different anions ( $\text{OH}^-$ ,  $\text{NO}_3^-$ ,  $\text{ClO}_4^-$ ).

Tab. 1: Fluorescence lifetimes and number of water molecules in the first coordination shell of Eu(III) in coprecipitation experiment.

Site	Fluorescence lifetime ( $\mu\text{s}$ )	$n(\text{H}_2\text{O})$
A	$460 \pm 80$	$1.7 \pm 0.3$
B	$3616 \pm 450$	$0.0 \pm 0.0$
C	$3661 \pm 220$	$0.0 \pm 0.0$

Tab. 2: Fluorescence lifetimes and number of water in nitrate present experiments.

Sample	Fluorescence lifetime ( $\mu\text{s}$ )	$n(\text{H}_2\text{O})$
Batch-exp. (34d)	$548 \pm 53$	$1.3 \pm 0.2$
Batch-exp. (53d)	$600 \pm 52$	$1.2 \pm 0.2$
MFR-exp.	$677 \pm 52$	$1.0 \pm 0.1$

[1] Horrocks (1979) J. Am. Chem. Soc. 101, 334.

[2] Schmidt (2008) Angew. Chem. Int. Ed. 47, 5846–5850.

## Ultrasensitive detection of actinides by accelerator mass spectrometry

G. Rugel,<sup>1</sup> S. Akhmadaliev,<sup>2</sup> S. Merchel,<sup>1</sup> S. Pavetich<sup>1</sup>

<sup>1</sup> Helmholtz Institute Freiberg for Resource Technology, Division Resource Analytics, Dresden, Germany

<sup>2</sup> Helmholtz-Zentrum Dresden-Rossendorf, Institute of Ion Beam Physics and Materials Research, Dresden, Germany

Accelerator mass spectrometry (AMS) represents an ultrasensitive technique for quantifying long-lived radionuclides. The new AMS facility DREAMS (DRESDEN AMS, Fig. 1) will broaden the spectrum of measurable radionuclides like  $^{10}\text{Be}$ ,  $^{26}\text{Al}$ ,  $^{36}\text{Cl}$ ,  $^{41}\text{Ca}$  [1] to actinides with the setup of a new time-of-flight (TOF) beam line.

AMS is capable of quantifying isotope ratios, i.e. stable nuclides are usually measured in Faraday-cups while radionuclides are counted by detectors like an ionization chamber. In comparison to  $\alpha$ -spectrometry a relative simple chemical sample preparation can be applied and isotopes like  $^{239}\text{Pu}$  and  $^{240}\text{Pu}$  can be distinguished at the detector. AMS determines ratios as low as  $10^{-16}$ , thus, providing the lowest detection limit of all mass spectrometry methods [2]. For long half-lives it is also more sensitive than decay counting techniques.

We expect about 100 events in the detector for samples containing an amount of about  $10^4$  to  $10^6$  atoms of the radionuclide in the ion source. As an example the sensitivity limit for a  $^{236}\text{U}/\text{U}$  ratio is about  $10^{-12}$  [3].

This high sensitivity allows many applications from nuclear forensics, radiation protection, environmental monitoring to astrophysics. Isotopes measured by AMS are e.g.  $^{236}\text{U}$ ,  $^{237}\text{Np}$ ,  $^{239,240,241,242,244}\text{Pu}$  [3].

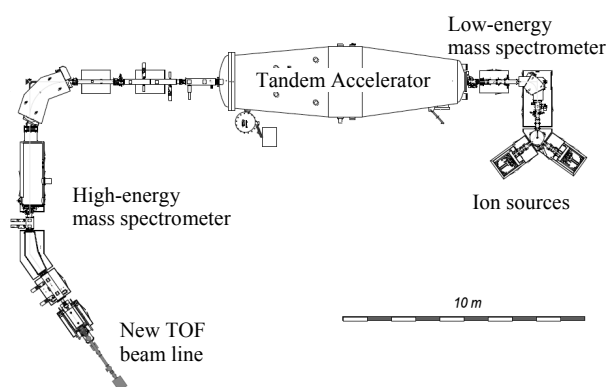


Fig. 1: AMS setup at DREAMS with the new TOF beam line.

This setup will be also used in the future analyzing geological samples with high lateral resolution – without chemical sample preparation – a so called Super-SIMS – a combination of a SIMS (Secondary Ion Mass Spectrometry) with an accelerator.

[1] Akhmadaliev, S. et al. (2012) Nucl. Instr. and Meth. in Phys. Res. B, doi: 10.1016/j.nimb.2012.01.053.

[2] Fifield, L. K. (2008) Quaternary Geochronology 3, 276-290.

[3] Steier, P. et al. (2010) Nucl. Instr. and Meth. in Phys. Res. B 268, 1045-1049.



## Bioaccumulation of uranium from contaminated waters by the acidophilic protozoan, *Euglena mutabilis*

S. Brockmann,<sup>1,2</sup> T. Arnold,<sup>1</sup> G. Bernhard<sup>1,2</sup>

<sup>1</sup> Helmholtz-Zentrum Dresden-Rossendorf, Institute of Resource Ecology, Dresden, Germany

<sup>2</sup> Dresden University of Technology, Radiochemistry, Dresden, Germany

To study the influence of eukaryotic microorganisms on the migration behavior of uranium in acid mine drainage (AMD) environments bioaccumulation experiments with aqueous uranium and *Euglena mutabilis*, a eukaryotic microorganism often identified in AMD environments, were carried out. Batch sorption experiments at pH 3 and 4 were performed in Na<sub>2</sub>SO<sub>4</sub> background solutions to mimic AMD conditions and in NaClO<sub>4</sub> background solutions, respectively. It was found that axenic cultures of *Euglena mutabilis* were able to bioaccumulate more than 90% of uranium from a  $1 \cdot 10^{-5}$  mol/L uranium solution.

Laser-induced fluorescence spectroscopy was used to identify the speciation of uranium immobilized by *Euglena* cells. A comparison of the recorded fluorescence spectra with uranium reference compounds indicated that the immobilized uranium species forming in *Euglena* cells or on euglenid pellicles were related to carboxylic groups and/or organophosphate groups.

Similar experiments with *Euglena mutabilis* cells were carried out with sterile filtrated AMD waters obtained from the underground uranium mine Königstein. In these experiments, reduced uranium immobilization rates were observed. However, the identified uranium speciation of the bioaccumulated uranium was identical in these experiments. The reduced rates were attributed to the competition by other cations present in the sterile filtrated water for available sorption sites on or in the *Euglena* cells. The results showed that *Euglena mutabilis* or components of it are able to immobilize aqueous uranium and thus may be used in future as promising agent for immobilizing uranium in low pH waste water environments.

---

[1] Brockmann, S. et al. (2012) International Journal of Environmental Science and Technology (submitted).

## Speciation and distribution of plutonium after uptake by Opalinus Clay using synchrotron microbeam techniques

S. Amayri,<sup>1</sup> U. Kaplan,<sup>1</sup> J. Drebert,<sup>1</sup> D. Grolimund,<sup>2</sup> T. Reich<sup>1</sup>

<sup>1</sup> Institute of Nuclear Chemistry, Johannes Gutenberg-Universität Mainz, Mainz, Germany

<sup>2</sup> Paul Scherrer Institut, Swiss Light Source, Villigen, Switzerland

Plutonium is a major concern for the risk assessment of high-level geologic nuclear waste repositories. It plays an important role because of its long half-life and high radiotoxicity [1]. Pu exhibits a complicated redox chemistry, where up to three oxidation states can coexist in natural waters [2]. In order to estimate the migration behavior of Pu in an accident scenario after its release from a repository of spent nuclear fuels into the environment, the interaction of Pu with the host rock formation has to be studied in detail. Argillaceous rocks are under consideration in several European countries as a potential host rock for high-level nuclear waste repositories. In clay formations diffusion and sorption are considered to be the main transport and retardation processes [3]. The interaction of <sup>242</sup>Pu(VI) with Opalinus Clay (OPA) from Mont Terri, Switzerland, was studied by batch and diffusion experiments. These macroscopic investigations were combined with microscopic X-ray synchrotron radiation techniques (micro X-ray absorption spectroscopy ( $\mu$ -XAS), micro X-ray fluorescence spectroscopy ( $\mu$ -XRF), and micro X-ray diffraction ( $\mu$ -XRD) to determine the distribution and the chemical speciation of Pu after sorption and diffusion processes. Several thin sections of OPA were contacted with 20  $\mu$ M <sup>242</sup>Pu(VI) in OPA pore water (pH = 7.6, I = 0.4 M) under aerobic conditions for at least 3 days. For comparison, a OPA bore core in a diffusion cell was contacted with 20  $\mu$ M <sup>242</sup>Pu(VI) under the same conditions for more than one month. The sorption and diffusion samples were investigated at the MicroXAS beamline at the Swiss Light Source, Paul Scherrer Institut, Switzerland [4].  $\mu$ -XRF mapping has been used to determine the elemental distribution of Pu and other elements contained in OPA, e.g., Fe and Ca. Regions of high Pu concentrations were subsequently investigated by  $\mu$ -XANES to identify the oxidation state of sorbed Pu on the surface of OPA. Further,  $\mu$ -XRD was employed to gain knowledge about reactive crystalline mineral phases in the vicinity of Pu enrichments. The results of Pu L<sub>III</sub>-edge  $\mu$ -XANES spectra on Pu hot spots showed that Pu(IV) is the dominating species on OPA, i.e., the highly soluble Pu(VI) was retained by OPA in the reduced and less mobile tetravalent oxidation state of Pu.  $\mu$ -XRD results indicated that Pu is localized on or in the close vicinity of the Fe(II)-bearing mineral siderite and the clay mineral illite. Siderite is one of the redox-active mineral phases of OPA, which determines the speciation on Pu after uptake on OPA. The obtained results indicate that OPA is a suitable host rock for a high-level nuclear waste repository.

**Acknowledgement.** This work was financed by the Federal Ministry of Economics and Technology (BMWi) under contract no. 02E10166 and Actinet-I3 under contract no. 232631. We are grateful to C. Borca at SLS for her support during the measurements. Further we thank Dr. C. Marquardt (INE, KIT) and M. Biegler (Max-Planck-Institute for Chemistry, Mainz) for providing OPA samples and preparation of the OPA thin sections.

[1] Gompper, K. (2000) Zur Abtrennung langlebiger Radionuklide. In: Radioaktivität und Kernenergie. Forschungszentrum Karlsruhe, p.153.

[2] Runde, W. (2000) Los Alamos Sci. 26, 392-411.

[3] Van Loon, L. R. et al. (2003) J. Contam. Hydrol. 61, 73-83.

[4] Borca, C. N. et al. (2009) J Phys: Conf Ser 186, 012003-1 to 012003-3.

## Index of Authors

Abraham, M. ....	34	Guillaumond, D. ....	30
Acker, M. ....	41	Guillaumont, R. D. ....	58
Adam, C. ....	45	Günther, A. ....	48, 55
Akhmadaliev, S. ....	61	Harley, S. ....	22
Amayri, S. ....	18, 63	Hashem, E. ....	31
Aoyagi, N. ....	16	Haupt, S. ....	46, 50
Arias, J. M. ....	20	Heim, K. ....	25, 36
Arnold, T. ....	62	Heine, A. ....	34, 53
Auriault, C. ....	35	Heller, A. ....	36
Baker, R. J. ....	31	Heuser, J. ....	26
Banerjee, D. ....	56	Hofmann, S. ....	60
Barkleit, A. ....	20, 24, 36, 41	Hohnstein, S. ....	51
Baumann, N. ....	38	Holliday, K. ....	49
Benedetti, M. ....	35	Huang, P. ....	22
Bernhard, G. ....	36, 41, 48, 52, 55, 57, 62	Huber, F. ....	29
Bosbach, D. ....	26, 49	Huittinen, N. ....	23
Boubals, N. ....	58	Husar, R. ....	52
Breher, F. ....	51	Janot, N. ....	35
Bremer, A. ....	47	Jeanson, A. ....	28
Brendler, V. ....	24, 57, 59	Jordan, N. ....	25
Brockmann, S. ....	62	Kaden, P. ....	45
Caciuffo, R. ....	29	Kaplan, U. ....	63
Carroll, S. ....	22	Kar, A. S. ....	37
Casas, I. ....	38	Karpov, A. ....	47
Cheng, M. ....	54	Kelly, N. ....	53
Colette-Maatouk, S. ....	35	Kerridge, A. ....	31
Comarmond, M. J. ....	59	Kersting, A. ....	22
Conradson, S. ....	30	Kersting, B. ....	46
Creff, G. ....	28	Kimura, T. ....	16
Dardenne, K. ....	19, 51	Klenze, R. ....	32
De Sio, S. ....	33	Knope, K. E. ....	27
Den Auwer, C. ....	28, 30, 33	Kremleva, A. ....	17
Denecke, M.A. ....	45	Kretzschmar, J. ....	24
Drebert, J. ....	18, 63	Krüger, S. ....	17
Dumas, T. ....	30	Kupcik, T. ....	32
Fenter, P. ....	27	Lee, S. S. ....	27
Fernández, I. ....	51	Lehto, J. ....	23
Fillaux, C. ....	30, 33	Li, J. ....	15
Finkeldei, S. ....	49	Lindner, K. ....	55
Flörsheimer, M. ....	32	Lindqvist-Reis, P. ....	51
Foerstendorf, H. ....	25, 36, 44, 56, 59	Löble, M. ....	51
Gareil, P. ....	35	Lorenzo Solari, P. ....	28
Geckeis, H. ....	19, 29, 32	Lübke, M. ....	18
Geipel, G. ....	41	Lütke, L. ....	57
Geist, A. ....	45, 47	Mansel, A. ....	46
Giménez, J. ....	38	Martí, V. ....	38
Girnt, D. ....	47	Martínez-Torrents, A. ....	38
Gloe, K. ....	34, 53	März, J. ....	34
Gloe, Ke. ....	34, 53	Masella, M. ....	43
Godbole, S. V. ....	37	Mason, H. ....	22
González-Muñoz, M. T. ....	20	Matioszek, D. ....	51
Grolimund, D. ....	63	Maxwell, R. ....	22
Gückel, K. ....	44, 59	Meca, S. ....	38
Guerrero Martinez, Y.O. ....	43	Merchel, S. ....	61
Guilbaud, P. ....	33, 58	Merroun, M. L. ....	20
		Meyer, J. ....	51

Moisy, P. ....	33	Vallet, V. ....	43
Moll, H. ....	57	Vidaud, C. ....	28
Morcillo, F. ....	20	Vitova, T. ....	29, 51
Moreau, P. ....	35	Vogel, M. ....	48
Müller, K. ....	59	Vuilleumier, R. ....	58
Müller, T. J. J. ....	47	Walther, C. ....	42, 49, 54
Müllich, U. ....	47	Weiss, S. ....	52
Nakai, A. ....	56	Wieland, E. ....	42
Neumeier, S. ....	49	Wilson, R. E. ....	27
Ohashi, A. ....	56	Yang, P. ....	13
Oña-Burgos, P. ....	51	Zänker, H. ....	52
Pablo, J. de ....	38	Zavarin, M. ....	22
Panak, P. J. ....	45, 47		
Pavetich, S. ....	61		
Payne, T. E. ....	59		
Persson, P. ....	14		
Plaschke, M. ....	19		
Platts, J. A. ....	31		
Poetsch, M. ....	46		
Polly, R. ....	32		
Prüßmann, T. ....	29		
Rabung, T. ....	32		
Raff, J. ....	48, 57		
Réal, F. ....	43		
Reich, T. ....	18, 63		
Reiller, P. E. ....	35		
Ribokaité, K. ....	33, 58		
Roesky, P. W. ....	47		
Roques, J. ....	28		
Rösch, N. ....	17		
Rossberg, A. ....	44, 48		
Rothe, J. ....	19, 29, 47, 51		
Ruff, Ch. M. ....	47		
Rugel, G. ....	61		
Saeki, M. ....	56		
Safi, S. ....	28		
Saito, T. ....	16		
Sarv, P. ....	23		
Sasaki, Y. ....	56		
Schäfer, T. ....	19, 29		
Scheinost, A. C. ....	30, 56		
Schimmelpfennig, B. ....	32, 43		
Schlenz, H. ....	26		
Schmidt, M. ....	27, 60		
Schnorr, R. ....	46, 50		
Shuh, D. ....	30		
Simoni, E. ....	28		
Soderholm, L. ....	27		
Steppert, M. ....	54		
Stumpf, T. ....	42, 49, 60		
Szabó, Z. ....	21		
Taube, F. ....	53		
Tits, J. ....	42		
Tomar, B. S. ....	37		
Trapp, I. ....	51		
Trumm, M. ....	43		
Tsushima, S. ....	36, 44		
Tyliszczak, T. ....	30		
Ullmann, S. ....	50		

